National Library of Canada
Acquisitions and Bibliographic Services Branch
395 Wellington Street
Ottawa, Ontario
K1A 0N4

Bibliothèque nationale du Canada
Direction des acquisitions et des services bibliographiques
395, rue Wellington
Ottawa (Ontario)
K1A 0N4

Your file Votre référence

Our file Notre référence

NOTICE

The quality of this microform is heavily dependent upon the quality of the original thesis submitted for microfilming. Every effort has been made to ensure the highest quality of reproduction possible.

If pages are missing, contact the university which granted the degree.

Some pages may have indistinct print especially if the original pages were typed with a poor typewriter ribbon or if the university sent us an inferior photocopy.

Reproduction in full or in part of this microform is governed by the Canadian Copyright Act, R.S.C. 1970, c. C-30, and subsequent amendments.

AVIS

La qualité de cette microforme dépend grandement de la qualité de la thèse soumise au microfilmage. Nous avons tout fait pour assurer une qualité supérieure de reproduction.

S'il manque des pages, veuillez communiquer avec l'université qui a conféré le grade.

La qualité d'impression de certaines pages peut laisser à désirer, surtout si les pages originales ont été dactylographiées à l'aide d'un ruban usé ou si l'université nous a fait parvenir une photocopie de qualité inférieure.

La reproduction, même partielle, de cette microforme est soumise à la Loi canadienne sur le droit d'auteur, SRC 1970, c. C-30, et ses amendements subséquents.

Canada

University of Alberta

Wall Moisture Simulation Model

by

© Kenneth Francis McRae

A thesis submitted to the Faculty of Graduate Studies and Research in partial fulfillment of

the requirements for the degree of Master of Science.

Department of Mechanical Engineering

Edmonton, Alberta

Spring 1995

National Library
of Canada

Acquisitions and
Bibliographic Services Branch

395 Wellington Street
Ottawa, Ontario
K1A 0N4

Bibliothèque nationale
du Canada

Direction des acquisitions et
des services bibliographiques

395, rue Wellington
Ottawa (Ontario)
K1A 0N4

Your file Votre référence

Our file Notre référence

THE AUTHOR HAS GRANTED AN IRREVOCABLE NON-EXCLUSIVE LICENCE ALLOWING THE NATIONAL LIBRARY OF CANADA TO REPRODUCE, LOAN, DISTRIBUTE OR SELL COPIES OF HIS/HER THESIS BY ANY MEANS AND IN ANY FORM OR FORMAT, MAKING THIS THESIS AVAILABLE TO INTERESTED PERSONS.

L'AUTEUR A ACCORDE UNE LICENCE IRREVOCABLE ET NON EXCLUSIVE PERMETTANT A LA BIBLIOTHEQUE NATIONALE DU CANADA DE REPRODUIRE, PRETER, DISTRIBUER OU VENDRE DES COPIES DE SA THESE DE QUELQUE MANIERE ET SOUS QUELQUE FORME QUE CE SOIT POUR METTRE DES EXEMPLAIRES DE CETTE THESE A LA DISPOSITION DES PERSONNE INTERESSEES.

THE AUTHOR RETAINS OWNERSHIP OF THE COPYRIGHT IN HIS/HER THESIS. NEITHER THE THESIS NOR SUBSTANTIAL EXTRACTS FROM IT MAY BE PRINTED OR OTHERWISE REPRODUCED WITHOUT HIS/HER PERMISSION.

L'AUTEUR CONSERVE LA PROPRIETE DU DROIT D'AUTEUR QUI PROTEGE SA THESE. NI LA THESE NI DES EXTRAITS SUBSTANTIELS DE CELLE-CI NE DOIVENT ETRE IMPRIMES OU AUTREMENT REPRODUITS SANS SON AUTORISATION.

ISBN 0-612-01636-6

Canada

University of Alberta

Library Release Form

Name of Author : Kenneth Francis McRae

Title of Thesis : Wall Moisture Simulation Model

Degree: Master of Science

Year this Degree Granted : 1995

Permission is hereby granted to the University of Alberta Library to reproduce single copies of this thesis and to lend or sell such copies for private, scholarly, or scientific research purposes only.

The author reserves all other publications and other rights in association with the copyright in the thesis, and except as hereinbefore provided, neither the thesis nor any substantial portion thereof may be printed or otherwise reproduced in any material form whatever the author's prior written permission.

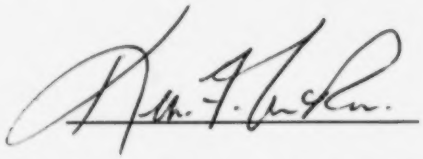

279, 10120 - 146 Avenue
Edmonton, Alberta
T5E 2K1

University of Alberta

Faculty of Graduate Studies and Research

The undersigned certify that they have read, and recommend to the Faculty of Graduate Studies and Research for acceptance, a thesis entitled, Wall Moisture Simulation Model submitted by Kenneth Francis McRae in partial fulfillment of the requirements for the degree of Master of Science.

Dr. T. Forest

Dr. J. Feddes

Dr. J. Yokota

Jan 30, 1995

DEDICATION

I would like to dedicate this thesis to my mother for her relentless support towards my educational efforts throughout my many years. Her support and encouragement have been greatly appreciated.

ABSTRACT

Moisture accumulation within a wall cavity can result in the degradation of insulation and structural damage to the exterior wood sheathing due to wood rot. Most homes are not "air-tight" and are susceptible to warm moist air exfiltrating through cracks and openings through the wall cavity to the outside. When this air flow comes in contact with the cold surface of the exterior sheathing moisture deposition occurs. The amount of air flow through the wall cavity is dependent upon the leakage path configuration, the leakage configuration of the house (vents, flues or fans) and meteorological conditions.

The Wall Moisture Simulation (WMS) model was developed to predict the amount and location of moisture deposited in a wall cavity as a function of time. This model is comprised of three different sub-models. The first is Walkers (1993) ventilation model which predicts the overall leakage of the building as a function of the leakage configuration, building geometry, shelter effect, and meteorological conditions. The second is Nikels (1991) two-dimensional, steady-state moisture deposition model which predicts the wall moisture deposition rate for a given leakage air flow rate. The third is the cavity flow model which predicts the wall leakage flow rate and couples the first two models together. The WMS model is the first model of its kind which first calculates the air leakage flow across the wall cavity and then determines the moisture deposition rate based on that air flow rate.

The WMS model was used to predict the seasonal variation in wood sheathing moisture content for five distinct regions across Canada. These regions included the East and West Coasts, Prairies, Central and Northern Canada. The East Coast represented by St.Johns, had the greatest moisture accumulation and potential for biological activity. Whitehorse (Northern), Winnipeg (Prairies) and Montreal (Central) all had comparable amounts of moisture accumulation. Vancouver with its mild winters and low wind speeds had the lowest moisture accumulation but surprisingly the second highest potential for biological activity.

ACKNOWLEDGMENT

I would like to acknowledge and thank Mr. Mark Ackerman for his assistance and throughout my research. I would especially like to thank my supervisor, Dr. Tom Forest, for his guidance, patience, and assistance throughout my research.

TABLE OF CONTENTS

Page

1 INTRODUCTION....1
1.1 Historical Development and Literature Review....4
1.2 Main Features of the Wall Moisture Simulation Model....6

2 DEVELOPMENT OF THE WALL MOISTURE SIMULATION MODEL....8
2.1 Ventilation Model....9
2.1.1 Weather Data....10
2.1.2 Shelter Effect....10
2.1.3 Building Geometry and Leakage Configuration....11
2.1.4 Wind Pressures....13
2.1.5 Indoor-Outdoor Temperature Difference Pressures....14
2.1.6 Reference Pressure, ΔP_{ref}....15
2.2 Moisture Deposition Model....18
2.2.1 Governing Equations....20
2.2.2 Boundary Conditions....21
2.2.3 Inlet Conditions....23
2.2.3.1 Temperature Profile....24
2.2.3.2 Indoor Relative Humidity....29
2.3 Development of the Cavity Flow Model....31
2.3.1 Infiltration Flow....33
2.3.2 Exfiltration Flow....42
2.3.3 Determination of the Flow Coefficient and Flow Exponent....44
2.4 Implementation of the WMS Model....51

3 VAPOR PRESSURE FOR WOOD SHEATHING....54
3.1 Base Case Simulation....55
3.2 Alternate Model for $P_{w,c}$ Below 0 ° C....56
3.3 Average Moisture Content Values....58

4 WALL MOISTURE SIMULATIONS....72
4.1 Base Case Analysis For the Five Cities....73
4.1.1 Flow Rates....74
4.1.2 Vapor Pressure Difference ($P_{w,inlet} - P_{w,c}$)....77
4.1.3 Cavity Mass Deposit Rate....80
4.1.4 Moisture Content Profile....83
4.1.5 Surface Moisture Accumulation....85
4.1.6 Biological Activity Potential....87
4.2 Variation in the Wall Cavity Depth....88
4.3 Exterior Retrofit....89
4.4 Variation in the Leakage Path Height....90
4.5 Constant Exfiltration Flow Rate....91

4.6 Summary....93

5 CONCLUSIONS AND RECOMMENDATIONS....136
5.1 Base Case Results....137
5.2 Parametric Changes to the Wall Cavity....138
5.3 Recommendations....138

REFERENCES....140

APPENDIX A Weather Data for Whitehorse, Winnipeg, Montreal, St.Johns and Vancouver....142

APPENDIX B Physical Constants....148

LIST OF TABLES

Table		Page
3-1	Building and wall cavity characteristics used in the WMS model to determine the relationship for $P_{w,e}$.	71
4-1	Summary of the hourly average and maximum flow rates, mass of water vapor, cavity mass deposit rates, and mass of water vapor exiting the cavity for each of the base case cities over a 1 year period.	133
4-2	Total number of hours showing only the top 10 and bottom 10 zones when the moisture content was greater than 20% (by weight) and the temperature of the inner surface of the exterior sheathing (Tc) was greater than 10 °C.	134
4-3	Summary of the hourly average and maximum flow rates, mass of water vapor, cavity mass deposit rates, and mass of water vapor exiting the cavity for St.Johns comparing the various wall cavity assemblies over a 1 year period.	135

LIST OF FIGURES

Figure — Page

2-1 Individual components of mass flow resulting from natural and mechanical sources within a house....12

2-2 Schematic diagram of the wall cavity used to derive the moisture deposition model....19

2-3 Sources of heat flux throughout the wall cavity for each nodal point....25

2-4 Typical mean indoor relative humidites for Canadian homes, Kent et al (1966) superimposed on the region of validity for 100 % relative humidity for the moisture deposition model....30

2-5 Wall cavity geometry showing the leakage sites locations and the various pressure difference locations used in the derivation of the cavity flow model....32

2-6 Flow exponents for various length to diameter ratios of short capillary tubes at low Reynolds numbers....46

2-7 Flow chart showing the major components of the Wall Moisture Simulation Model....53

3-1 Vapor pressure of wood as a function of the temperature and moisture content for various relative humidities....60

3-2 Schematic showing the moisture bound within the cell walls for Tc = - 20 °C for a constant moisture content and a moisture content calculated using Cleary's expression for vapor pressure....61

3-3 Comparison of the daily averaged vapor pressure difference (Pwinlet-Pwc) over a 1 year period (July-June) in Winnipeg for the base case and extrapolated values methods of determining the vapor pressure, Pwc....62

3-4 Comparison of the daily averaged cavity mass deposit rate for the base case method and the extrapolated values methods over a 1 year period (July-June) in Winnipeg....63

3-5 Comparison of the daily averaged moisture content of zone 1 over a 1 year period (July-June) in Winnipeg for the base case and extrapolated values method of determining the vapor pressure using Cleary's expression....64

Figure Page

3-6 Daily average unbound moisture within the cell walls for zone 1 over a 1 year period (July-June) in Winnipeg. Surface moisture accumulation is uniformly distributed over zone 1 which is 50 mm high and 368 mm wide....65

3-7 Comparison of the daily averaged vapor pressure difference (Pwinlet-Pwc) over a 1 year period (July-June) in Winnipeg for the base case and average moisture content methods....66

3-8 Comparison of the daily averaged cavity mass deposit rate for the base case method and average moisture content method over a 1 year period (July-June) in Winnipeg....67

3-9 Comparison of the daily averaged moisture content of zone 1 over a 1 year period in Winnipeg for the base case and the average moisture content methods....68

3-10 Comparison of the daily averaged surface moisture accumulation of zone 1 over a 1 year period (July-June) in Winnipeg for the base case and average moisture content methods. Surface moisture accumulation is uniformly distributed over zone 1 which is 50 mm high and 368 mm wide....69

3-11 Isometric view of the building characteristics used in all simulations ran using the WMS model....70

4-1 Wall pressure coefficients for an isolated buildings over a wind angle range of 360 ° 95

4-2 Daily averaged flow rate and vapor pressure difference over a one year period (July-June) in Whitehorse....96

4-3 Daily averaged cavity mass deposit rate over a one year period (July-June) in Whitehorse....97

4-4 Daily averaged moisture content profiles for various zones over a 1 year period (July-June) in Whitehorse....98

4-5 Daily averaged surface moisture accumulation for zone 1 over a 1 year period (July-June) in Whitehorse. Surface moisture accumulation is uniformly distributed over zone 1 which is 50 mm high and 368 mm wide....99

4-6 Daily averaged flow rate and vapor pressure difference over a 1 year period (July-June) in Winnipeg....100

Figure Page

4-7 Daily averaged cavity mass deposit rate over a 1 year period (July-June) in Winnipeg....101

4-8 Daily averaged moisture content profiles for various zones over a 1 year period (July-June) in Winnipeg....102

4-9 Daily averaged surface moisture accumulation for zone 1 over a 1 year period (July-June) in Winnipeg. Surface moisture accumulation is uniformly distributed over zone 1 which is 50 mm high and 368 mm wide....103

4-10 Daily averaged flow rate and vapor pressure difference over a 1 year period (July-June) in St.Johns....104

4-11 Daily averaged cavity mass deposit rate over a 1 year period (July-June) in St.Johns....105

4-12 Daily averaged moisture content profiles for various zones over a 1 year period (July-June) in St.Johns....106

4-13 Daily averaged surface moisture accumulation for zones 1 and 2 over a 1 year period (July-June) in St.Johns. Surface moisture accumulation is uniformly distributed over zones 1 and 2 which is 100 mm high and 368 mm wide....107

4-14 Daily averaged flow rate and vapor pressure difference over a 1 year period (July-June) in Montreal....108

4-15 Daily averaged cavity mass deposit rate over a 1 year period (July-June) in Montreal....109

4-16 Daily averaged moisture content profiles for various zones over a 1 year period (July-June) in Montreal....110

4-17 Daily averaged surface moisture accumulation for zone 1 over a 1 year period (July-June) in Montreal. Surface moisture accumulation is uniformly distributed over zone 1 which is 50 mm high and 368 mm wide....111

4-18 Daily averaged flow rate and vapor pressure difference over a 1 year period (July-June) in Vancouver....112

4-19 Daily averaged cavity mass deposit rate over a 1 year period (July-June) in Vancouver....113

Figure Page

4-20 Daily averaged moisture content profiles for various zones over a 1 year period (July-June) in Vancouver....114

4-21 Hourly values of the flow rate, and vapor pressure difference (top figure) and the cavity mass deposit (bottom figure) rate for July 1 - 3 in Winnipeg....115

4-22 Comparison of the daily averaged moisture content of zone 1 for a cavity depth of 89 mm (3.5") and 140 mm (5.5") over a 1 year period (July-June) in St.Johns....116

4-23 Comparison of the daily averaged surface moisture accumulation for zone 1 for a cavity depth of 89 mm (3.5") and 140 mm (5.5") over a 1 year period (July-June) in St.Johns. Surface moisture accumulation is uniformly distributed over zone 1 which is 50 mm high and 368 mm wide....117

4-24 Comparison of the moisture content of zone 1 for a standard wall configuration with an exterior retrofit wall over a 1 year period (July-June) in Whitehorse....118

4-25 Comparison of the daily averaged surface moisture accumulation in zone 1 for a standard wall configuration with an exterior retrofit wall over a 1 year period (July-June) in Whitehorse. Surface moisture accumulation is uniformly distributed over zone 1 which is 50 mm high and 368 mm wide....119

4-26 Comparison of the daily averaged moisture content of zone 1 for a standard wall configuration with an exterior retrofit wall over a 1 year period (July-June) in Winnipeg....120

4-27 Comparison of the daily averaged surface moisture accumulation in zone 1 for a standard wall configuration with an exterior retrofit wall over a 1 year period (July-June) in Winnipeg. Surface moisture accumulation is uniformly distributed over zone 1 which is 50 mm high and 368 mm wide....121

4-28 Comparison of the daily averaged moisture content in zone 1 for a standard wall configuration with an exterior wall retrofit over a 1 year period (July-June) in St.Johns....122

4-29 Comparison of the daily averaged surface moisture accumulation in zone 1 for a standard wall configuration with an exterior retrofit wall over a 1 year period (July-June) in St.Johns. Surface moisture accumulation is uniformly distributed over zone 1 which is 50 mm high and 368 mm wide....123

Figure Page

4-30 Comparison of the daily averaged moisture content in zone 1 for a standard wall configuration with an exterior retrofit wall over a 1 year period (July-June) in Montreal....124

4-31 Comparison of the daily averaged surface moisture accumulation in zone 1 for a standard wall configuration with an exterior retrofit wall over a 1 year period (July-June) in Montreal. Surface moisture accumulation is uniformly distributed over zone 1 which is 50 mm high and 368 mm wide....125

4-32 Comparison of the daily averaged moisture content in zone 1 for a standard wall configuration with an exterior retrofit wall over a 1 year period (July-June) in Vancouver....126

4-33 Comparison of the daily average moisture content in zone 1 (top figure) and zone 40 (bottom figure) for a leakage path height of 1.931 m and 0.966 m over a 1 year period (July-June) in Vancouver....127

4-34 Comparison of the daily averaged moisture content in zone 1 (top figure) and zone 40 (bottom figure) for a leakage path height of 1.931 m and 0.966 m over a 1 year period (July-June) in St.Johns....128

4-35 Comparison of the daily averaged surface moisture accumulation in zone 1 for a leakage path height of 1.931 m and 0.966 m over a 1 year period (July-June) in St.Johns. Surface moisture accumulation is uniformly distributed over zone 1 which is 50 mm high and 368 mm wide....129

4-36 Comparison of the daily averaged cavity mass deposit rate for a variable flow rate (base case) with a fixed flow rate of 0.0244 m^3/hour over a 1 year period (July-June) in St.Johns....130

4-37 Comparison of the daily averaged moisture content in zone 1 for a variable flow rate (base case) with a fixed flow rate of 0.0244 m^3/hour over a 1 year period (July-June) in St.Johns. Surface moisture accumulation is uniformly distributed over zone 1 which is 50 mm high and 368 mm wide....131

4-38 Comparison of the daily averaged surface moisture accumulation in zone 1 for a variable flow rate (base case) with a fixed flow rate of 0.0244 m^3/hour over a 1 year period (July-June) in St.Johns....132

NOMENCLATURE

A_C	Cavity cross-sectional area [m^2]
A_t	Throat area [m^2]
C	Flow coefficient [m^4 s/kg]
C_d	Discharge coefficient
C_p	Wall pressure coefficient
D	Mass diffusivity of water vapor [m^2/s]
d	Depth of wall cavity [m]
F_{d-grnd}	View factor from the exterior sheathing to the ground
F_{d-sky}	View factor from the exterior sheathing to the sky
g	Gravitational acceleration [m/s^2]
H_C	Height of wall cavity [m]
h	Convective heat transfer coefficient [W/m^2 K]
I_{total}	Total solar radiation [W/m^2]
K	Permeability of insulation [m^2]
L	Width of wall cavity [m]
M_w	Molecular mass of water [kg/kmol]
$\dot{M}_w$	Mass of water entering the wall cavity [kg/s]
$\dot{m}_w$	Moisture deposition rate [kg/s]
$\dot{m}_{w,exit}$	Amount of water vapor exiting the wall cavity [kg/s]
MC	Wood moisture content by weight
n	Summation index
n	Flow exponent of air
P_{atm}	Atmospheric pressure [Pa]
$P_{w,e}$	Vapor pressure of water on the inner surface of the exterior sheathing [Pa]
$P_{w,inlet}$	Inlet water vapor pressure [Pa]
$P_{w,s}$	Saturation pressure of water [Pa]
ΔP_i	Pressure difference across a crack at height, i [Pa]
ΔP_{ref}	Reference pressure difference at grade [Pa]
ΔP_T	Pressure difference due to indoor-outdoor temperature differences [Pa]
ΔP_w	Pressure difference due to wind effects [Pa]
Q	Volumetric flow rate [m^3/s]
q	Heat flux [W/m^2]
Re	Reynolds number
R_o	Universal gas constant [J/kmol K]
S_w	Wind shelter factor
T_a	Temperature of wall at inner surface [K]
T_C	Cavity temperature, [K]
T_{in}	Indoor temperature [K]
T_{out}	Outdoor temperature [K]
U	Wind speed at eave height [m/s]

v	Air velocity in the y direction [m/s]

GREEK SYMBOLS

α	Solar absorptivity of exterior sheathing
β	Ratio of the obstruction diameter to the upstream diameter
μ	Dynamic viscosity [kg/m s]
ρ	Density [kg/m^3]
ϕ	Relative humidity
ε	Long wave emissivity for the exterior sheathing
σ	Stefan-Boltzmann constant [$W/m^2/K^4$]

SUBSCRIPTS

a	Interior surface of the drywall
b	Interface between the drywall and the insulation
c	Interface between the insulation and the exterior sheathing
d	Exterior surface of the exterior sheathing
i, I	Inside
o, O	Outside
w	Water
1	Location of interior leakage site
2	Location of exterior leakage site

Chapter
ONE

INTRODUCTION

Indoor moisture-related problems, consisting of dampness and mustiness, window condensation, and mold and mildew are known to occur in homes. Tsongas (1992) visually inspected 86 newly constructed homes in the Pacific Northwest and found that one-third of the homes had mold and mildew. It was observed on window frames, walls and ceilings of all types of rooms. Almost all of the problems were worst in cold climate regions. Moisture damage visually apparent on the walls, and ceilings is not only a nuisance, but also causes additional maintenance and repair costs and is a potential health problem. Of greater concern is the amount of moisture damage caused by moisture deposition within wall and ceiling cavities. By visual inspection the wall may appear to be unaffected but the exfiltration of warm moist air during the cold winter months may covertly be causing damage to the wall cavity. Moisture in the form of water or ice may unknowingly be accumulating within the wall cavity which could lead to several different moisture related problems.

The exfiltration of warm moist indoor air is the main reason for moisture deposition within wall cavities of residential homes. Moisture deposition within wall cavities often leads to deterioration of the insulation and wood components and the presence of biological activity such as mold and fungi.

The amount of moisture deposition is dependent upon the air flow rate across the various leakage sites of the building envelope. The air flow is dependent upon the outdoor

weather conditions and the condition of the building envelope. Air exfiltrating through cracks and openings causes a great deal of heat loss when there is a high indoor-outdoor temperature difference. Warped, damaged, or deteriorated trim around windows and doors often leads to drafts which are one cause of a "leaky" house resulting in great deal of exfiltration. Another contributing factor of a "leaky" house is poor craftsmanship. Examples of poor craftsmanship include not taking the proper precautions in sealing around electrical outlets, windows and doors, and at the joints where the wall and floor and wall and ceiling meet.

The warm moist air exfiltrating through the leakage site up along the wall cavity will result in moisture depositing on the cold surface of the exterior sheathing. There are two possible methods to try to eliminate the possibility of moisture deposition caused by air exfiltration. First, the house could be built "air-tight" void of any possible leakage sites. This "air-tight" building would be void of any air leakage but the occupants would require a minimum of 8.5 m^3/hour/person (ASHRAE 1989), of fresh air supplied by some type of mechanical ventilation system. Unfortunately, most older homes do not have ventilation systems solely dedicated to the supply of fresh air. The second and more feasible option would be to take the necessary preventative maintenance precautions and reduce the possibility of moisture deposition. This would include such things as sealing around electrical outlets, ensuring weather striping around doors and windows are well maintained, and properly insulating the walls of the house.

However, even by taking the necessary precautions some moist air may find its way though some leakage site and enter the wall by two possible mechanisms: vapor

convection and vapor diffusion. When the partial pressure of water vapor of the indoor environment is greater than the partial pressure of water vapor of the outdoor conditions, vapor diffusion will occur through the wall cavity initiating at the drywall and travel towards the exterior sheathing. The only manner in which to stop vapor diffusion is the use of a vapor retarder such as a polyethylene sheet. A vapor retarder will also stop the flow of air infiltrating and exfiltrating through the wall cavity. Vapor convection associated with air movement is the result of a pressure difference across the building envelope caused by temperature and wind effects and some defect in the wall. Normally, in most residential buildings the amount of water vapor carried through walls caused by vapor convection is 10 to 4000 times greater than vapor diffusion, (TenWolde and Suleski, 1984).

Breaks in the vapor barrier occur in the wall cavity as a result of poor installation and openings cut to allow for the installation of electrical outlets, windows and doors. A break in the vapor barrier allows the moist air to travel past the vapor barrier, vertically along the wall cavity and deposit moisture upon the cold surface of the exterior sheathing. The amount of moisture deposition is a function of the air flow rate which is dependent upon the weather conditions, building leakage configuration, building shelter and cavity geometry. As the air flow convects along the wall cavity, moisture deposits on the cold exterior surface causing an increase in the moisture content of the exterior sheathing.

The moisture content of the sheathing increases from the start of the summer, eventually reaching a maximum during the cold winter months and then declines with the onset of spring and summer. The surface deposition reaches a maximum during the cold

winter months and gradually declines with the onset of warmer weather until there is no surface deposition remaining. The amount of deposition varies from one region to another within Canada. It is not possible to generalize and say that the coastal areas have a greater chance of more moisture deposition because of their higher relative humidities than areas such as the prairies. Wind direction, wind speed, outdoor temperature and relative humidity all must be taken into account when predicting if there will be a potential problem with moisture deposition in the wall cavity.

1.1 Historical Development and Literature Review

There are a number of different numerical models used to predict the amount of moisture deposition in a wall cavity. One of these is a transient, one dimensional, finite difference model developed by Burch and Thomas (1992) which predicts the horizontal distribution of heat and moisture in a multilayer wall under nonisothermal conditions. The model is capable of calculating the moisture transfer for diffusing water vapor through the capillary regimes. Capillary transfer occurs when a continuous path of liquid exists within the insulation or porous material. The model predicts the transient average moisture content of the sheathing and siding of a wood-frame wall as a function of the time of the year. The model is also capable of accounting for convective moisture transfer assuming an exfiltration flow rate or cavity ventilation rate of six volume changes per hour. Because the amount of moisture deposition for vapor diffusion is very small compared to that of vapor convection this model is limited in its use. It also does not predict a vertical distribution of moisture.

Ojanen and Kumaran (1992), on the other hand developed a numerical method model to predict the amount of moisture accumulation in residential wall cavities due to vapor convection. The computer model used for the simulations uses a finite-difference technique to solve the transient heat, air, and moisture transfers in two dimensional multilayer building structures. They studied the results for a number of wall cavities exposed to Canadian and Finnish weather conditions at various locations. An appreciable amount of moisture accumulated during the heating season and subsequently dried out during the warmer periods. The maximum mass of moisture ranged from 1.0 kg/m^2 of wall area for Vancouver to 28.1 kg/m^2 for Resolute Bay. Unfortunately, similar to Burch and Thomas (1992), instead of calculating the air flow rate across the wall cavity they also assumed a constant exfiltration flow rate. It will be shown in Chapter 4 that assuming a constant exfiltration flow rate is a viable alternative only if this value approximates the yearly mean exfiltration rate.

TenWolde and Carll (1992) on the other hand measured the air flow rate across the wall cavity based on an imposed 4 Pa pressure differential across the wall envelope. They used the measured air flow rates to predict the moisture flows, wetting and drying potentials assuming a steady-state, one-dimensional, thermal conduction, and water vapor diffusion. TenWolde and Carll's prediction is somewhat limited since the majority of moisture deposition is the result of vapor convection and not vapor diffusion.

One of the better models developed was by Nikel (1991) whose two dimensional model coupled heat transfer and mass transfer together to predict the moisture deposition in a wall cavity. The moisture deposition model is based on the analytical solution to the

two dimensional, steady-state differential equation governing the diffusion of air through a porous medium. The model takes into account the vapor diffusion in the horizontal direction and vapor convection associated with the air flow in the vertical within the wall cavity. However, in verifying the model, the air flow rates had to be first measured using an orifice meter and then input into his moisture deposition model. An orifice meter located 1.55 m from the base of the wall was installed in the interior wall of the wall cavity. Located on the exterior side of the wall cavity were two leakage sites. There was one leakage site located at the top and bottom of the wall cavity. The model proved to be a simple method of predicting the amount of moisture deposition but limited in scope since the air flow rate across the wall cavity leakage path had to be known. These leakage flow rates are generally not known for varying meteorological conditions.

1.2 Main Features of the Wall Moisture Simulation Model

The moisture deposition model presented is called the Wall Moisture Simulation (WMS) model and is a culmination of 3 different works. The first model calculates the pressure difference across the building envelope as a function of the weather data, building leakage configuration, building geometry, and shelter. This model has been recently developed by Walker(1993) in order to predict the whole house ventilation rate. The second model predicts the amount and distribution of moisture in a vertical wall cavity for a given leakage air flow rate through the wall cavity. This model has been developed by Nikel (1991). The third model developed in Chapter 2 is the cavity flow model. This model calculates the pressure difference across the wall cavity as a function of the overall

leakage configuration, wind and temperature effects, and the mass flow rates through the wall cavity.

The Wall Moisture Simulation model was developed to be used as a tool to better understand the behavior of moisture deposition in a wall cavity for different climatic regions across Canada. Chapter 2 outlines the development of the WMS model showing the contribution of the ventilation model (Walker, 1993), moisture deposition model (Nikel, 1991) and the derivation of the cavity flow model which has not been done previously. Chapter 3 discusses how the vapor pressure, $P_{w,c}$ relates to the moisture deposition model for temperatures both above and below 0 ° C. Chapter 4 presents yearly simulations including the flow rate, cavity mass deposition rate, sheathing moisture content profile, and surface moisture accumulation for five different climatic regions across Canada. These results are then used as the base for comparison with various wall assemblies. Chapter 5 summarizes and makes recommendations based on the results of Chapter 4 which can then be used to improve the building construction practices of residential housing.

Chapter
TWO

DEVELOPMENT OF THE WALL MOISTURE SIMULATION MODEL

Most residential buildings have some air leakage through the walls of the house. During the cold winter months, the air leakage exfiltrating from within the house carries moisture with it which tends to condense on the cold outer sheathing causing an accumulation of moisture. This is generally followed by a drying period during the spring and summer months. This cycle of moisture accumulation and drying may continue for years going unnoticed. Depending on the weather conditions, there is the unfortunate possibility that the exterior sheathing may not dry out in the spring and summer and the high moisture content within the wooden structures may result in some form of structural damage.

The objective of this chapter is to show the development of the Wall Moisture Simulation (WMS) model which will predict the amount of moisture deposition and subsequent moisture content of the exterior sheathing within the wall cavity. A review of ventilation model developed by Walker (1993) and moisture deposition developed by Nikel (1991) model for air flow through wall cavities model will first be covered followed by the derivation of the cavity flow model . The major components reviewed in Walker's ventilation model include: some of the main features which the model was developed, weather data, shelter effect, building geometry and leakage configuration, wind pressures, and indoor-outdoor temperature difference pressures. This is followed by a review of the

moisture deposition model which includes: governing equations, boundary conditions, and inlet conditions. After reviewing the main features of the ventilation model and moisture deposition model, the critical connection between these two models will be outlined in the derivation of the cavity flow model.

2.1 Ventilation Model

The ventilation model developed by Walker estimates the air mass flow rates through all house leaks which includes major leakage such as flues, open windows or doors, vents and fans and minor leaks which are distributed over the walls and ceilings. Input to the ventilation model includes the weather data, shelter type, and building geometry and leakage configuration. Some of the important features of the model are :

- The building has a rectangular floor plan. The floor plan must not have the longest side greater than about three times the shorter side because the wind pressure coefficients used in the model will be incorrect.
- Leakage is distributed between the ceiling, floor, and walls for the four walls.
- All wind pressure coefficients are averaged over the wall surface. This means that extremes of wind pressure occurring at the corner flow separation are not included.
- Upwind obstacles are assumed to shade the entire wall height of the downwind building when calculating wind shelter.

2.1.1 Weather Data

Weather data required for the ventilation model are the hourly averaged wind speed, wind direction, outdoor relative humidity, and outdoor temperature. Meteorological data generated by Canada Mortgage and Housing (CHMC)[1] is used as input to run the WMS model and includes; wind speed at 10 m height, wind angle, outdoor relative humidity, outdoor temperature, cloud cover index and total solar radiation on the four vertical walls oriented N, S, E and W. Simulations will be run using the CHMC meteorological data collected for Whitehorse, Winnipeg, St.Johns, Montreal and Vancouver.

2.1.2 Shelter Effect

The wind shelter effect is dependent upon the surrounding buildings and obstacles. The reduction in velocity caused by upwind obstacles can be determined using a method called the Wind Shadow Wake Shelter developed by Walker (1993). The reduction in wind speed in the shadow is assumed to be proportional to the decrease in velocity at the eave height on the centerline of the wake generated by the upwind obstacle. The shelter model further assumes that the downwind building of interest is sufficiently far enough downstream of the obstacle that it does not affect the wake flow structure.

---

[1] Meteorological data in a standard format is available from CHMC.

2.1.3 Building Geometry and Leakage Configuration

The building geometry of the house which the WMS model takes into account includes the ceiling height, floor height, floor area, and volume of the building. The specific dimensions of the building geometry used in the simulations ran in Chapter 4 can be seen in Table 3-1. The building geometry together with the leakage configuration is input into Walker's ventilation model in order to calculate the leakage across the building envelope.

The building leakage configuration is dependent upon a number of different factors as shown in Fig. 2-1. Air flow across a leakage site may result from the pressure difference caused by mechanical ventilation or natural causes. Mechanical ventilation within a house includes such things as a flue, fan, or vent. Natural causes of ventilation include the effects due to wind and temperature differences. The mass flow of air through each leakage site, i, resulting from either mechanical or natural pressure differences can be expressed as

$$\dot{m}_i = \rho_i C \Delta P_i^{n} \quad \text{(infiltration)} \tag{2.1a}$$

$$\dot{m}_{ex} = \rho_o C \Delta P_i^{n} \quad \text{(exfiltration)} \tag{2.1b}$$

where ρ is the density of the ambient air,

C is the flow coefficient of each leak,

ΔP_i is the pressure difference across the leakage site, and

n is the flow exponent of each leakage site.

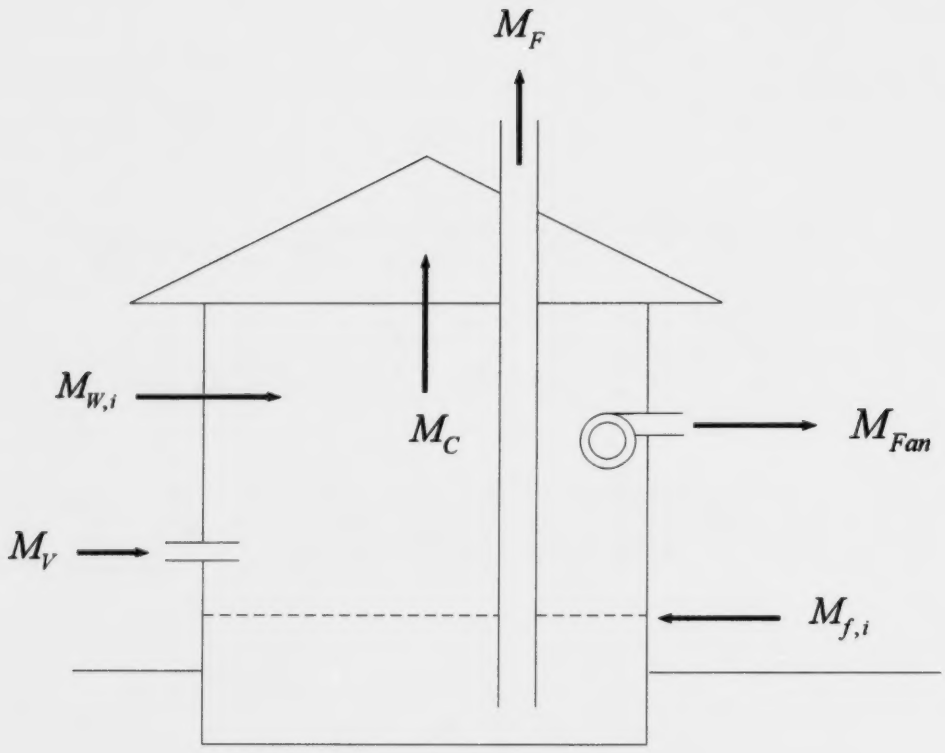

Mass Flow Rates where:

M_F	-	Flue
M_{Fan}	-	Fan
$M_{f,i}$	-	Floor level leaks below wall i
M_V	-	Vent
$M_{W,i}$	-	Wall i
M_C	-	Ceiling

Figure 2-1 **Individual components of mass flow resulting from natural and mechanical sources within a house.**

Density, ρ , of the ambient air is dependent upon the direction of the air flow. For example, if the air flow is from the exterior to the interior (infiltration) of the house then the outdoor density, ρ_{out} is used; if exfiltration, then the indoor density, ρ_i would be used. The flow coefficient C , is related to the leakage area and air properties and may differ depending on the direction of the flow. The flow exponent n_i , describes the nature of the air flow. The flow exponent is a number between 1/2 for turbulent flow and 1 for laminar flow. The pressure difference ΔP_i is the result of the pressure differences caused by wind and temperature (stack) effects which can be expressed as

$$\Delta P_i = \Delta P_{ref} + \Delta P_{wind} + \Delta P_{stack} \tag{2.2}$$

where: ΔP_{wind} is the wind induced pressure difference,

ΔP_{stack} is the temperature effect pressure difference, and

ΔP_{ref} is the reference pressure difference at grade.
(This term will be discussed in Sec. 2.1.6)

2.1.4 Wind Pressures

The wind induced pressure difference on a surface of a house is defined as

$$\Delta P_{wind} = C_p \frac{\rho_{out} U^2}{2} S_w^2 \tag{2.3}$$

where: C_p is the wind pressure coefficient,

ρ_{out} is the outdoor density,

U is the reference wind speed at eave height, and

S_W is the shelter factor.

ΔP_{wind} is the difference between the pressure on the surface of the building due to the wind and the atmospheric pressure P_∞. The pressure coefficients, C_p have been determined from wind tunnel studies which are generally positive for upwind surfaces due to flow stagnation and negative on downwind surfaces due to flow separation (the variation of C_p wind direction will be discussed in Chapter 4). The outdoor density was chosen as the reference density because the pressure coefficients are in terms of wind speed. U is the wind speed which corresponds to the wind speed at the eaves height. The wind speed data from the CHMC meteorological data files were measured at a 10 m height. A correction was made to account for the height difference between the 10 m measured values and eaves height. For no shelter, the shelter effect, S_W = 1 and for complete shelter S_W = 0 which implies that there is no wind effect.

2.1.5 Indoor-Outdoor Temperature Difference Pressures

The pressure difference due to the indoor - outdoor temperature difference (stack effect) can be expressed as

$$\Delta P_{stack} = -\rho_{out}\ g\ H_i\left(\frac{T_{in} - T_{out}}{T_{in}}\right) \tag{2.4}$$

where: ρ_{out} is the outdoor density,

g is the gravitational acceleration,

H_i is the height of the leakage site, i,

T_{in} is the indoor temperature, and

T_{out} is the outdoor temperature.

ΔP_{stack} is the pressure difference across the building envelope resulting from the difference between the indoor and outdoor densities. By using single indoor and outdoor densities, assumes that the indoor and outdoor air are homogeneous and well mixed. The pressure difference is the outdoor pressure minus the indoor pressure which will be the convention so positive pressures result in flow entering the building from the outside. H_i is the height of the leakage site which is taken above grade level (reference height). The indoor and outdoor temperatures are both assumed to be constant for any given height above grade.

2.1.6 Reference Pressure, ΔP_{ref}

An in-depth look at how ΔP_{ref} is defined and its significance to the cavity flow model is beneficial. For any given height, H_i , the pressure inside the house can be expressed as

$$P_i = P_{i,ref} - \rho_i g H_i \tag{2.5}$$

where $P_{i,ref}$ is the inside reference pressure at grade level. The pressure on the wall induced by wind at grade level is

$$P_{o,ref} = P_\infty + C_p \frac{\rho_o U^2}{2} Sw^2 \tag{2.6}$$

The pressure on the outside of the wall at height, H_i becomes

$$P_{oi} = P_{o,ref} - \rho_o g H_i \tag{2.7}$$

Now eliminating $P_{o,ref}$ from Eqn.2.7 using Eqn. 2.6 gives

$$P_{oi} = P_\infty - \rho_o g H_i + C_p \frac{\rho_o U^2}{2} S_w^{\,2} \tag{2.8}$$

The complete expression for the pressure difference between the outside and inside across the leakage site i at height, H_i can now determined using Eqns. 2.5 and 2.8 and expressed as

$$P_{oi} - P_i = P_\infty - \rho_o g H_i - P_{i,ref} + \rho_i g H_i + C_p \frac{\rho_o U^2}{2} Sw^2 \qquad (2.9)$$

ΔP_{ref} is now defined as $(P_\infty - P_{i,ref})$. Combining the two terms with densities together, using the ideal gas equation and the outdoor-indoor pressure difference across a leakage site at height, H_i can now be expressed as

$$\Delta P_i = \Delta P_{ref} - \rho_o g H_i \left(\frac{T_{in} - T_{out}}{T_{in}} \right) + C_p \frac{\rho_o U^2}{2} S_w^2 \qquad (2.10)$$

For brevity, Eqn. 2-10 can be expressed in a more general form as

$$\Delta P_i = \Delta P_{ref} - \Delta P_T H_i + C_{p_i} \Delta P_w S_{w_i}^2 \qquad (2.11)$$

where: $\Delta P_T = \rho_o g \left(\frac{T_{in} - T_{out}}{T_{in}} \right)$, and

$$\Delta P_w = \frac{\rho_o U^2}{2}.$$

The value of ΔP_{ref}, is determined by iteratively solving the mass balance for the mass flow from Eqn. 2.1 of air flowing through each leakage site as a result of mechanical or natural ventilation within the house. Because the flow through the wall cavity is small compared to the total flow across the building envelope, the ventilation model is not

influenced by the leakage through the wall cavity. The value of ΔP_{ref} is not affected by the presence of the leakage path in the wall cavity and will be used as an input in the cavity flow model.

2.2 Moisture Deposition Model

Nikel (1991) developed a simple mass transfer model which predicts the amount of moisture accumulation based on forced convective flow through a wall cavity. Input parameters for the model include indoor and outdoor relative humidity, ambient temperature and air flow rate. The cavity model used in the derivation of the moisture deposition model can be seen in Fig.2-2. Some important features of the moisture deposition model are:

- The wall cavity can be of any rectangular construction as long as it has a large aspect ratio (height/depth >>1) and is assumed to be two dimensional.
- The velocity has a uniform profile (plug flow) which flows only in the y direction. There is no forced convective flow in the x and z directions.
- The inlet vapor pressure, $P_{w,inlet}$ is assumed to be constant at the inlet.
- The vapor pressure, $P_{w,c}$ is assumed to be constant along the height of the wall cavity.
- Moisture is deposited by diffusion in the x direction on the inner cold surface of the exterior sheathing and not within the insulation.

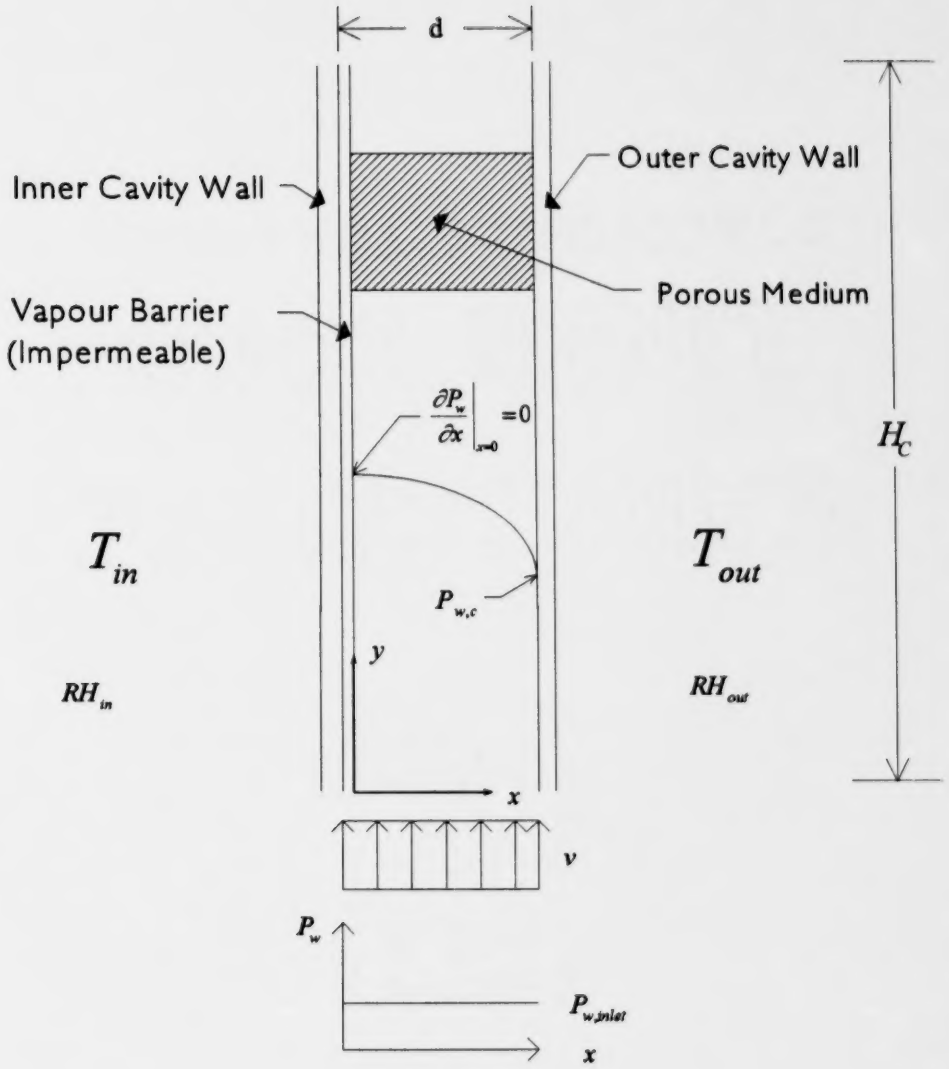

Figure 2-2 **Schematic diagram of the wall cavity used to derive the moisture deposition model.**

- There is negligible effect due to latent energy when the moisture vapor condenses on the cold surface.
- The porous medium is assumed homogeneous, and isotropic. Darcy's Law applies if the local Reynolds number based on the average velocity and $K^{1/2}$ does not exceed $O(1)$.

2.2.1 Governing Equations

The two dimensional, steady-state differential moisture diffusion equation governing the diffusion of a gas through the porous medium is expressed as

$$v\frac{\partial P_w}{\partial y} = D\frac{\partial^2 P_w}{\partial x^2} \tag{2.12}$$

where: P_w is the partial pressure of water vapor,

v is the velocity in the y direction, and

D is the mass diffusivity of the porous medium.[1]

Since the velocities in the x and z directions are assumed to be zero, Eqn.2.12 reduces to moisture deposition in the y direction only. Before we can solve Eqn. 2.12 we must first review the boundary conditions.

---

[1] All physical constants are listed in Appendix-B.

2.2.2 Boundary Conditions

The first boundary condition is at $x = 0$. This is the interface between the drywall and the vapor barrier. Since the vapor barrier is assumed to be impermeable to any moisture vapor, the first boundary condition states that no moisture will be able to diffuse through the vapor barrier to the inner wall. Mathematically this boundary condition translates into a zero mass flux at $x = 0$ and can be expressed as,

$$\frac{\partial P_w(0,y)}{\partial x} = 0 \tag{2.13}$$

Since no moisture can permeate the vapor barrier, the only place moisture can enter the cavity wall is through a leakage path entrance. This leakage path entrance could be the result of not properly sealing the entire cavity wall due to poor construction practice.

The second boundary condition is at the outer wall cavity $x = d$ which has a constant vapor pressure given by $P_w(d,y) = P_{w,c}$. The vapor pressure, $P_{w,c}$ depends on the moisture content and the temperature T_C at the inner surface of the external sheathing. Though the moisture content of the sheathing varies greatly along the height of the cavity, the value of $P_{w,c}$ is assumed to be constant along the wall cavity.

The third boundary condition states that since the inlet relative humidity and temperature are assumed to be constant, the inlet vapor pressure must therefore also be assumed to be constant. This is expressed as

$$P_w(x,0) = P_{w,inlet} \tag{2.14}$$

After using separation of variables and applying the three boundaries conditions, the general solution for Eqn. 2.12 in terms of P_w can be expressed as

$$P_w(x,y) = P_{w,c} + \left(P_{w,inlet} - P_{w,c}\right)\sum_{n=1}^{\infty}\frac{2\sin\lambda_n}{\lambda_n}\cos\left(\frac{\lambda_n x}{d}\right)\exp\left[-\frac{D\lambda_n^{\,2}}{d^2 v}y\right] \tag{2.15}$$

where: λ_n is the separation constant $\left(\lambda_n = \frac{(2n-1)\pi}{2},\ n = 1,2,3,\ldots\right)$

The vapor pressure gradient can now be obtained by taking the derivative of Eqn. 2.15 with respect to x.

$$\frac{\partial P_w(x,y)}{\partial x} = \left(P_{w,inlet} - P_{w,c}\right)\sum_{n=1}^{\infty}\frac{-2\sin\lambda_n}{d}\sin\left(\frac{\lambda_n x}{d}\right)\exp\left[-\frac{D\lambda_n^{\,2}}{v d^2}y\right] \tag{2.16}$$

The total mass deposited on the surface at $x = d$ can be determined by integrating Eqn. 2.16

$$\dot{m}_w = -DL\frac{M_w}{R_o T}\int\frac{\partial P_w}{\partial x}dy \tag{2.17}$$

where D is the diffusivity of the porous medium,

L is the cavity width,

M_w is the molecular mass of water,

R_o is the universal gas constant, and

T is the mean cavity temperature.

Integrating Eqn 2.17 yields the complete expression for the total mass deposited between the limits of integration .

$$\dot{m}_w = -DL\frac{M_w}{R_o T}\left(P_{w,inlet} - P_{w,c}\right)\sum_{n=1}^{\infty}\frac{-2\sin\lambda_n}{d}\sin\left(\frac{\lambda_n x}{d}\right)\left(\frac{-\nu d^2}{D\lambda_n^{\,2}}\right)$$

$$\left(\exp\left[-\frac{D\lambda_n^{\,2}}{\nu d^2}y_j\right] - \exp\left[-\frac{D\lambda_n^{\,2}}{\nu d^2}y_i\right]\right) \qquad (2.18)$$

2.2.3 Inlet Conditions

The two main inlet conditions which are essential to the moisture deposition model are the vapor pressure at the inner surface of the exterior sheathing, $P_{w,c}$ and the inlet vapor pressure, $P_{w,inlet}$. The inlet vapor pressure is simply the product of the relative humidity and the saturation vapor pressure for the inlet temperature. The direction of the flow through the wall cavity will determine whether to use the indoor or outdoor

temperature and relative humidity. The value of the inlet conditions for infiltrating flow can easily be determined since the values of the outdoor temperature and relative humidity are read into the model as input parameters. However, before the inlet conditions for exfiltrating flow and the vapor pressure $P_{w,c}$ can be determined, the value of T_C must first be calculated.

2.2.3.1 Temperature Profile

In order to determine the value of T_C, an energy balance at each node within the wall cavity is performed using a one-dimensional steady-state analysis. Nikel (1991) determined that the addition of forced flow through the wall cavity does not alter the steady state heat flux calculations. The induced air flow through the wall cavity tends to affect a small region of about $2d$ long (approximately 18 cm), near the entrance to the wall cavity which is small in comparison to the entire height of the wall cavity. Therefore, a linear temperature profile is assumed throughout the entire height of the wall cavity. Fig. 2-3 shows the nodal point locations a through d and the indoor and outdoor temperatures. The steady state energy balance at each node can be expressed as

$$\sum_{i=1}^{\infty} q_i = 0 \tag{2.19}$$

where q_i are the heat fluxes due to conduction, convection and radiation.

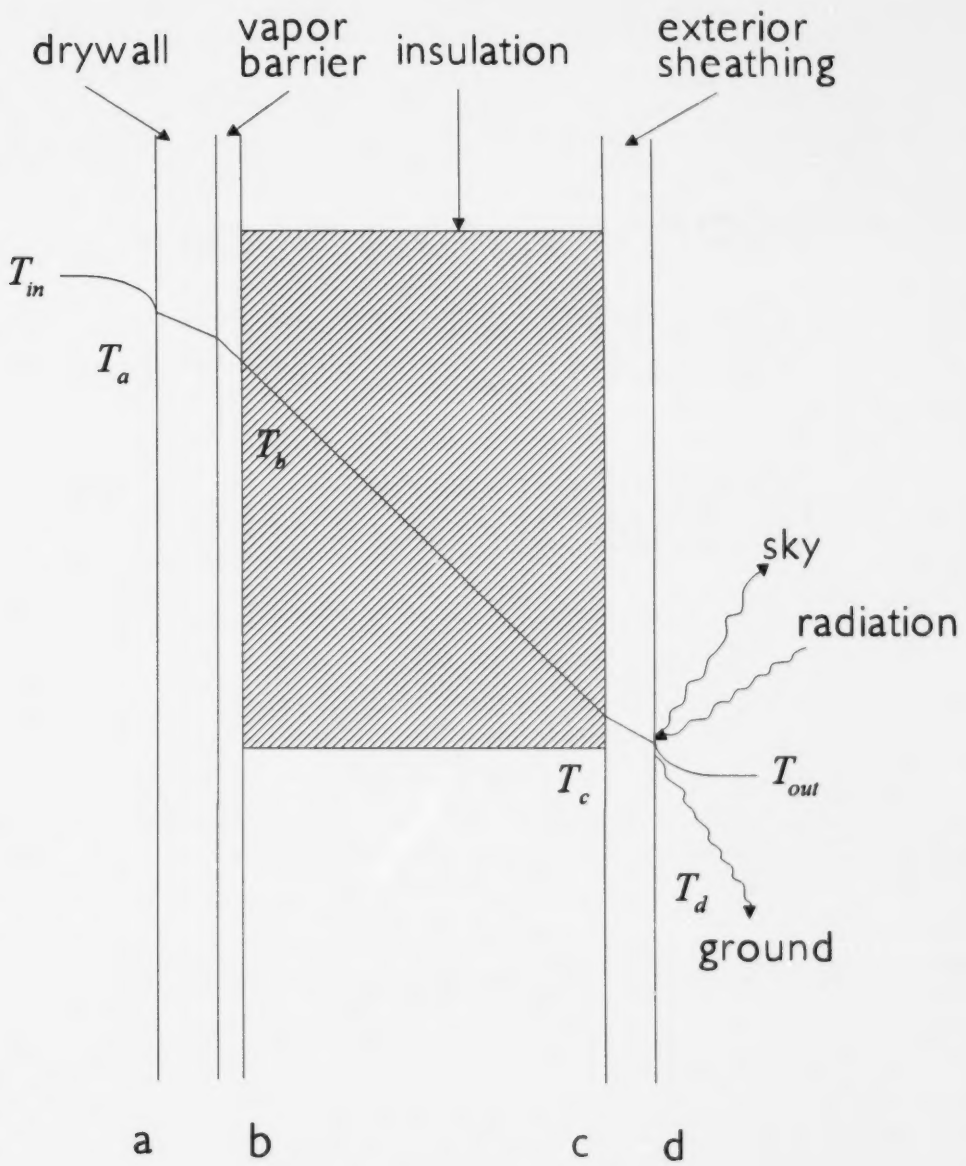

Figure 2-3 **Sources of heat flux throughout the wall cavity for each nodal point.**

Convention for heat flux into a node will be positive and negative for heat flux leaving a node. For node a, the sum of the heat fluxes are due to convection and conduction can be expressed as

$$h_a A_a (T_{in} - T_a) - \frac{A_a}{R_{ab}} (T_a - T_b) = 0 \qquad (2.20)$$

where: h_a convective heat transfer coefficient for node a,

A_a is the cross sectional area,

T_{in} is the indoor temperature,

T_a, T_b are the temperatures at nodes a and b, respectively, and

R_{ab} is the thermal resistance of the drywall between nodes a and b.

The value of the convective heat transfer for node a is the ASHRAE(1989) value based on the assumption for still air on a vertical surface with horizontal heat flux. The thermal resistance of the vapor barrier is assumed to be negligible. The heat fluxes for node b are solely due to conduction and can be expressed as

$$\frac{A_a}{R_{ab}} (T_a - T_b) - \frac{A_b}{R_{bc}} (T_b - T_c) = 0 \qquad (2.21)$$

where R_{bc} is the thermal resistance of the insulation. The heat fluxes at node c are also due to conduction only and can be expressed as

$$\frac{A_b}{R_{bc}}(T_b - T_c) - \frac{A_c}{R_{cd}}(T_c - T_d) = 0 \qquad (2.22)$$

where R_{cd} is the thermal resistance of the exterior sheathing. The heat fluxes at node d are due to conduction, convection and radiation and can be expressed as

$$\frac{A_d}{R_{cd}}(T_c - T_d) + A_d I_{total}\alpha + h_{R,d-sky} A_d (T_{sky} - T_d) + h_{R,d-grnd} A_d (T_{out} - T_d) + h_d A_d (T_{out} - T_d) = 0 \qquad (2.23)$$

where: I_{total} is the total solar radiation on the exterior sheathing,

α is the solar absorptivity of the exterior sheathing,

$h_{R,d-sky}$ is the radiation heat transfer coefficient from node d to the sky,

T_{sky} is the sky temperature,

$h_{R,d-grnd}$ is the radiation heat transfer coefficient from the node d to the ground, and

h_d is the convective heat transfer coefficient for the exterior sheathing.

The total solar radiation which is one of the input parameters to the WMS model includes both the direct and diffuse radiation. The value of the solar absorptivity of the exterior sheathing was chosen to be equal to 0.8 which lies between 0.7 for red brick and 0.9 for

black oil paint. The convective heat transfer coefficient for the exterior sheathing is based on an ASHRAE (1989) mean value of 28.40 W/m °C for any position, moving air at 6.7 m/s in the winter (34.08 W/m °C) and 3.4 m/s in the summer (22.72 W/m °C). The radiation heat transfer coefficients form node d (exterior sheathing) can be defined from node d to the ground and to the sky as

$$h_{R,d-grnd} = \frac{\sigma(T_d + T_{out})(T_d^2 + T_{out}^2)}{\frac{1-\varepsilon}{\varepsilon} + \frac{1}{F_{d-grnd}}} \tag{2.24}$$

$$h_{R,d-sky} = \frac{\sigma(T_d + T_{sky})(T_d^2 + T_{sky}^2)}{\frac{1-\varepsilon}{\varepsilon} + \frac{1}{F_{d-sky}}} \tag{2.25}$$

where: σ is the Stefan-Boltzmann Constant (5.669×10^{-8} W/m^2/K^4),

ε is the long wave emissivity of the exterior sheathing,

F_{d-grnd} is the view factor from the exterior sheathing to the ground,

T_{sky} is the sky temperature which is defined as,

$T_{sky} = T_{out}\left(0.55 + 5.68x10^{-3}\sqrt{P_{w,s}}\right)^{0.25}$ (Parmelee and Aubele, 1952),

F_{d-sky} is the view factor from the exterior sheathing to the sky.

The view factor from the node d to the sky is defined as $F_{d-sky} = 0.5(1 - CCI)$ where CCI is the cloud cover index (Ford, 1982). A value of $CCI = 1$ implies that there is complete cloud cover whereas a value of $CCI = 0$ implies that the sky is clear. Since the two view factors must add up to unity, the view factor from node d to the ground is $F_{d-grnd} = 1 - F_{d-sky}$. Once the energy balances have been determined for nodes a - d, Gaussian elimination is used to solve the Eqns. 2.20 to 2.23 for the four unknowns temperatures, T_a, T_b, T_c, and T_d.

2.2.3.2 Indoor Relative Humidity

Nikel (1991) ran his moisture deposition model using an inlet relative humidity varying from 5 to 100 %, indoor temperature of 20 ° C, outer wall cavity temperature varied from -30 ° C to 10 ° C for a maximum velocity of 0.01 m/s. He showed that for a given wall cavity temperature T_C, there is a minimum RH_{inlet} above which moisture will begin to deposit within the insulation as well as on the sheathing. Since his simplified model could not handle condensation within the insulation, the RH_{inlet} was limited to a specific range of values depending on the value of T_C. This range of values is shown in Fig. 2-4 together with typical measured indoor relative humidity values in Canadian homes as a function of temperature. Since the indoor relative humidity values for the typical Canadian homes below -13.8 $°C$ would result in deposition within the insulation, the WMS model uses indoor relative humidity values which are determined from the limiting values shown in Fig. 2-4.

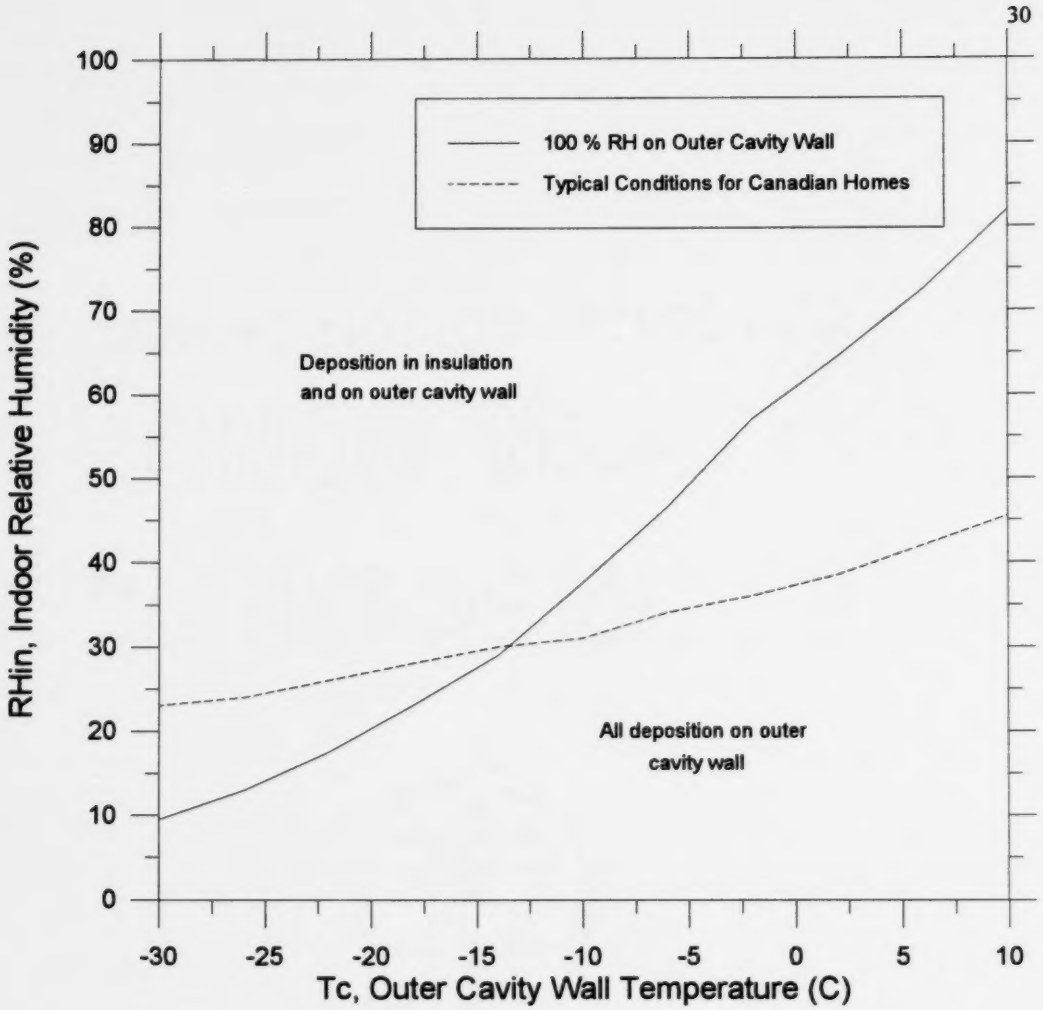

Figure 2-4 Typical mean indoor relative humidites for Canadian homes, Kent et al (1966) superimposed on the region of validity for 100 % relative humidity for the moisture deposition model.

By utilizing the value of ΔP_{ref} which is a function of the leakage characteristics calculated from Walker's ventilation model and coupling this with the moisture deposition model a more comprehensive realistic model has developed. Before the ventilation model and moisture deposition model can be coupled together, the air flow rate through a wall cavity must be determined utilizing the cavity flow model. This is where the WMS model differs from the other moisture deposition models developed to date. The WMS model calculates the air flow rate across the wall cavity based on the leakage configuration of the house and the meteorological data.

2.3 Development of the Cavity Flow Model

The main objective of the cavity flow model is to determine the flow rate across the wall cavity and subsequently determine the air velocity which can then be used as input to the moisture deposition model. The cavity mass flow rate is determined from the overall pressure difference, $P_{O2} - P_{I1}$ as shown in Fig. 2-5 and the characteristics of the leakage path. The expression for the pressure difference $P_{O2} - P_{I1}$ is in terms of the wind effect and stack effect. The derivation of the cavity flow model is first shown for infiltrating flow followed then by a summarized derivation for exfiltrating flow. With the mass flow rate known, the velocity through the insulation can subsequently be determined. The velocity is then used as an input into the Eqn.2.18 and the hourly moisture deposition rate calculated. The cavity flow model is based on the following:

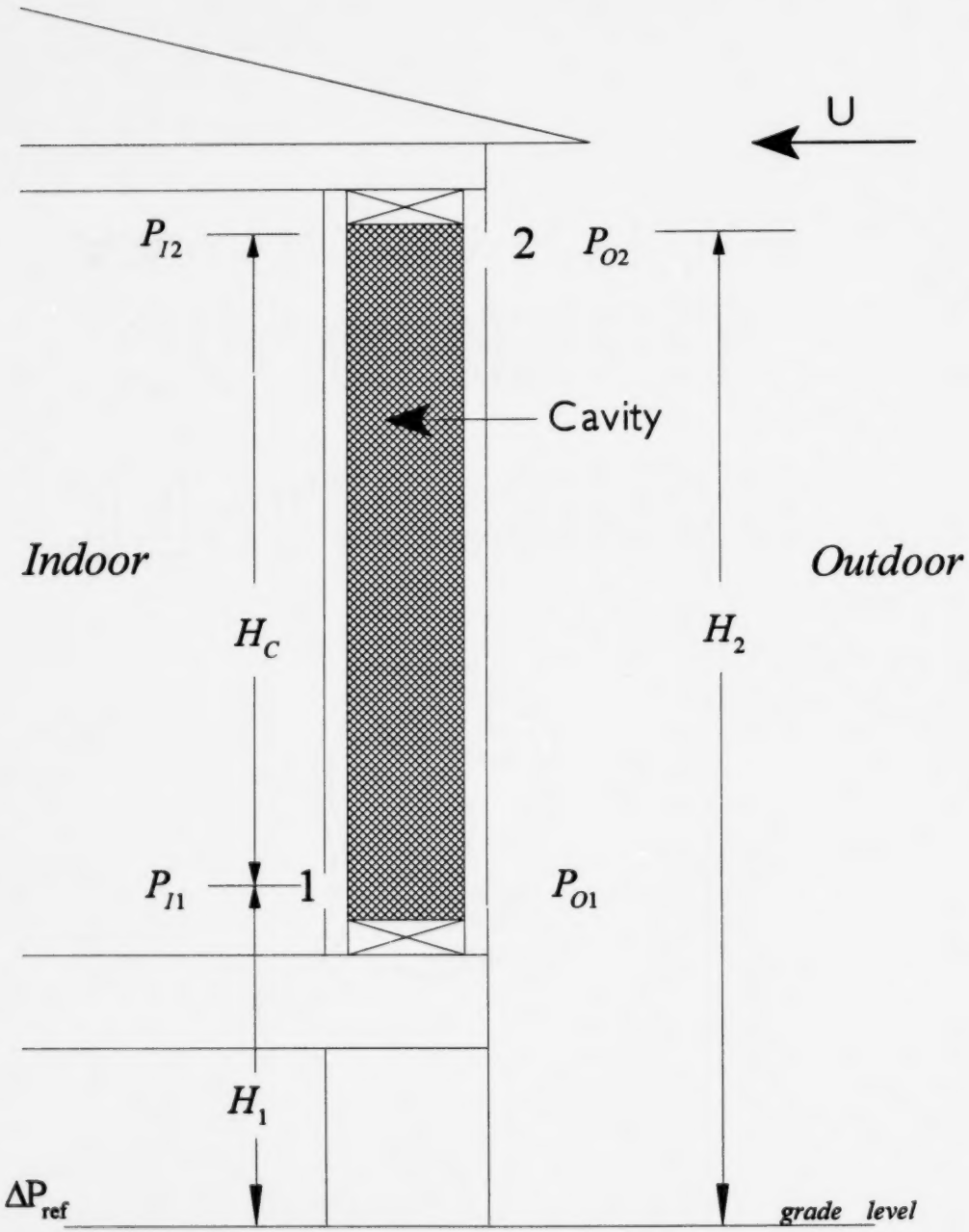

Figure 2-5 **Wall cavity geometry showing the leakage site locations and the various pressure difference locations used in the derivation of the cavity flow model.**

- The air flow leakage path is two dimensional. Air enters horizontally through an inlet slit approximately 2mm high and 368 mm wide, travels vertically through the insulation, and then exits the wall cavity through another slit of similar dimensions into the surrounding ambient conditions.

- The flow through the leakage path is assumed to be either turbulent, developing or laminar flow.
- The amount of leakage through the wall cavity is small compared to the total amount of distributed leakage through the building. Therefore, ΔP_{ref} from the ventilation model can be utilized in the development of the cavity flow model.
- The flow coefficient and flow exponent for the cavity have different values than the building's.
- The absolute temperature throughout the cavity insulation is the mean temperature between the indoor and outdoor temperature. Consequently, the density of the cavity insulation is based upon the cavity mean temperature.

2.3.1 Infiltrating Flow

Recall the expression from Eqn. 2.11 for the pressure distribution across a leakage site i, is a combination of the wind and stack effects.

$$\Delta P_i = \Delta P_{ref} - \Delta P_T H_i + C_{p_i} \Delta P_w S_{w_i}^2$$

$$\text{where } \Delta P_T = \rho_o \, g \left(\frac{T_{in} - T_{out}}{T_{in}} \right), \text{ and}$$

$$\Delta P_w = \frac{\rho_o U^2}{2}$$

Using this expression, the pressure difference for the leakage site at location 2 where the wall cavity meets the ceiling as shown in Fig. 2-5 can be expressed as

$$P_{O2} - P_{I2} = \Delta P_{ref} + C_{p_2} \Delta P_w \, S_w^{\,2} - \Delta P_T \, H_2 \tag{2.29}$$

Here P_{O2} is the pressure at the outside of the site 2 and P_{I2} is the pressure at the inside of the wall cavity at location 2. Similarly, for location 1 at the base of the wall cavity where the floor meets the wall, the expression for the pressure difference across the opening at location site 1 can be expressed as

$$P_{O1} - P_{I1} = \Delta P_{ref} + C_{p_1} \Delta P_w \, S_w^{\,2} - \Delta P_T \, H_1 \tag{2.30}$$

The pressure at locations I1 and I2 or O1 and O2 are related by the hydrostatic terms

$$P_1 = P_2 + \rho g \, H_C \tag{2.31}$$

where ρ is either the indoor density for locations I1 and I2 or outdoor density for locations O1 and O2. The term H_C has been substituted for the height difference $H_2 - H_1$. By substituting the expression for P_{I2} from Eqn. 2.31 into Eqn. 2.29 the expression for P_{O2} becomes,

$$P_{O2} = P_{I1} - \rho_i g H_C + \Delta P_{ref} + C_{p_2} \Delta P_w S_w^2 - \Delta P_T H_2 \tag{2.32}$$

By substituting the expression for P_{O1} from Eqn.2.31 into Eqn. 2.30, P_{I1} becomes,

$$P_{I1} = P_{O2} + \rho_o g H_C - \Delta P_{ref} - C_{p_1} \Delta P_w S_w^2 + \Delta P_T H_1 \tag{2.33}$$

A general expression for the pressure difference across the leakage path in terms of the stack and wind effects can now be obtained by subtracting Eqn. 2.33 from Eqn. 2.32.

$$P_{O2} - P_{I1} = -\left(\frac{\rho_i + \rho_o}{2}\right) g H_C + \Delta P_{ref} - \Delta P_T \left(\frac{H_1 + H_2}{2}\right) + \Delta P_w C_p S_w^2 \tag{2.34}$$

Since the value of ΔP_{ref} is calculated from the ventilation model, the pressure difference in Eqn. 2.34 can be determined.

For a given pressure difference $(P_{o2} - P_{i1})$, the mass flow rate can de calculated if the flow resistance of the leakage path can be characterized. For the path shown in Fig. 2-5, there are three flow resistances in series: the inlet crack at location 2, the cavity filled with porous insulation, and the outlet crack at location 1. The mass flow rate through the leakage path can be calculated by expressing the pressure difference across each resistance in terms of the mass flow rate and equating the sum of the three pressure differences to $(P_{o2} - P_{i1})$. The mass flow through any resistance can be expressed as

$$\dot{m} = \rho C \Delta P^n \tag{2.35}$$

where ρ is the density,

C is the flow coefficient,

ΔP is the pressure difference across the leakage site and,

n is the flow coefficient.

The density term is dependent upon the direction of the air flow through the wall cavity. For infiltrating flow the outdoor density will be used whereas the indoor density will be used for exfiltrating flow. The flow coefficient, C, is determined from the geometry of the inlet and flow characteristics such as density and viscosity. The flow exponent specifies the behavior of the flow through the leakage site. For fully developed flow, $n = 1$, whereas for

turbulent flow $n = 1/2$. Selection of the values for the flow coefficient and flow exponent will be discussed later in this section.

The mass flow rate from the outside at location 2 through the inlet into the wall cavity can be expressed as

$$\dot{m}_C = \rho_o C_2 \left(P_{O2} - P_{C2}\right)^{n_2} \tag{2.36}$$

where P_{O2} is the pressure at the outside of location 2,

P_{C2} is the pressure just after the air enters the cavity at location 2, and

C_2, n_2 are the unknown flow coefficient and flow exponent respectively.

Similarly, the mass flow for an infiltrating flow exiting the cavity and entering the indoor space through inlet 1 can be expressed as

$$\dot{m}_C = \rho_C C_1 \left(P_{C1} - P_{I1}\right)^{n_1} \tag{2.37}$$

where ρ_C is the density of air within the cavity,

P_{C1} is the pressure just after the air enters the cavity at location 1,

P_{I1} is the inside of the house at location 1, and

C_1, n_1 are the unknown flow coefficient and flow exponent respectively.

Finally, in order to consider the mass flow through the insulation of the cavity wall we must first review the governing equation for flow through a porous medium.

In fluid mechanics of porous medium, the momentum or force balances can be summarized mathematically by the Darcy Law (Bejan 1984). Since the velocity flows only in the y direction the expression for velocity from the Darcy Law in the presence of a body force (gravity) is expressed as,

$$v = \frac{K}{\mu}\left(-\frac{dP}{dy} - \rho g\right) \tag{2.38}$$

where K is the permeability of the insulation and μ is the viscosity of air seeping through the porous material . For infiltrating flow traveling in the negative y direction Eqn. 2.38 becomes

$$v = \frac{K}{\mu}\left(\frac{dP}{dy} + \rho g\right) \tag{2.39}$$

This form of Darcy's Law assumes that the velocity v is uniform across the cross-sectional area of the wall cavity. (i.e. plug flow through the insulation). Integrating Eqn. 2.39 over the height of the wall cavity height the expression for the velocity in the y direction in terms of pressure difference becomes

$$v = \frac{K}{\mu_c H_c}\left[(P_{c2} - P_{c1}) + \rho g H_c\right] \tag{2.40}$$

The mean temperature of the cavity will be used to determine the variations in density and viscosity with temperature. The mean temperature of the cavity is the mean value of outdoor and the indoor temperatures. Using the power law to account for variations in viscosity with temperature , the viscosity of the air within the cavity can be determined as follows (Wilson 1994)

$$\frac{\mu_c}{\mu_{ref}} = \left(\frac{T_C}{300}\right)^1 \tag{2.41}$$

where μ_{ref} is the reference viscosity = 1.98 x 10^{-5} (Ns/m^2) at $T_{ref} = 300\ K$, and

T_C is the mean cavity temperature.

To determine the variation in the air density with temperature within the cavity, the ideal gas equation is used assuming a constant pressure. A simple ratio between the unknown density and the reference density, ρ_{ref} is used to determine the density of the cavity.

$$\frac{\rho_C}{\rho_{ref}} = \frac{293}{T_C} \tag{2.41}$$

The mass flow rate within the wall cavity can now be determined knowing the values of the density and viscosity within the cavity. Using the expression derived for the velocity from Eqn. 2.40, the mass flow through the porous medium within the cavity is,

$$\dot{m}_C = \frac{\rho_C A_C K}{\mu_C H_C}\left[(P_{C2} - P_{C1}) + \rho_C g H_C\right] \tag{2.42}$$

By equating mass flows in Eqns. 2.36 and 2.37, the pressure difference across the outlet at location 1 becomes

$$P_{C1} - P_{I1} = \left(\frac{\rho_o C_2}{\rho_C C_1}\right)^{1/n_1} (P_{O2} - P_{C2})^{n_2/n_1} \tag{2.43}$$

Similarly, by equating the mass flows in Eqns. 2.37 and 2.42 the pressure difference within the cavity between inlets 1 and 2 becomes,

$$P_{C2} - P_{C1} = \frac{C_1 \mu_C H_C}{A_C K}(P_{C1} - P_{I1})^{n_1} - \rho_C g H_C \tag{2.44}$$

Subtracting P_{I1} from both sides, Eqn. 2.44 becomes,

$$P_{C2} - P_{I1} = P_{C1} - P_{I1} + \frac{C_1 \mu_C H_C}{A_C K}(P_{C1} - P_{I1})^{n_1} - \rho_C g H_C \tag{2.45}$$

Now, by substituting the expression from Eqn. 2.43 for the pressure difference $P_{C1} - P_{I1}$ into Eqn. 2.45 an expression for the pressure difference ($P_{O2} - P_{I1}$) across the wall cavity can be expressed as,

$$P_{O2} - P_{I1} = (P_{O2} - P_{C2}) + \left(\frac{\rho_o C_2}{\rho_C C_1}\right)^{1/n_1} (P_{O2} - P_{C2})^{n_2/n_1} + \frac{C_2 \mu_C H_C \rho_o}{A_C K \rho_C} (P_{O2} - P_{C2})^{n_2} - \rho_C g H_C \tag{2.46}$$

By equating the expression for the pressure difference $P_{O2} - P_{I1}$ across the leakage path from Eqn. 2.34 with the pressure difference, $P_{O2} - P_{I1}$ from Eqn. 2.46 in terms of the mass flow rates, a general expression for the pressure difference across the wall cavity can be determined and expressed as,

$$(\Delta P_{OC2}) + \left(\frac{\rho_o C_2}{\rho_C C_1}\right)^{1/n_1} (\Delta P_{OC2})^{n_2/n_1} + \frac{C_2 \mu_C H_C \rho_o}{A_C K \rho_C} (\Delta P_{OC2})^{n_2} - \Delta P_{inf} = 0 \tag{2.47}$$

where ΔP_{OC2} is $P_{O2} - P_{C2}$

$$\Delta P_{inf} = \Delta P_{ref} - \Delta P_T \left(\frac{H_1 + H_2}{2}\right) + \Delta P_w C_p S_w^2 \tag{2.48}$$

It should be noted that the C and n values in Eqn. 2.47 depend on the flow rate through the wall cavity which depends on ΔP_{OC2}. The evaluation of C and n will be discussed in

Sec. 2.3.3. Thus for a given C and n Eqn. 2.47 is nonlinear and the unknown quantity ΔP_{OC2} of Eqn. 2.47 is solved using Newton's method. Once the unknown quantity ΔP_{OC2} has been determined, the mass flow can be calculated by substituting the value for ΔP_{OC2} back into Eqn. 2.36.

2.3.2 Exfiltrating Flow

The derivations for determining the pressure difference across the cavity wall for exfiltrating flow are exactly the same as those for infiltrating flow. The mass flow equations across leakage site 2, site 1, and through the insulation are respectively,

$$\dot{m}_C = \rho_C C_2 (P_{C2} - P_{O2})^{n_2}, \tag{2.49}$$

$$\dot{m}_C = \rho_i C_1 (P_{I1} - P_{C1})^{n_1}, \text{ and} \tag{2.50}$$

$$\dot{m}_C = \frac{\rho_C A_C K}{\mu_C H_C}\left[(P_{C1} - P_{C2}) - \rho_C g H_C\right] \tag{2.51}$$

Equating the mass flow equations (2.49) and (2.50) an expression for the pressure across the cavity wall at location 1 becomes

$$P_{I1} - P_{C1} = \left(\frac{\rho_C C_2}{\rho_i C_1}\right)^{1/n_1} (P_{C2} - P_{O2})^{n_2/n_1} \tag{2.52}$$

Now equating the mass flow Eqns. 2.50 and 2.51 the pressure difference between locations I1 and C2 becomes,

$$P_{I1} - P_{C2} = P_{I1} - P_{C1} + \frac{C_1 \mu_C H_C \rho_i}{A_C K \rho_C} (P_{I1} - P_{C1})^n + \rho_C g H_C \qquad (2.53)$$

Substituting the expression for the pressure difference $P_{I1} - P_{C1}$ across leakage site 1 from Eqn. 2.52 into Eqn. 2.53 will yield the expression for the pressure difference across the leakage path.

$$P_{I1} - P_{O2} = (P_{C2} - P_{O2}) + \left(\frac{\rho_C C_2}{\rho_i C_1}\right)^{1/n_1} (P_{C2} - P_{O2})^{n_2/n_1} + \frac{C_2 \mu_C H_C}{A_C K} (P_{C2} - P_{O2})^{n_2} + \rho_C g H_C$$

(2.54)

For exfiltrating flow, the expression for the pressure difference $P_{I1} - P_{O2}$ is,

$$P_{I1} - P_{O2} = \left(\frac{\rho_i + \rho_o}{2}\right) g H_C - \Delta P_{ref} + \Delta P_T \left(\frac{H_1 + H_2}{2}\right) + \Delta P_w C_p S_w^2 \qquad (2.55)$$

Equating Eqns. 2.54 and 2.55 for the pressure difference $P_{I1} - P_{O2}$ across the cavity wall results in the following expressions,

$$(\Delta P_{CO2}) + \left(\frac{\rho_C C_2}{\rho_I C_1}\right)^{1/n_1} (\Delta P_{CO2})^{n_2/n_1} + \frac{C_2 \mu_C H_C}{A_C K} (\Delta P_{CO2})^{n_2} - \Delta P_{ex} = 0 \qquad (2.56)$$

where: ΔP_{CO2} is $P_{C2} - P_{O2}$

$$\Delta P_{ex} = -\left(\Delta P_{ref} - \Delta P_T \left(\frac{H_1 + H_2}{2}\right) + \Delta P_w C_p S_w^{\,2}\right) \qquad (2.57)$$

The mass flow rate for exfiltrating flow can be determined by solving for ΔP_{CO2} using Newton's method and substituting the value of ΔP_{CO2} back into Eqn. 2.49.

2.3.3 Determination of the Flow Coefficients and Flow Exponents

The flow coefficient and exponent describing the resistance of the inlet and outlet cracks are dependent on the nature of the flow (i.e. whether the flow is laminar, turbulent, fully developed or developing). For a given crack geometry, the C and n will therefore depend on the mass flow rate through the wall cavity. Thus, the solution to Eqns. 2.47 and 2.56 requires iteration where an initial guess is made for C and n and then verified by checking the flow regime.

The flow exponent n, must first be determined since the flow coefficient C, is dependent upon its value. Kreith and Eisenstadt (1957) performed an experiment to determine the pressure drop and flow characteristics of short capillary tubes at low Reynolds numbers. The inlet cracks of the wall cavity were assumed to behave in a similar manner as the short capillary tubes. The length to diameter (L/d) ratios ranged from 0.45 to 18 at diameter Reynolds numbers ranging from 8 to 1500. The air flow rate was plotted against the pressure drop for each (L/d) ratio and the corresponding slope was the flow exponent. With the flow exponent known, a relationship between the flow exponent and the corresponding (L/d) ratio can be determined as shown in Fig. 2-6. This figure is very useful in determining the flow exponent for a given (L/d) geometry. Unfortunately, this leads to two further problems. One problem is that the (L/d) ratio is not known for a given leakage site and secondly, the flow coefficient is difficult to calculate for intermediary values of n. By assuming a (L/d) ratio of 5 and using three intermediary values of $n = 1/2,\ 2/3$, and 1 the corresponding flow coefficients can be calculated. The value of the (L/d) changes for differing values of flow exponents but a (L/d) ratio of 5 will be assumed to be constant regardless of the value of the flow exponent. This is based on the assumption that the geometry of the leakage path throughout the wall cavity is seldom straight from the leakage site to the surrounding environment but rather is complex changing directions several times across the cavity wall.

The air flow rate is first determined based on an initial guess that $n = 2/3$ for the flow exponent. Jones (1987) calculated the relationship for the flow for $n = 2/3$ from the

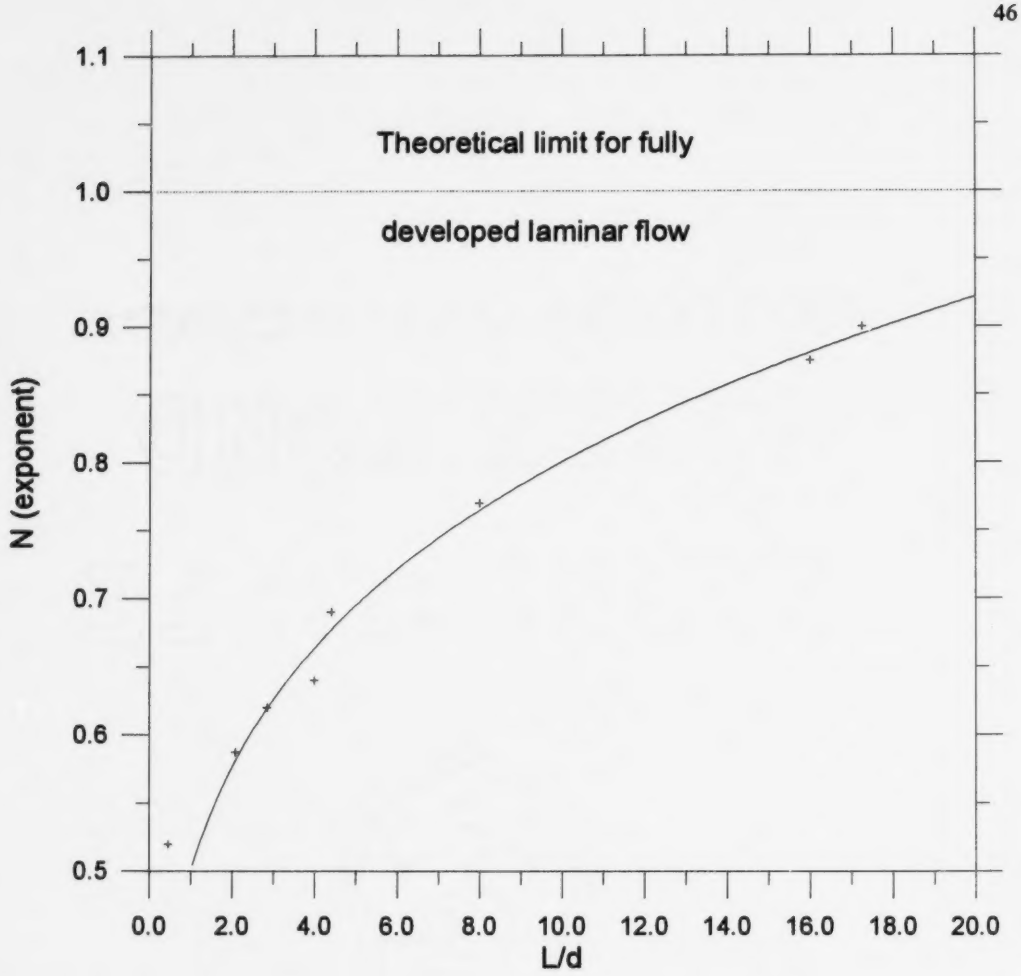

$$n = 0.5005\left(\frac{L}{d}\right)^{0.2038}$$

Figure 2-6 **Flow exponents for various length to diameter ratios of short capillary tubes at low Reynolds Numbers.**

experimental results of Shapiro, Siegel and Kline (1954). The expression for the flow rate in a tube when n=2/3 is

$$Q = \left(\frac{\pi^3 D^8}{16 \rho \mu k^2 L} \right)^{1/3} \Delta P^{2/3} \tag{2.58}$$

where: D is the diameter of the tube,

ρ, μ are the density and viscosity of the air ,

k is an experimental constant equal to 13.74,

L is the length of the tube and,

ΔP is the pressure drop along the tube from the entrance to the axial distance L.

Replacing the term for the tube's diameter in equation (2.58) with the hydraulic diameter for a two-dimensional crack and recalling that (L/d)=5, Eqn. 2.58 can now be expressed as,

$$Q = \left(\frac{0.2628(wh)^7}{\rho \mu (w+h)^7} \right)^{1/3} \Delta P^{2/3} \tag{2.59}$$

where: w is the width and h is the height of the leakage crack, and

$\left(\frac{0.2628(wh)^7}{\rho\mu(w+h)^7}\right)^{1/3}$ is the expression for the flow coefficient for $n = 2/3$.

After solving for the mass flow rate based on $n = 2/3$ the Reynolds number based on the hydraulic diameter is calculated . If the value of the ratio of(L/d) to the Reynolds number falls within the limits

$$10^{-3} \rangle \left(\frac{L}{d\,\mathrm{Re}}\right) \rangle 10^{-5} \tag{2.60}$$

then the assumption was correct and n=2/3. However, if the value of the ratio is greater that 10^{-3} than the flow is approaching laminar flow and the mass flow rate is then recalculated for a flow exponent equal to 1. The expression for the flow rate in a tube for laminar flow is

$$Q = \left(\frac{\pi R^4}{8\mu L}\right)\Delta P \tag{2.61}$$

where: R is the radius and L is the length of the tube,

μ is the viscosity, and

ΔP is the pressure drop along the distance L of the tube.

Replacing the radius term with the hydraulic radius Eqn. 2.61 can be expressed now for non circular geometries as

$$Q = \left(\frac{\pi (wh)^3}{640 \mu (w+h)^3} \right) \Delta P \tag{2.62}$$

where: w is the width and h is the height of the leakage crack, and

$\frac{\pi (wh)^3}{640 \mu (w+h)^3}$ is the expression for the flow coefficient.

If the value of the ratio is less than 10^{-5} then the flow is approaching turbulent flow and the process is repeated using a flow exponent equal to 1/2. For turbulent flow the flow coefficient is equal is equal to 1/2 which corresponds to flow through an obstructed opening. From White (1986) the expression for flow as a function of pressure drop is expressed as

$$Q = C_d A_1 \left(\frac{2 \Delta P}{\rho (1 - \beta^4)} \right)^{1/2} \tag{2.63}$$

where: C_d is the discharge coefficient,

A_t is the area at the throat (inlet),

ρ is the density of the air flow,

ΔP is the pressure drop across the inlet, and

β is the ratio of the obstruction diameter to the upstream diameter .

The density of the air flow depends on whether the flow is infiltrating or exfiltrating. When the upstream diameter is much greater that the obstruction diameter, $\beta = 0$. Rearranging the terms in Eqn. 2.63 and by setting $\beta = 0$ the expression for the flow rate becomes,

$$Q = \left(\left(\frac{2}{\rho} \right)^{1/2} A \right) \Delta P^{1/2} \tag{2.64}$$

where: $\left(\frac{2}{\rho} \right)^{1/2} A$ is the expression for the flow coefficient for $n = 1/2$.

Note that the area A is the product of the discharge coefficient and the inlet area.

Once the flow coefficient and flow exponent have been determined the mass flow rate can be determined using Eqn. 2.36 or 2.49. The velocity of the air through the wall cavity is then calculated by dividing the mass flow rate from Eqn. 2.36 by the product of the density and cavity cross-sectional area.

2.4 Implementation of the WMS Model

The WMS model divides the wall cavity into 40 equal zones with each zone being less than 5 cm in height. Zone number 1 is the bottom zone which is adjacent the interior leakage crack at the junction where the floor and wall meet. The zone numbers sequentially range from 1 to 40 with zone 40 being adjacent the exterior leakage crack where the ceiling and wall meet. If the leakage path height is reduced and the zone height is calculated to be less than 1 cm then the WMS model reduces the number of zones from 40 to 23. The zone height was chosen to be a maximum of 5 cm in order to compare results from the WMS model with the moisture deposition model. Nikel (1991) used a 5 cm zone height to compare the predicted values from his moisture deposition model with the actual values of moisture deposited which were cut out of the exterior sheathing each 5 cm in diameter.

The WMS model calculates the hourly moisture deposition rate which is then used to determine the moisture content and surface moisture accumulation for each zone along the wall cavity as shown in Fig. 2-8. This figure also shows the major components of the WMS model including the contribution of the ventilation, moisture deposition and cavity flow models. When moisture is deposited in a zone it is assumed to be distributed uniformly over the height and width of that zone. The moisture is also assumed to be absorbed instantaneously increasing the moisture content of the exterior sheathing. Once the exterior sheathing reaches its saturation point, moisture then deposits on the surface of the sheathing.

However, before the moisture deposition rate can be calculated, two important questions must be addressed. The first questions deals with the relationship between the moisture content (MC), temperature, T_C and the vapor pressure, $P_{w,c}$ and the second questions deals with which value of $P_{w,c}$ should be chosen (i.e which zone should used). Chapter 3 will discuss these two questions in detail.

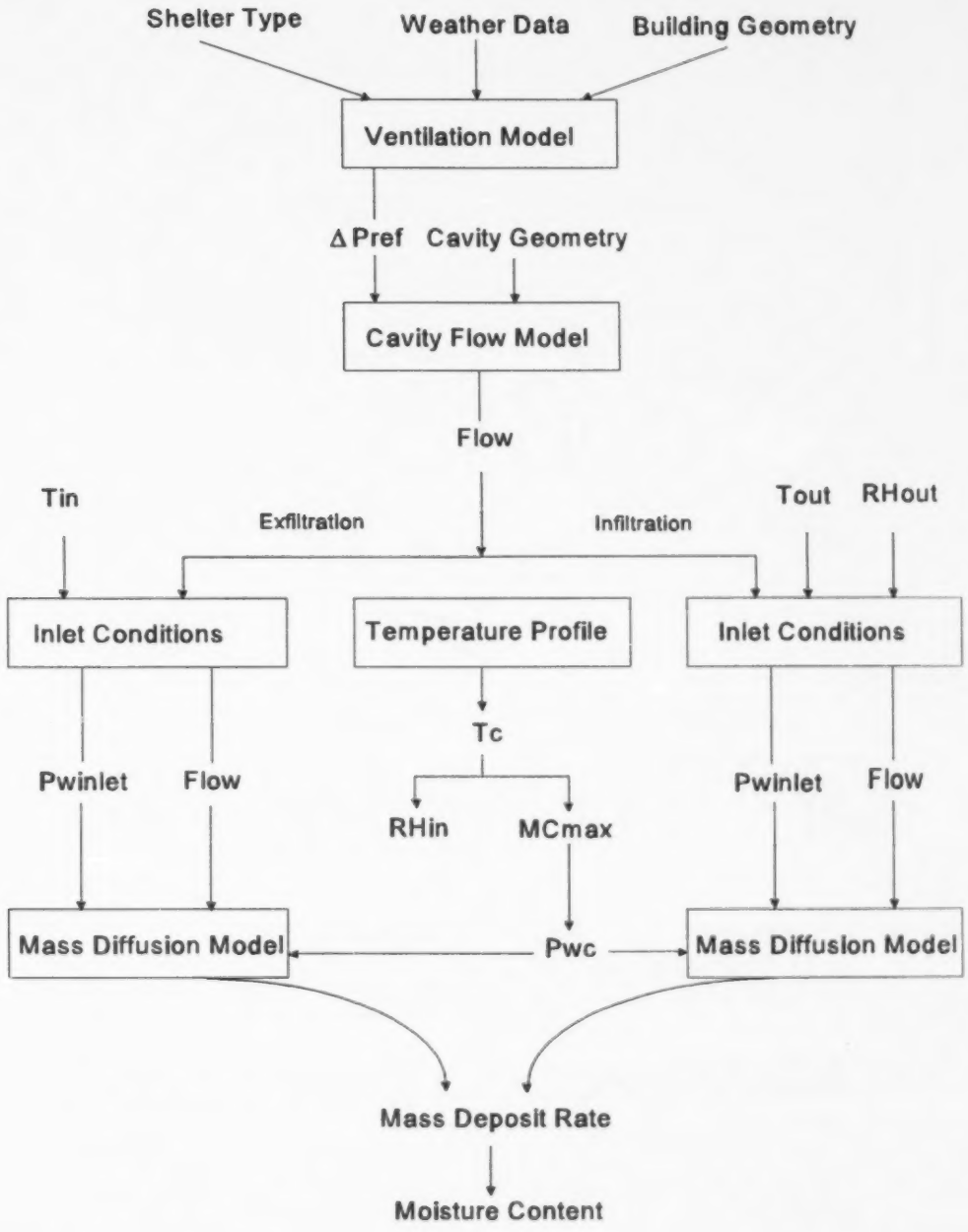

Figure 2-7 Flow chart showing the major components of the Wall Moisture Simulation Model.

Chapter
THREE

VAPOR PRESSURE FOR WOOD SHEATHING

Before the WMS simulation model can be used, there are two important questions to be resolved. The first deals with the relationship between the vapor pressure $P_{w,c}$, moisture content (MC), and temperature for wood. As moisture is deposited or removed from the exterior sheathing, the moisture content of the sheathing changes resulting in a change in the value of $P_{w,c}$ which changes the flux of moisture to or from the sheathing. At temperatures above 0 ° C, the relationship between $P_{w,c}$, MC, and temperature has been measured and the results have been described by the correlation developed by Cleary (1985). However, for temperatures below 0 ° C, there are no measured data for this relationship. The first part of this chapter discusses two alternatives for the relationship between $P_{w,c}$, MC, and temperature below 0 ° C.

The second question deals with the appropriate value of $P_{w,c}$ to be used in the moisture deposition model. Recall, that the moisture deposition model developed by Nikel (1991) requires that the cold surface of the exterior sheathing have a uniform vapor pressure. However, when moisture is initially deposited on the sheathing, the moisture content will not be uniform over the height of the wall cavity because the flux of vapor to the cold sheathing varies with height (as given by Eqn. 2.18). This implies that the vapor pressure $P_{w,c}$ will vary with height. Two alternatives for choosing the value of $P_{w,c}$ are compared using the WMS model to generate yearly simulations. In the first analysis the

values for the vapor pressure $P_{w,c}$, are obtained by extrapolating Cleary's expression for temperatures below 0 ° C. The second alternative utilizes the same procedure as the base case model for determining the vapor pressure but utilizes the arithmetic average moisture value as the input for moisture content into the expression for the vapor pressure, $P_{w,c}$.

3.1 Base Case Simulation

The absorption characteristics of wood sheathing is given Cleary's empirical expression for the vapor pressure for values of temperature above 0 ° C ,

$$P_{w,c} = \frac{P_{atm}}{0.622} \exp\left(\frac{T_C}{15.8\,^\circ C}\right)\left(-0.0015 + 0.053\,MC - 0.184\,MC^2 + 0.233\,MC^3\right)$$

The input variables into this expression are the temperature T_C , which is the temperature between the insulation and the exterior sheathing and the moisture content. For temperature (T_C) values below 0 ° C the base case method assumes that the moisture content is constant for a given value of relative humidity as shown in Fig. 3-1 . Physically this implies that water absorbed within the cell walls for temperatures below 0 ° C for a given relative humidity is assumed to be constant[1]. The cell walls will not absorb any additional moisture unless the relative humidity increases.

---

[1] Wood is composed of hollow cells and the cell walls are made of cellulose. Moisture is first absorbed in the cell walls until it reaches saturation beyond which excess moisture appears as free water inside the hollow cell.

For the base case simulation, the meteorological data for Winnipeg was chosen for its extremes in indoor-outdoor temperature. The wall cavity and building geometry used in all simulations ran can be seen in Fig. 3-11 and Table 3-1.

3.2 Alternative Model for $P_{w,c}$ Below 0° C

An alternative model for the vapor pressure of wood below 0 ° C, results from a simple extrapolation of Cleary's correlation below 0° C. These extrapolated values are shown in Fig. 3-1 as the dashed curve for a given relative humidity. Physically, this model predicts that as the temperature decreases (below 0 ° C) moisture that is bound in the cell wall is forced out and ultimately some of this moisture appears as unbound water inside the cell. For example, if a wood sample initially at 0° C and a moisture content of 16.5 % (i.e. in equilibrium at a relative humidity of 80 %) were cooled down to -10° C, the cell wall would just reach saturation and corresponding vapor pressure of 260 Pa. A further reduction in the temperature to -20 ° C would reduce the moisture content in the cell wall to 11 % and the excess amount of moisture would appear as unbound water inside the cell as shown in Fig.3-2. The corresponding vapor pressure would be the saturation pressure value for the given temperature.

The main difference between this model and the previous model (solid line below 0 ° C in Fig. 3-1) is the vapor pressure of the wood at a given moisture content and temperature. In the example above, the first model would predict a vapor pressure of 260 Pa at a moisture content of 16.5 % and temperature of -10 ° C as opposed to 208 Pa for

the second method. For the cavity moisture deposition model, this difference in the vapor pressure will affect the flux of vapor to the exterior sheathing.

In the simulations that were used in this chapter, the inlet vapor pressure, $P_{w,inlet}$ remained constant and only the value of the vapor pressure $P_{w,c}$ changed causing the vapor pressure difference $(P_{w,inlet} - P_{w,c})$ to differ form the base case simulation. As a consequence using the extrapolated method would result in a vapor pressure value that is always lower than the base case method. This results in only a slightly greater vapor pressure difference $(P_{w,inlet} - P_{w,c})$ using the extrapolated method of determining $P_{w,c}$ compared to the base case model as shown in Fig. 3-3. This small increase in the vapor pressure difference $(P_{w,inlet} - P_{w,c})$ results in a marginal increase in the moisture deposition rate as shown in Fig. 3-4. From Fig. 3-5 the behavior of the moisture content profile of zone 1 shows a strong temperature dependency using the extrapolated method of determining the value of $P_{w,c}$ compared to the base case. The difference in the moisture content values of zone 1 between the base case and extrapolated methods can be used to determine the amount of unbound water. Though the maximum amount of the daily averaged surface moisture deposition is less than 1 gram, the daily averaged unbound water for zone 1 can reach values as high as 23 grams as shown if Fig. 3-6.

Though there was only a small difference in the results for the two methods presented, the base case method was chosen as the preferred method for determining the value of $P_{w,c}$. The moisture content profile for the base case seemed to demonstrate a better response to the weather conditions than the extrapolated method increasing with the

onset of colder weather, reaching saturation value during mid winter, and then declining with the onset of warmer weather in the spring. More measurements for the vapor pressure of the wood for temperatures below 0 ° C should be done.

3.3 Average Moisture Content Values

The second question relates to which value of vapor pressure $P_{w,c}$ or (i.e. which zone) should be used. With most of the deposition occurring in zone 1 it would seem reasonable to use the value of the moisture content of zone 1 to determine the value of the vapor pressure, $P_{w,c}$. However, moisture deposition does occur in the other zones along the wall cavity and depending on the flow conditions, the moisture content may for example be greater in zone 40 than zone 1 for any particular time. The moisture content of zone 1 was therefore chosen as input for the moisture content for exfiltrating flow and zone 40 for infiltrating flow. However, since the moisture content of each of the 40 zones is different, it was difficult choosing the appropriate value for the moisture content as the input when determining the value of $P_{w,c}$.

One possible alternative was to use the value of the arithmetic average moisture content of the 40 zones as the input for the moisture content when determining the value for the vapor pressure. Since the value of the average moisture is lower than the moisture content of zone 1 and zone 40, inputting this value into the expression for the vapor pressure, $P_{w,c}$ resulted in a lower value of $P_{w,c}$ and a greater vapor pressure difference ($P_{w,inlet} - P_{w,c}$) as shown in Fig. 3-7. This produced a greater moisture deposition rate as

shown in Fig. 3-8. The result was a significant increase in the moisture deposition rate, which caused an increase in the wood moisture content and surface moisture accumulation as shown in Figs. 3-9 and Fig 3-10, respectively.

Using the arithmetic average moisture content as the input for the moisture when determining the vapor pressure $P_{w,c}$ was not a reasonable approach after examining the moisture content profiles as shown in Fig. 3-9. The moisture content profile using the average moisture content value showed a rapid increase over a short period of time in the fall and early winter. The maximum moisture content was sustained over a substantially longer period than the base case and showed only a 4 % decrease in the moisture content at the end of the simulation during the spring and summer period. This moisture content profile did not seem to reflect the weather conditions for Winnipeg having moderate wind speeds and indoor-outdoor temperatures.

Having chosen zone 1 for exfiltrating flow and zone 40 for infiltrating as the values for the moisture content when calculating the value of the vapor pressure $P_{w,c}$, the mass deposition rate will now be determined for five different climatic regions across Canada in Chapter 4.

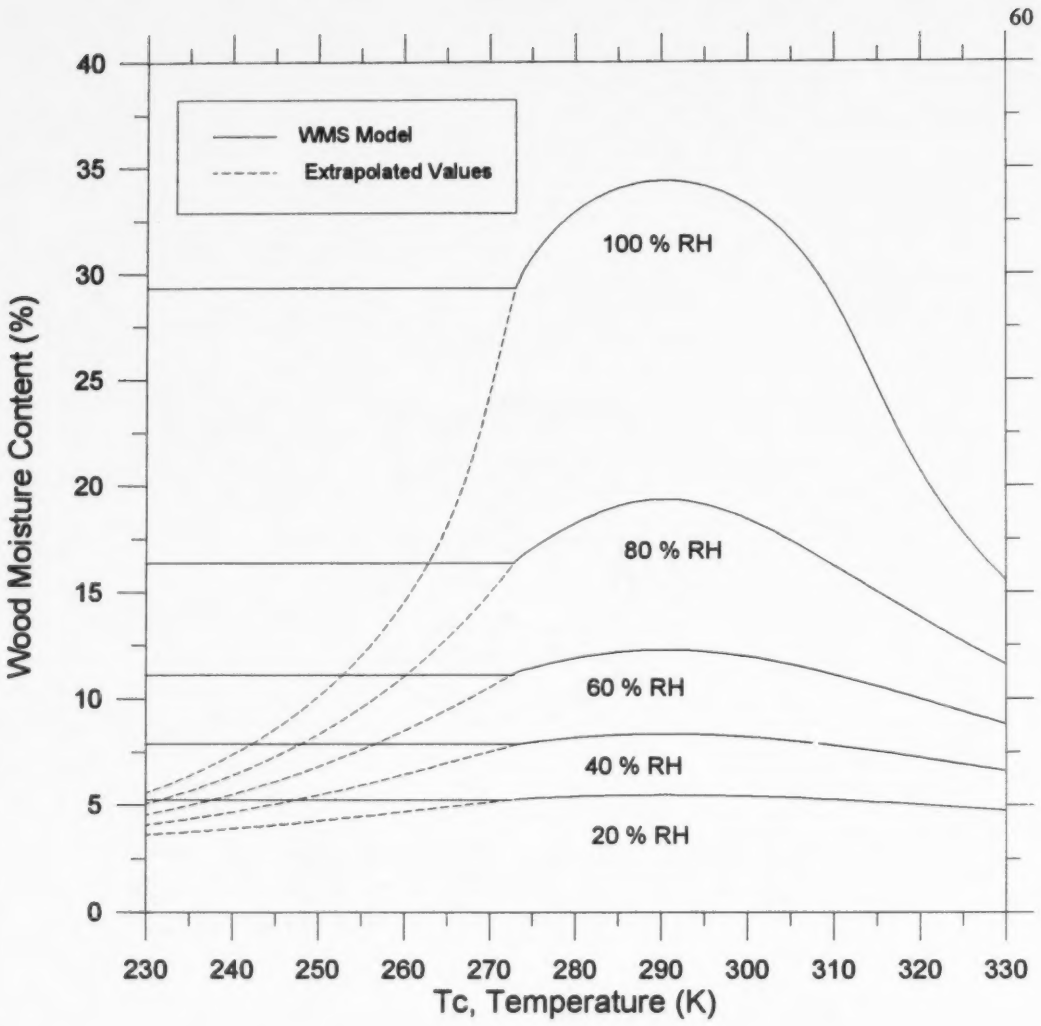

Figure 3-1 Vapor pressure of wood as a function of the temperature and moisture content for various relative humidites.

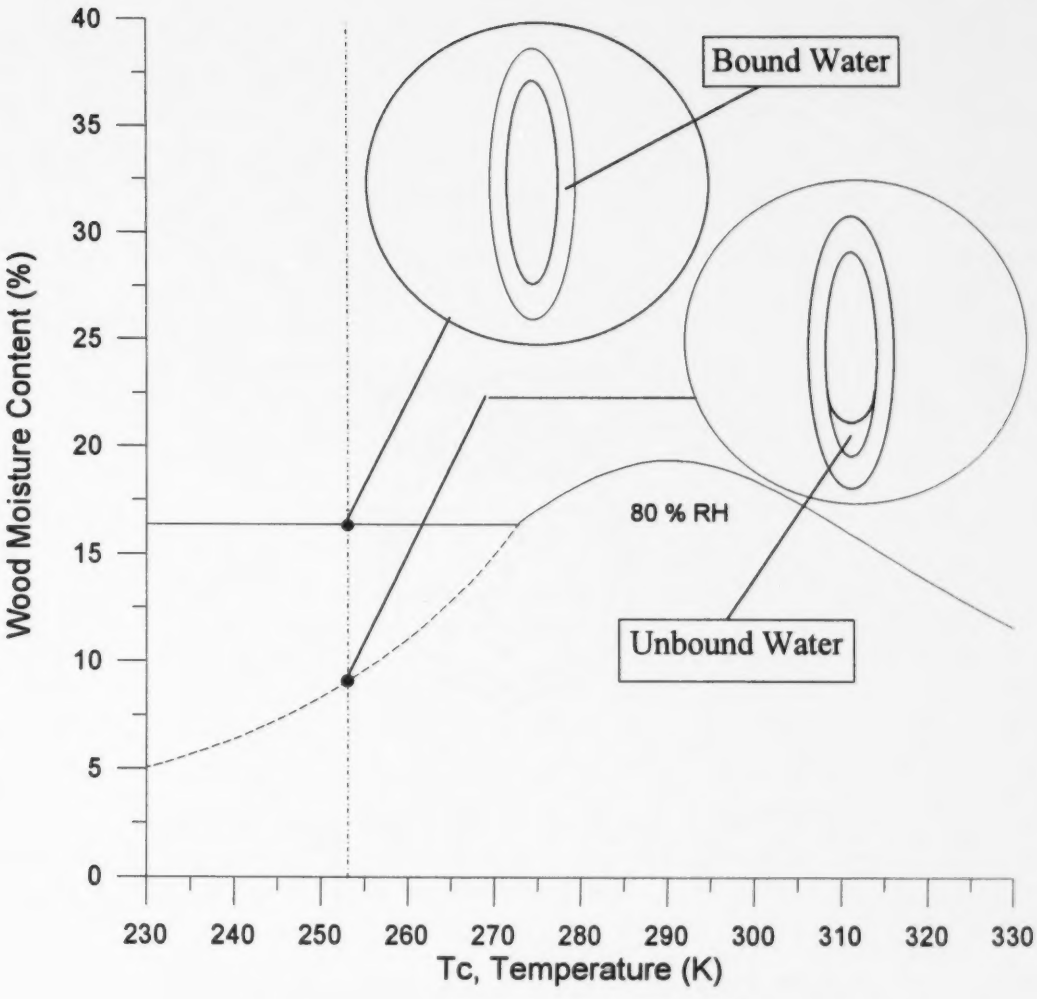

Figure 3-2 Schematic showing the moisture bound within the cell walls for Tc = - 20 °C for a constant moisture content and a moisture content calculated using Clearly's expression for vapor pressure.

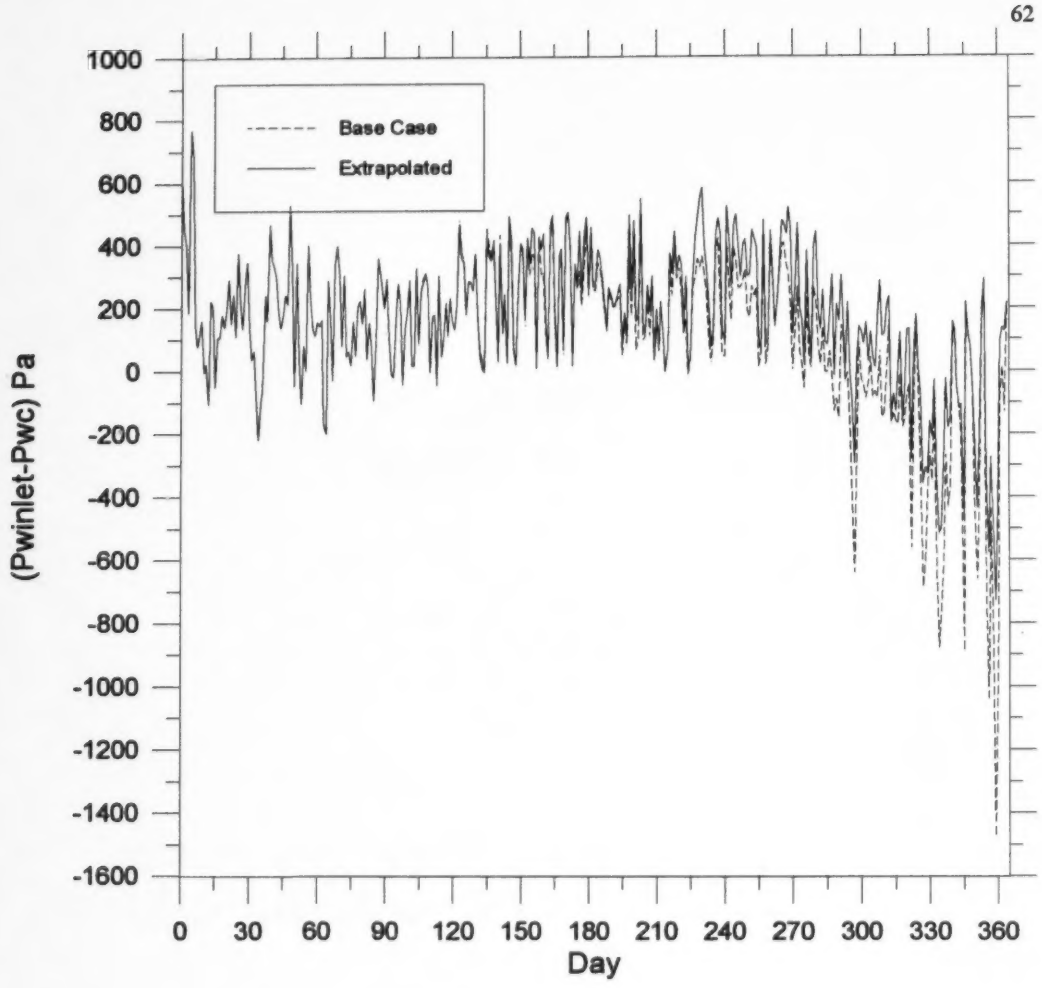

Figure 3-3 Comparison of the daily averaged vapor pressure difference (Pwinlet-Pwc) over a 1 year period (July-June) in Winnipeg for the base case and extrapolated values methods of determining the vapor pressure, Pwc.

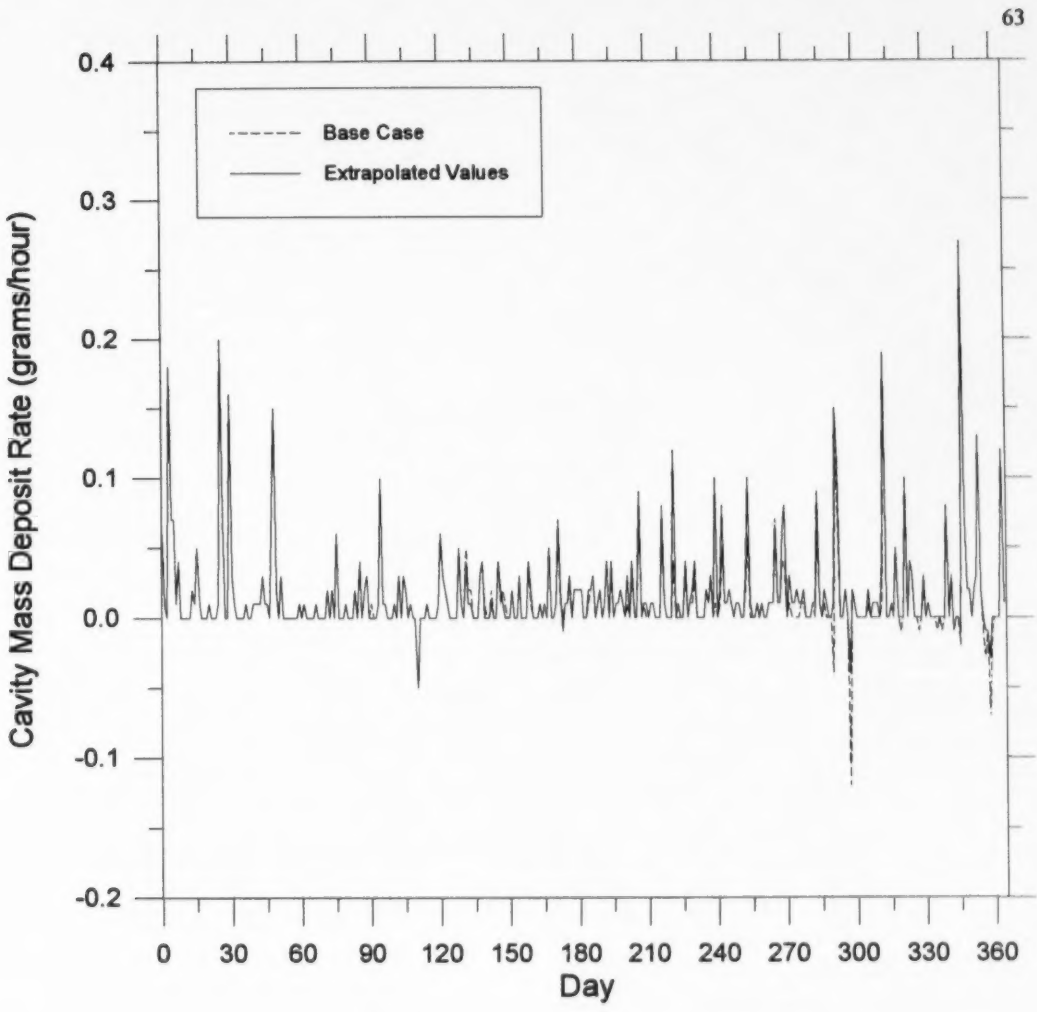

Figure 3-4 Comparison of the daily averaged cavity mass deposit rate for the base case method and the extrapolated values method over a 1 year period (July-June) in Winnipeg.

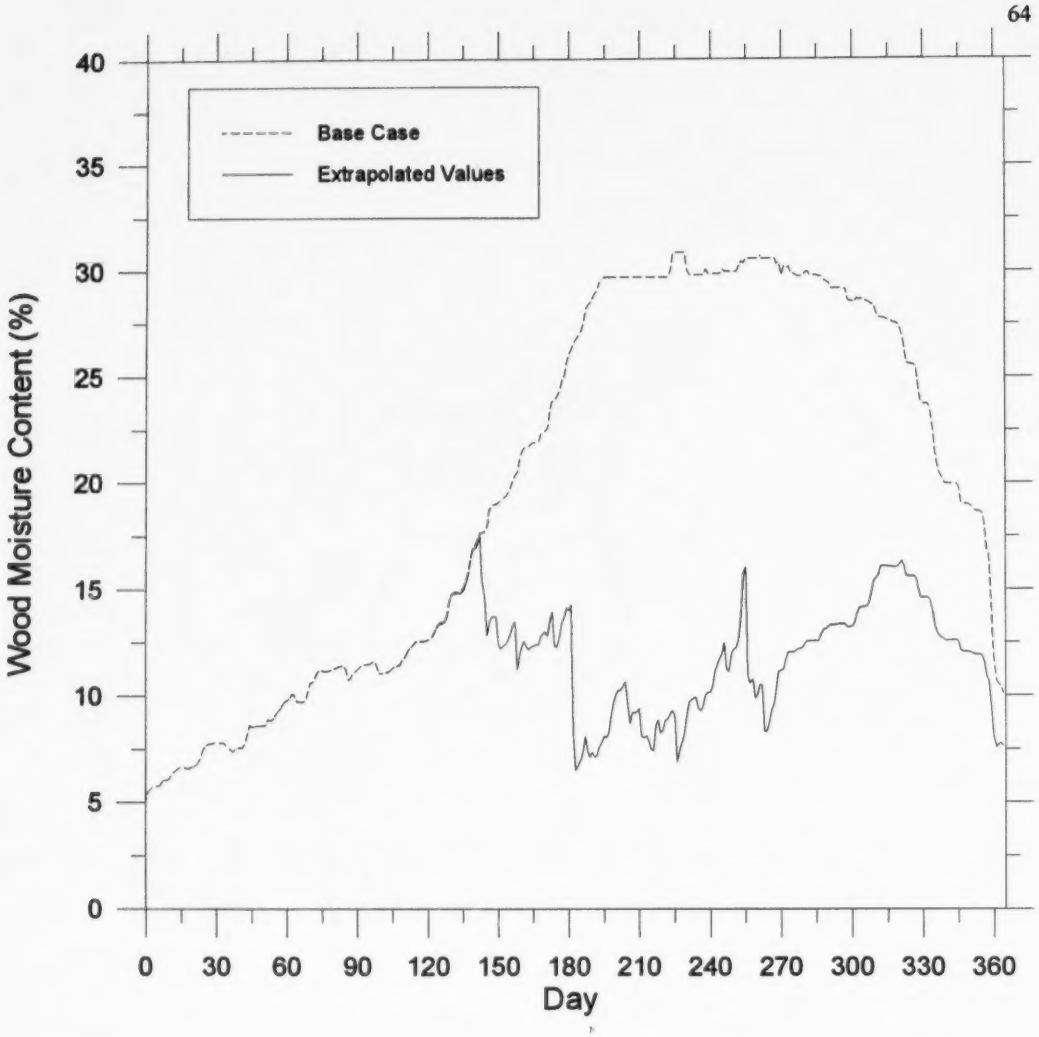

Figure 3-5 Comparison of the daily averaged moisture content of zone 1 over a 1 year period (July-June) in Winnipeg for the base case and extrapolated values method of determining the vapor pressure using Cleary's expression.

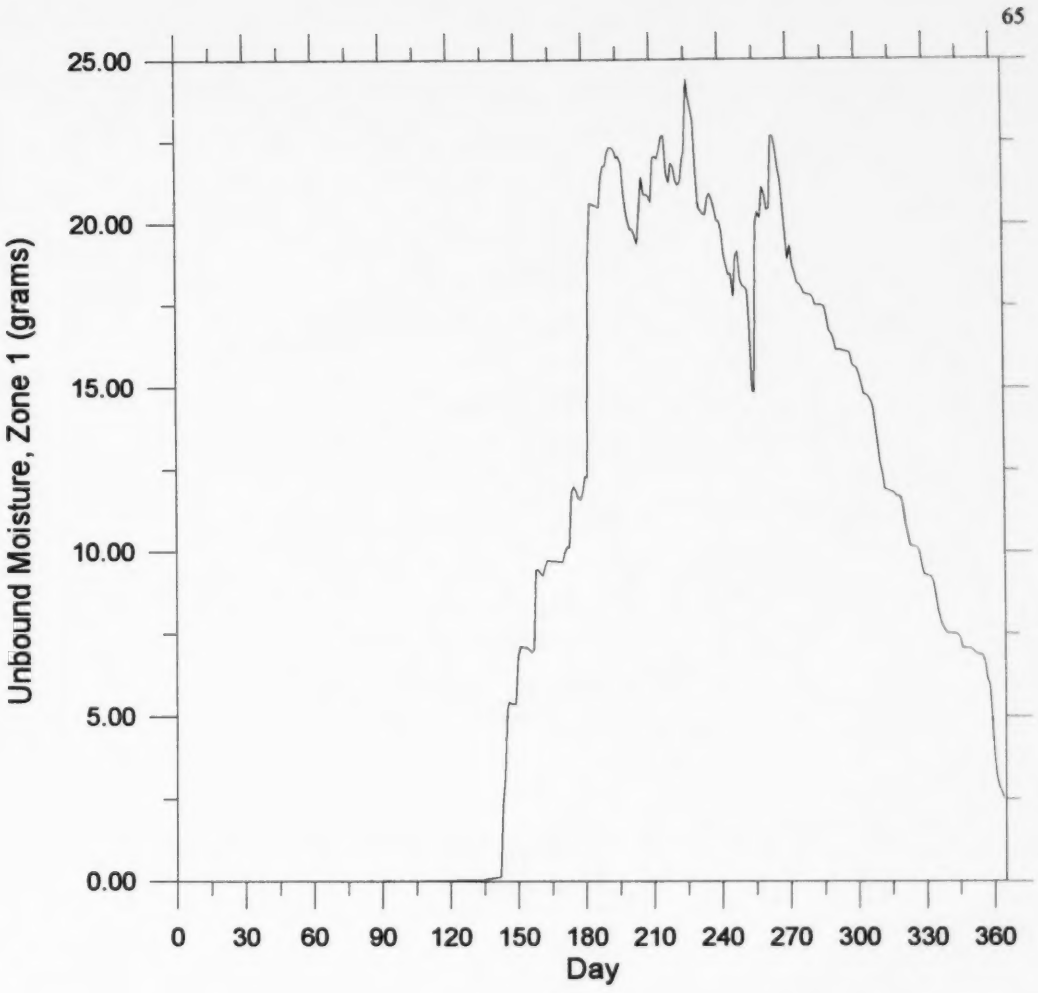

Figure 3-6 Daily average unbound moisture within the cell walls for zone 1 over a 1 year period (July-June) in Winnipeg. Surface moisture accumulation is uniformly distributed over zone 1 which is 50 mm high and 368 mm wide.

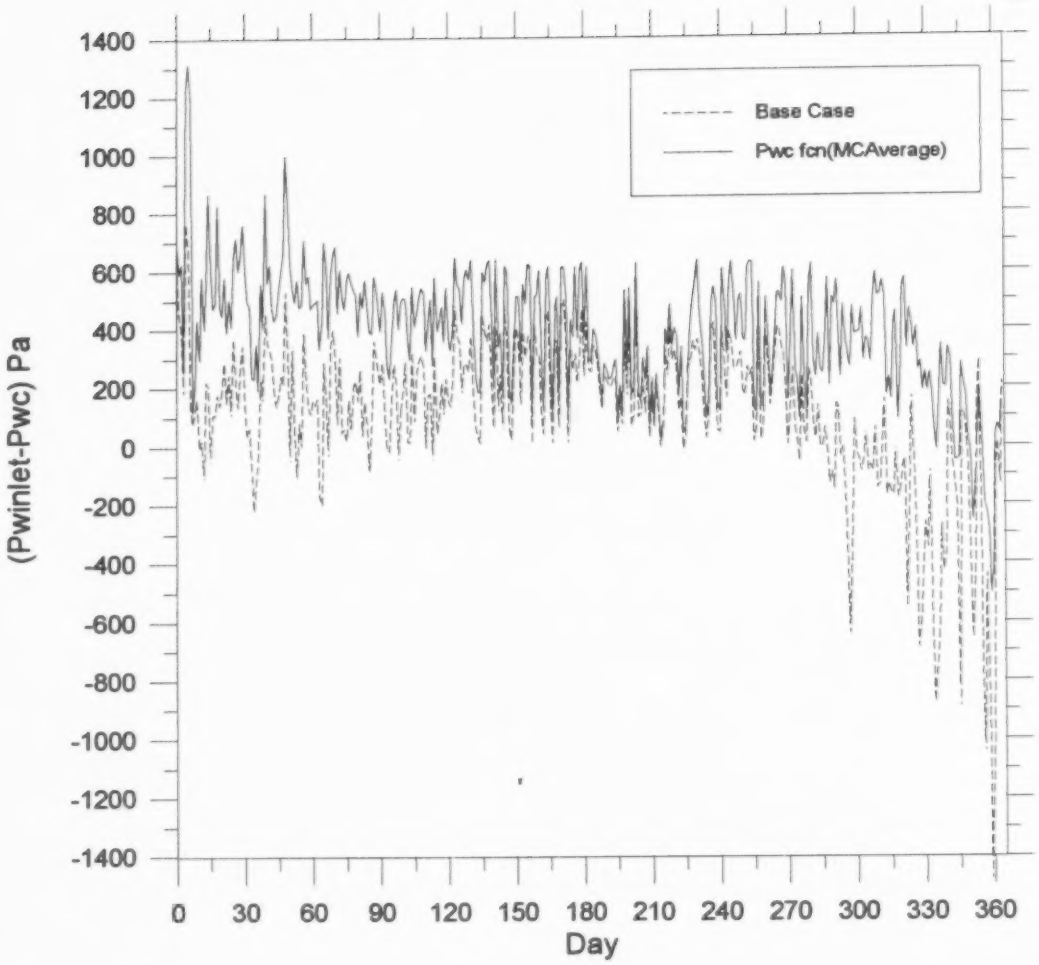

Figure 3-7 Comparison of the daily averaged vapor pressure difference (Pwinlet-Pwc) over a 1 year period (July-June) in Winnipeg for the base case and average moisture content methods.

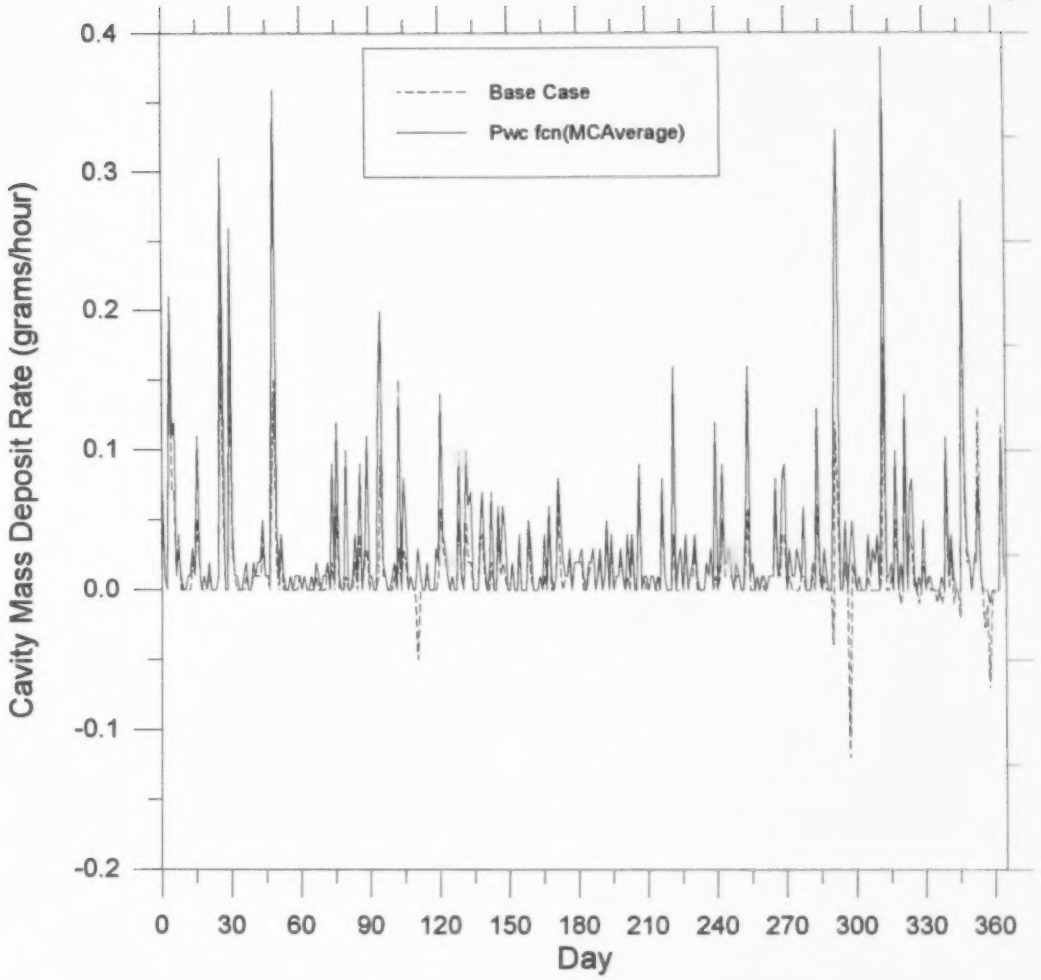

Figure 3-8 Comparison of the daily averaged cavity mass deposit rate for the base case method and average moisture content methods over a 1 year period (July-June) in Winnipeg.

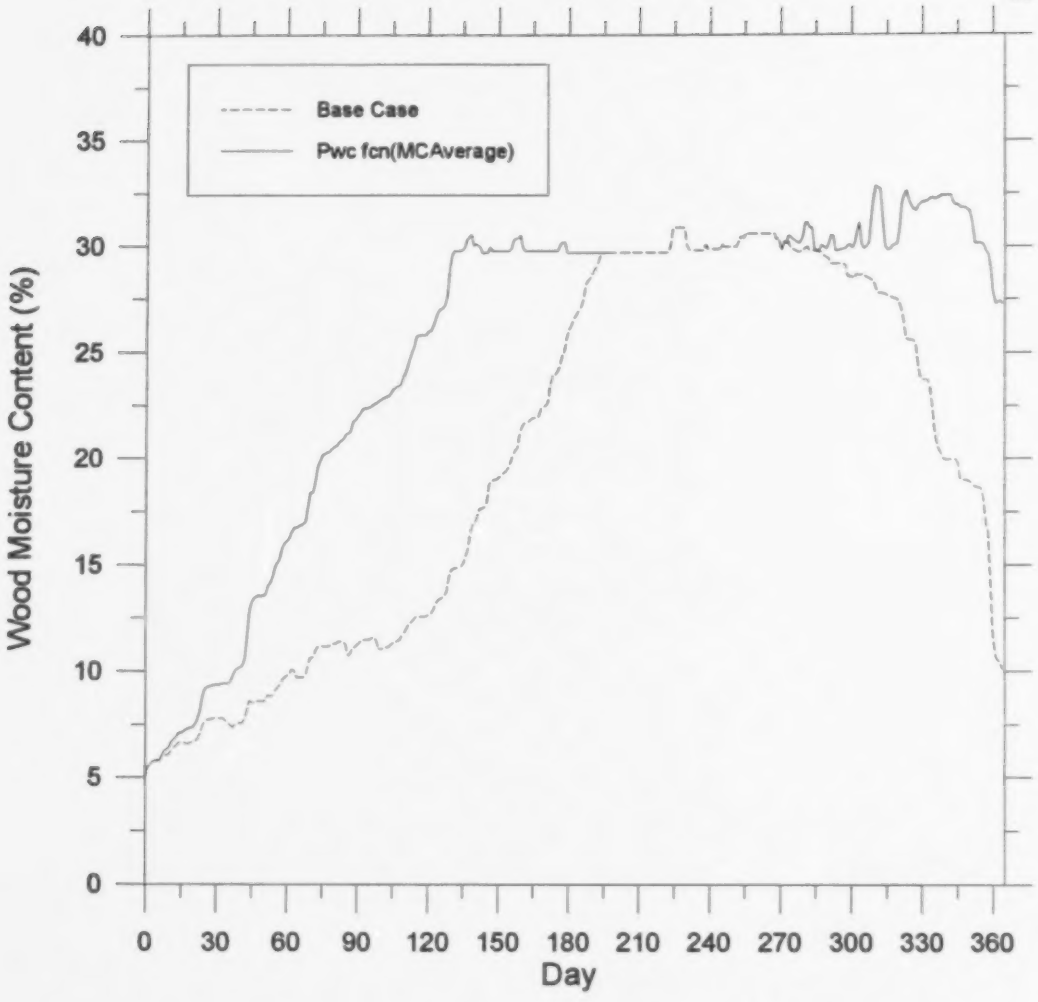

Figure 3-9 Comparison of the daily averaged moisture content of zone 1 over a 1 year period in Winnipeg for the base case and average moisture content methods.

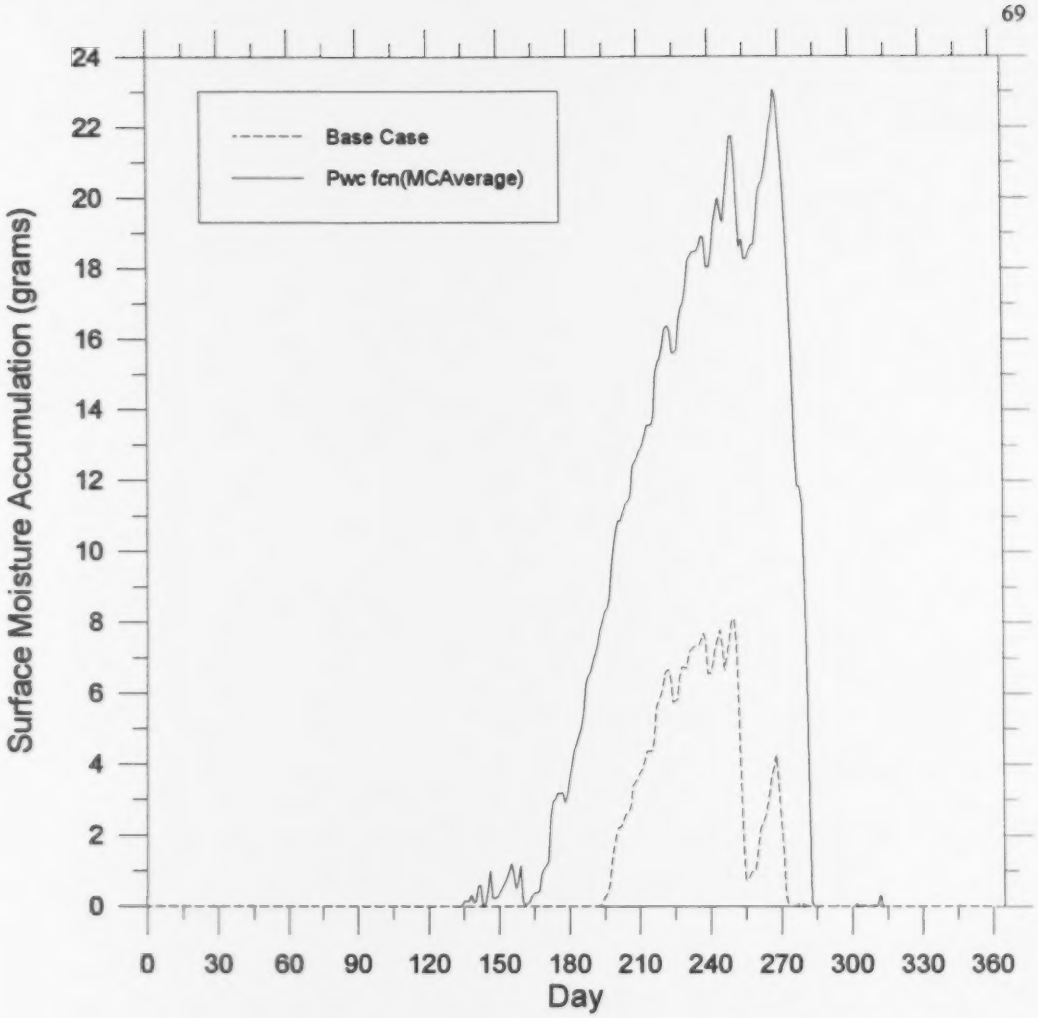

Figure 3-10 Comparison of the daily averaged surface moisture accumulation of zone 1 over a 1 year period (July-June) in Winnipeg for the base case and average moisture content methods. Surface moisture accumulation is uniformly distributed over zone 1 which is 50 mm high and 368 mm wide.

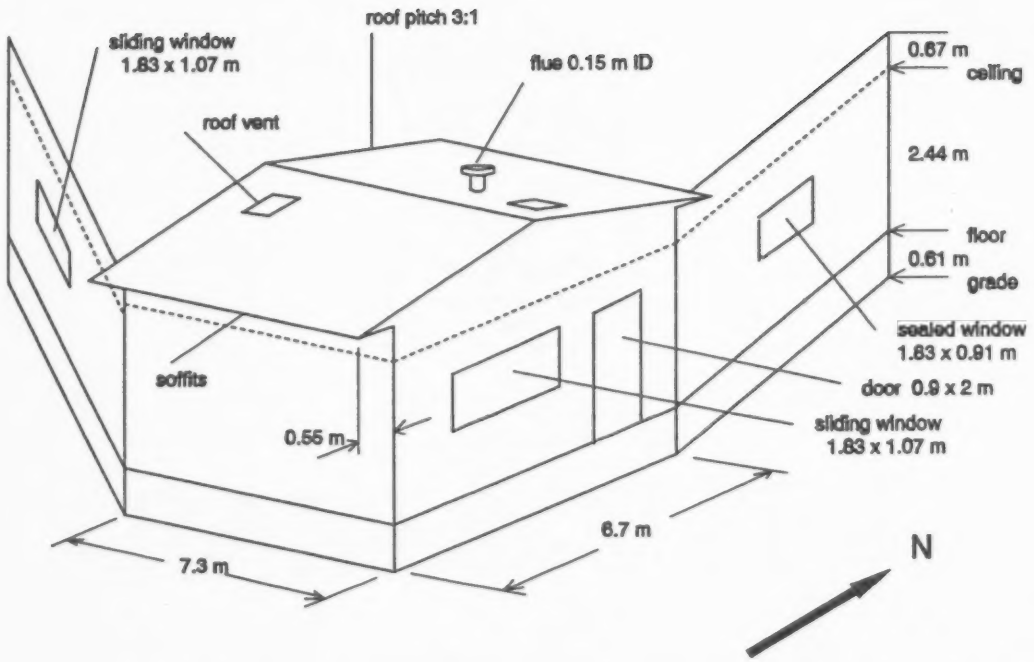

Figure 3-11 Isometric view of the building characteristics used in all simulations ran using the WMS model.

Building Characteristics	
Ceiling height of building	3 m
Floor height of building	0.61 m
Volume of building	200 m^3
Building flow coefficient	0.00845
Building flow exponent	0.681
Fraction of distributed leakage:	20% Floor: 10% ceiling: 70% walls
Fraction of distributed leakage in walls	25% in each wall
Fraction of floor leakage below walls	25% in each wall
Fraction of attic leakage above each wall	25% in each wall
Wall Cavity Characteristics	
Width of exterior slit	368 mm
Height of exterior slit	1.9 mm
Height of exterior inlet	2.684 m
Width of interior slit	368 mm
Height of interior slit	2.6 mm
Height of interior inlet	0.753 m
Width of Cavity	406.4 mm
Depth of Cavity	89 mm
Direction cavity wall is facing	North

Table 3-1 Building and wall cavity characteristics used in the WMS model to determine the relationship for $P_{w,c}$.

Chapter
FOUR

WALL MOISTURE SIMULATIONS

Development of a comprehensive numerical model enables manufacturers and builders involved with the building science industry the ability to predict potential problem areas which may arise and probable solutions without having to incur the time and expense of setting up field experiments. The Wall Moisture Simulation Model (WMS) was used to predict the moisture in walls of residential buildings of 5 different climatic regions across Canada. The meteorological data for five cities across Canada were chosen to represent different climatic regions. These 5 cities include Whitehorse (Arctic Region), Winnipeg (Prairie Region), St.Johns (Eastern Coastal Region), Montreal (Central Region) and Vancouver (Western Coastal Region). This chapter will first discuss the results generated for the 5 different cities across Canada which will be used as the basis for comparison purposes in the second part of the chapter. In the first section, it will be shown how the climatic conditions influence the leakage flows and hence the moisture conditions in the wall cavity and potential for biological growth in the sheathing. The meteorological conditions determine the moisture deposition pattern by imposing a total pressure and vapor pressure difference across the wall. It was also instructive to examine how the leakage flows are affected by the climatic conditions.

In the second part of the chapter, various wall assemblies were simulated to reflect current building practises of building walls of 140 mm (5.5") thickness and renovating existing walls by adding an exterior insulating sheathing. Simulations were also carried out

for varying leakage path length to determine the sensitivity of the results to this parameter. A final simulation was carried out using the base case and imposing a constant leakage flow on the wall. This type of simulation has been reported before by Ojanen and Kumaran (1992) and TenWolde and Carll (1992).

Each of the simulations were for an isolated, unsheltered bungalow, with a north facing wall cavity having a typical leakage path. A north facing wall was chosen since the moisture deposition would be greater for the north facing wall than the other 3 cardinal directions because of the lower amount of solar gain and hence lower sheathing temperatures. The results generated by the WMS model were calculated on an hourly basis over a 1 year period commencing in July and finishing in June. All simulations began in July when the moisture content of the sheathing is generally dry having an initial moisture content of 5.5 %. It was expected that the sheathing moisture content would increase from a low value in the summer reaching a maximum in the winter and then gradually decreasing with the return of the warmer weather in the spring.

4.1 Base Case Analysis For the Five Cities

In this section, we discuss the flow rate, vapor pressure difference ($P_{w,inlet} - P_{w,c}$), cavity mass deposit rate, moisture content profile, and surface moisture accumulation for the 5 cities and how these depend on the meteorological data. The flow rate and vapor pressure difference, ($P_{w,inlet} - P_{w,c}$), will first be analysed to determine the effect they have on the mass deposit rate. Meteorological data for each of the 5 cities included the outdoor temperature and relative humidity, wind speed as measured at a standard height of 10 m,

and wind direction which can be seen in Appendix A. The combination of air flow rate, vapor pressure difference ($P_{w,inlet} - P_{w,c}$), and moisture deposition rate will then be used to explain the behaviour of the moisture content profile and surface moisture accumulation along the wall cavity.

The leakage path for all simulations ran comprised of air entering horizontally through an inlet slit, traveled vertically through the insulation, and then exited horizontally through another slit into the surrounding ambient conditions. The wall cavity was built of 50 mm x 100 mm (2" x 4"s) on 406 mm (16") centers. The wall cavity was composed of 13 mm gypsum wallboard, 0.1 mm polyethylene vapor barrier, 90 mm glass fiber batt insulation, and 9.5 mm wooden exterior sheathing. The specific dimensions of the leakage path inlet slits and the wall cavity can be seen in Table 3-1.

4.1.1 Flow Rate

The air flow through the wall cavity can be either infiltrating or exfiltrating and its rate has a direct affect on the amount, location, and whether the moisture is either deposited or removed from the exterior sheathing. The amount of moisture deposition or removal is partially determined by the magnitude of the air velocity which is calculated from the volumetric flow rate. The direction of the flow determines whether the majority of the moisture is deposited or removed near the top or bottom leakage sites of the wall cavity.

Recall from Secs. 2.1.4 and 2.1.5 that the two main factors affecting the pressure difference across the leakage path are the wind and temperature differences (stack) on the envelope and are given by the following expressions.

$$\Delta P_{wind} = C_p \frac{\rho_{out} U^2}{2} S_w^2 \tag{2.3}$$

$$\Delta P_{stack} = -\rho_{out} g H_i \left(\frac{T_{in} - T_{out}}{T_{in}} \right) \tag{2.4}$$

The majority of the flow across the wall cavity in the summer is due to wind effect when the indoor-outdoor temperature difference is negligible or zero. As the outdoor temperature decreases , the indoor-outdoor temperature difference increases and the flow subsequently due to the stack effect increases. For cold climate locations such as Whitehorse and Winnipeg where the daily average outdoor temperatures can reach values colder than -30 ° C, the flow due to the stack effect is quite significant. Conversely, for fair weather locations such as Vancouver where the daily averaged outdoor temperature reach values of only -5 ° C during the winter months, the pressure difference due to the stack effect is only half that of Whitehorse or Winnipeg.

Superimposed on the stack effect is the variable effect of wind. The magnitude of the flow due to wind effects is not only due to the wind speed acting on the surface of the wall surface but also the wind direction. For an isolated house, with the wall leakage path

facing on a north wall, the pressure coefficient, C_p , for northerly blowing winds is approximately +0.6 , -0.4 for southerly winds, and -0.6 for easterly and westerly blowing winds. The variation of the pressure coefficient, C_p over a wind angle range of 360 ° for an isolated house can be seen in Fig. 4-1. This variation is included in the ventilation model. Positive values of pressure coefficient tend to result in infiltrating flow while negative values result in exfiltration. Note from Fig. 4-1 that the pressure coefficient is sensitive to wind direction and can change from positive to negative for a small change in wind direction. Thus, the wind direction will determine whether the flow is infiltrating or exfiltrating. On the other hand, the wind speed, U determines the magnitude of the flow. For example, St.Johns daily averaged wind speeds reach values as high as 65 kph, resulting in a flow rate 4 times greater than Vancouver where the wind speeds reach maximum values of only 33 kph.

Table 4-1 summarizes the number of hours of infiltration and exfiltration, flow rates, mass of water vapor entering the leakage site, cavity mass deposit rates, and mass of water vapor exiting the leakage site for each of the 5 cities. The mean infiltration flow rate for St.Johns calculated over 2908 hours was 0.0215 m^3/hour and 0.0244 m^3/hour over 5852 hours of exfiltration. This is largely due to the high wind speeds in St.Johns compared to the other locations. Vancouver on the other hand, with its seasonable warm temperatures and moderately low wind speeds, only reached a mean infiltration flow rate of 0.0011 m^3/hour calculated over 3849 hours and 0.0056 m^3/hour over 4911 hours of

exfiltration. Figures 4-2 [1], 4-6, 4-10, 4-14 and 4-18 show the daily averaged flow rates for 5 base case cities. The mean hourly infiltration flow rates over a 1 year period for Whitehorse, Winnipeg and Montreal were 0.0054 m^3/hour, 0.0212 m^3/hour, and 0.0090 m^3/hour respectively. For the most part, the mean hourly exfiltration flow rates were lower than the infiltration rates because of the difference in the magnitude of the pressure coefficients i.e. for a given wind speed, northerly winds produce +0.6 while southerly winds produce only -0.4. Throughout a 1 year period, the mean hourly exfiltration flow rates for Whitehorse, Winnipeg and Montreal were 0.0050 m^3/hour, 0.0067 m^3/hour, and 0.0087 m^3/hour respectively.

In general, the leakage flow rate directly influences the amount of moisture deposition. The leakage flow direction determines where the moisture is predominately deposited or removed along the wall cavity and the vapor pressure difference ($P_{w,inlet} - P_{w,c}$) determines the magnitude of the moisture deposition or removal rates from the exterior sheathing as the flow convects through the wall cavity.

4.1.2 Vapor Pressure Difference ($P_{w,inlet} - P_{w,c}$)

Similar to leakage flow, the magnitude of the vapor pressure difference partially determines the amount of moisture deposited since the sign of the vapor pressure

---

[1] Reference to figures will be made out of sequence when discussing the results for the 5 base cases. The results are grouped together in order for Whitehorse, Winnipeg, St.Johns, Montreal, and Vancouver.

difference ($P_{w,inlet} - P_{w,c}$) determines whether the flow is depositing or removing moisture along the wall cavity as can be seen in Eqn. 2.18,

$$\dot{m}_w = -DL\frac{M_w}{R_o T}\left(P_{w,inlet} - P_{w,c}\right)\sum_{n=1}^{\infty}\frac{-2\sin\lambda_n}{d}\sin\left(\frac{\lambda_n x}{d}\right)\left(\frac{-\nu d^2}{D\lambda_n^{\,2}}\right)$$
$$\left(\exp\left[-\frac{D\lambda_n^{\,2}}{\nu d^2}y_j\right] - \exp\left[-\frac{D\lambda_n^{\,2}}{\nu d^2}y_i\right]\right) \quad (2.18)$$

Recall from Sec. 2.2.3 that the inlet vapor pressure, $P_{w,inlet}$, is a function of the ambient temperature and relative humidity. The direction of the flow through the wall cavity determines whether the indoor or outdoor temperature and relative humidity values will be used. With the indoor temperature set at 20 ° C, the inlet vapor pressure for exfiltrating flow can vary from 234 Pa for a minimum indoor relative humidity of approximately 10 % to 1053 Pa for maximum indoor relative of 45 %. The variation in the indoor relative humidity as a function of the temperature T_C can be seen in Fig. 2-4. For an infiltrating flow, the inlet vapor pressure can range from 17 Pa for an outdoor temperature of - 30 ° C and relative humidity of 45 % to 3821 Pa for an outdoor temperature of + 30° C and relative humidity of 90 %. Recall from Sec. 3.1 that the vapor pressure along the exterior sheathing surface, $P_{w,c}$, is a function of the temperature, T_C, moisture content, and the relative humidity, RH_C. The vapor pressure for a maximum moisture content of 34 %, relative humidity of 100 %, and temperature, T_C of

28.5 ° C is 3753 Pa and 47 Pa for a minimum moisture content of 5.5 %, and temperature, T_C of - 28.5 ° C.

There are 4 possible combinations between the air flow direction and the vapor pressure difference which can occur. The first two possibilities occur when the vapor pressure difference is positive. For this case the inlet vapor pressure is greater than the vapor pressure along the wall surface and as the exfiltrating or infiltrating air flow convects upward or downward, the diffusion of moisture from the flow to the wall surface occurs in the form of moisture deposition. The other possibilities occur if the vapor pressure difference is negative. When the inlet vapor pressure is less than the vapor pressure then the diffusion of moisture is from the wall surface to the convective flow as moisture is removed from the wall surface for either exfiltrating or infiltrating flows. Examples of moisture removal and deposition for either infiltrating or exfiltrating flows can be seen in Table 4-1 by observing the range of the average cavity mass deposit rates for the 5 base case cities.

During the late summer and early fall the values and sign of the pressure difference fluctuate a great deal. The vapor pressure difference will generally be positive during the cold winter months, reaching a maximum value of approximately 500 Pa and will be predominately negative in the spring. Figures 4-2, 4-6, 4-10, and 4-14 show these trends of increasing vapor pressure difference fluctuating between 0 and 400 Pa as the weather becomes colder. As the year progresses and warmer weather approaches, the vapor pressure differences gradually becomes more negative. These trends can also be seen for

Vancouver in Fig. 4-18 but the fluctuations are smaller because of the small indoor-outdoor temperature difference during the winter months.

4.1.3 Cavity Mass Deposit Rate

The mass deposit rate is determined predominately by the velocity v, through the cavity which is calculated from the leakage air flow rate, and the vapor pressure difference $(P_{w,inlet} - P_{w,c})$ as shown in Eqn. 2.18 for the mass deposit rate. The cavity depth, d, has been set for the base case at 89 mm (3.5") and the cavity width, L, at 406 mm. The cavity temperature, T, is the mean temperature between the indoor and outdoor temperatures. The hourly sum of the mass deposit rate for all zones along the wall cavity is the cavity mass deposit rate. The distribution of the moisture deposition is non-linear along the height of the wall cavity, having the greatest deposition just adjacent the leakage sites and exponentially decreasing along the height of the wall cavity. The moisture deposition rate can be either positive or negative for an infiltrating or exfiltrating flow. To illustrate this phenomenon, hourly values are shown in Fig.4-21 for a 3 day period (July 1- 3) in Winnipeg. In the top diagram the flow rate is predominately positive (infiltration) over the first 3 days of July in Winnipeg and in the bottom diagram the vapor pressure difference $(P_{w,inlet} - P_{w,c})$, is also predominately positive. The result is a positive cavity mass deposit rate (moisture deposition) except for hours 15 and 63 where the rate is negative (moisture removal) as shown in the bottom diagram of Fig.4-21. When the moisture deposition rate is positive and the flow is infiltrating as shown in Fig. 4-21 the moisture is being deposited first at zone 40 and then exponentially decreasing as the flow descends down the wall

cavity. At hour 48 the flow is exfiltrating and the moisture deposition rate is positive resulting in moisture deposition beginning at zone 1 and exponentially decreasing as the flow ascends up the wall cavity. During hour 63, the cavity mass deposit rate is negative resulting from the inlet vapor pressure being less than the vapor pressure at the exterior surface. Moisture is removed from the sheathing as the flow convects down the wall cavity.

Of the simulations carried out, the greatest daily average deposition rate is for St.Johns as shown in Fig. 4-11 reaching a maximum of 0.54 grams/hour. St.Johns with its strong winds, moderate to high indoor-outdoor temperature differences and vapor pressure differences produced a deposition rate ranging between a maximum moisture deposition rate of 0.861 grams/hour to a maximum moisture removal rate of 0.641 grams/hour. Vancouver conversely, had the lowest deposition rate resulting from it very low flow rates and vapor pressure differences. The maximum deposition rate for Vancouver was 0.100 grams/hour as shown in Fig. 4-19. Comparing St.Johns to Vancouver, there was, on average, a difference of 2.3 and 24.6 times greater moisture deposition rates during infiltration and exfiltration, respectively.

Whitehorse with its extremes in indoor-outdoor temperatures had a moderately low moisture deposition rate compared to St.Johns. The maximum daily averaged deposition rate for Whitehorse was only 0.08 grams/hour as shown in Fig. 4-3. Though Winnipeg has similar weather conditions to Whitehorse, its maximum mass deposit rate was approximately three times greater (0.27 grams/hour) as shown in Fig. 4-7. The lower deposition rate for Whitehorse can be attributed to its lower wind speeds and vapor

pressure difference. The maximum daily averaged moisture deposition rate for Montreal was comparable to Winnipeg at 0.32 grams/hour as shown in Fig. 4-15 but its mean deposition rate calculated over 5053 hours was approximately 30 % higher.

A high moisture deposition rate is always a concern since a sustained rate will result in a significant amount of moisture deposition. However, the amount of moisture which enters the wall cavity is not always completely deposited along the wall surface but may exit through the leakage site at the top of the wall to the ambient conditions or into the interior room. When this occurs there is the potential for an accumulation of moisture in the form of liquid or ice near the exterior leakage site. The mass of water vapor exiting through either of the leakage sites can be calculated by subtracting the amount deposited within the cavity from the total amount of moisture entering the wall cavity. The total amount of moisture entering the cavity can be determined by multiplying the air flow rate and humidity ratio together.

From Table 4-1 it can be seen that there is more moisture leaving the leakage site than being deposited along the sheathing. For example, for St.Johns during exfiltrating flow, the average mass of water vapor entering the cavity over the period of 5852 hours is 0.1694 grams/hour. Out of this amount of water vapor, an average of 0.0.0344 grams/hour deposited as moisture along the wall cavity and the remaining 0.1331 grams/hour on average will exit through one of the leakage sites. If the vapor pressure of the water vapor exiting the wall cavity is less than the saturation pressure (based on the outdoor temperature) than there will be no problem with condensation. However, during the winter when the outdoor temperature is always a few degrees cooler than the inner

surface of the exterior sheathing the water vapor will condense and freeze near the leakage site. The result is ice accumulation surrounding the leakage site. This is a definite concern for all of the 5 cities since the amount of moisture exiting the leakage sites is approximately 5 times the amount being deposited within the wall cavity.

4.1.4 Moisture Content Profiles

The moisture deposition rate was integrated over the zone height and calculated for each zone along the wall cavity. The moisture content of each zone along the wall surface was determined by recording the amount of moisture deposition or removal for each hour. The moisture content profiles are the running cumulative values for each zone for anytime throughout the year. These profiles are useful in determining when throughout the year, there may be a potential moisture deposition problem.

Since the majority of the moisture is deposited in the first few zones near the leakage inlets, only the moisture content profiles for zones 1, 2, 3, 5, 20, 36, 38,39, and 40 for each of the 5 cities are shown. The general trend of the moisture content profiles is a continual increase in the moisture content while the temperature progressively drops as the season changes from summer to fall reaching a maximum during the colder periods during mid-winter. As the weather begins to warm up with the onset of spring the magnitude of the vapor pressure difference begins to decline and change sign from positive to negative. The sign change in the vapor pressure difference results in the removal of moisture from the exterior sheathing causing a decline in the wood moisture content. In the spring

the values of the outdoor relative humidity begin to decrease causing the magnitude of the inlet vapor pressure to fall resulting in a negative vapor pressure difference.

The moisture content profile in Fig. 4-4 for Whitehorse shows that zone 1 reached saturation at day 178 (beginning of January) and remained there for over 210 days. The moisture content of zones 2, 3, 5 and 20, along the wall cavity, were negligible. It was interesting to note that there was a small increase of approximately 10% from the initial moisture content of zone 40 due to infiltration early in the year during the early fall periods. Results for Winnipeg given in Fig. 4-8 showed a similar trend for the moisture content profile of both zone 1 and zone 40 as compared to Whitehorse. The maximum moisture content of 30 % in zone 1 stayed at that value for a shorter period of 180 days. Figure 4-16 shows a similar trend in the moisture content for zones 1 and 40 for Montreal compared to both Whitehorse and Winnipeg. Comparing the mean moisture deposition rates of Whitehorse, Winnipeg and Montreal from Table 4-1 of 0.0057 grams/hour, 0.0065 grams/hour and 0.0082 grams/hour respectively it is easy to see why the moisture content profiles for these three cities were similar. St.Johns on the other hand, showed the same trend in the moisture content profile as Whitehorse for zone 1, but reached saturation earlier at day 136 (mid December) and had a much higher moisture content for zones 2 through 5 as shown in Fig. 4-12. The difference in the trends of the moisture content profiles for zone 2-5 during the last few months can largely be attributed to the variations in the vapor pressure difference. The greater the magnitude of a negative vapor pressure difference, the more "drying potential" the air flow has when convecting through the wall cavity. It is important to note that the vapor pressure difference for St.Johns

during the last month of the simulation only reached values as low as -300 Pa compared to Whitehorse and Winnipeg which reached values as low as -800 Pa and -1400 Pa respectively. Therefore for St.Johns, the air which convected through the wall cavity during the last month of the simulation did not have a very strong ability to remove moisture from the sheathing as compared to Whitehorse or Winnipeg. Vancouver with its very low mass deposit and flow rates conversely showed that the moisture content in zone 1 was unable to reach the maximum moisture content of 30 % as shown in Fig. 4-20. The moisture content of zone 40 did show some increase from its original value of 5.5 % to approximately 13 %. The potential for surface moisture accumulation is possible only if the moisture content values exceeded 34% for temperatures above 0° C or above 30 % for temperatures below 0°C.

4.1.5 Surface Moisture Accumulation

Moisture which is deposited onto the wall cavity surface is first absorbed into the sheathing and retained as bound water in the cell walls of the wooden structure. Each time moisture is deposited or removed from the surface the moisture content is calculated for each zone along the wall cavity height. Once the saturation point of the wood has been reached, any additional moisture then deposits on the surface as water or ice depending on the sheathing temperature, T_C . The saturation point or maximum moisture content of the wood is dependent upon the temperature, T_C . For temperatures above 0° C the maximum moisture content is 34 % by weight and when the temperatures are below 0° C, the maximum moisture content for 100 % relative humidity is 30 % by weight. It is easy to

predict from the moisture content profile figures when and for which zones there will be an accumulation of moisture on the surface of the wall cavity.

For Whitehorse, the maximum moisture content is reached first at day 178 and surface moisture for zone 1 then begins to accumulate until it reaches a maximum value of 3.44 grams. With the onset of warmer weather the surface moisture accumulation begins to drop from its maximum value until at day 298 when there is no surface moisture remaining as shown in Fig. 4-5. Winnipeg followed the same trend for zone 1 as Whitehorse as shown in Fig. 4-9 commencing in day 195 but reaching a maximum surface moisture accumulation of 8.08 grams in zone 1 which is approximately two and a half times greater than for Whitehorse. St.Johns followed roughly the same trend as Winnipeg but the magnitude of the surface moisture accumulation for St.Johns was approximately three times greater than Whitehorse as a result of its high moisture deposition rates as shown in Fig. 4-13. The deposition rates were large enough that there was a small deposition of surface moisture in zone 2 and a substantial amount accumulated in zone 1. St.Johns was the only city which had surface moisture accumulation other than in zone 1. A total of 23.0 grams accumulated in zone 1 for St.Johns which corresponds to 2.4 mm of ice uniformly distributed over the complete zone. Montreal had a comparable amount of moisture accumulation compared to Winnipeg as shown in Fig. 4-17. Vancouver with its very low moisture deposition rate was unable to reach the maximum moisture content and subsequently had no surface moisture accumulation.

It is important to note that the WMS model is unable to account for liquid drainage down the wall cavity. Any moisture which is deposited is assumed to be absorbed

into the sheathing instantaneously until the saturation point is reached then deposit as surface moisture accumulation. This is a realistic assumption since a majority of the surface moisture accumulation occurs during the mid-winter months. However, with the onset of spring and the temperatures reaching values above 0 ° C the accumulation of moisture from one zone may condense and drain down into another.

4.1.6 Biological Activity Potential

The combination of moisture and moderately warm temperatures can lead to the growth of bacteria, mould or fungi in wood. Biological activity can occur for temperatures as low as 0° C or as high as 60 ° C for a variety of moisture contents. The excessive biological activity within the wall cavity can lead to odour problems, deterioration of the insulation, unsightly staining of the wood, wood rot, and potential health problems to the inhabitants of the house.

Although there is considerable disagreement, a wood moisture content of 20 % and a temperature greater than 10 °C was chosen as the criteria for biological activity in this study. The number of hours for each zone was recorded when these conditions were meet or exceeded. Table 4-2 shows the results for the top and bottom 10 zones of the cavity. The greatest risk for biological activity along the height of the wall cavity was for St.Johns followed next by Vancouver. The city with the least possibility of biological activity was Montreal.

4.2 Variation in the Wall Cavity Depth

This section compares the difference in the moisture content and surface moisture accumulation of zone 1 for a standard wall built with a 89 mm (3.5") cavity depth and 140 mm (5.5") cavity depth. Since the differences and trends for the moisture content profiles and surface moisture accumulation for all 5 cities were minimal, only the results for St.Johns with its high moisture content profiles and surface moisture accumulation was used for comparison purposes.

Increasing the cavity depth, d, affects the air flow rate, insulation thermal resistance value, R_{sc}, and mass deposit rate. Since the moisture deposition rate is a function of the cavity depth, any increase in the value of the cavity depth results in an increase in the moisture deposition rates for both infiltrating and exfiltrating flows as shown in Table 4-3. There was an increase of 33 % and 13 % in the mean hourly moisture deposition rates for infiltration and exfiltration flows respectively. The moisture deposition rate is also affected by the velocity of air which decreased by 28 % when the cross sectional area of the wall cavity was increased. Increasing the thermal resistance, R_{sc}, on the other hand, from 2.11 m^2K/W to 3.287 m^2K/W had little or no effect on the sheathing temperature, T_c or moisture deposition rate.

Increasing the cavity depth and decreasing the velocity overall had a minimal effect on the moisture content profile and a moderate effect to the surface moisture accumulation as seen in Figs. 4-22 and 4-23 for St.Johns respectively. The moisture content profile for zone 1 with a 140 mm (5.5") cavity depth followed essentially the same trend as the base case with the 89 mm (3.5") cavity depth.

4.3 Exterior Retrofit

This section compared the simulations for the base cases for the 5 cities consisting of the standard wall configuration with a 89 mm (3.5") cavity wall depth which had an exterior retrofit consisting of an additional 25 mm of expanded polystyrene extruded rigid insulation and aluminium siding. An exterior retrofit to a home is done to reduce heat loss and to generally improve the aesthetics.

The addition of the rigid insulation causes the thermal resistance of R_{ed} to increase from 0.083 m^2K/W to 0.959m^2K/W. This results in a larger temperature difference between T_C and the outdoor temperature. Increasing the temperature T_C causes a number of changes to occur which include increasing the maximum moisture content and vapor pressure, $P_{w,c}$. For example, if the outdoor temperature was - 22 ° C, the temperature T_C, would increase from -21.5 ° C to -10.5 ° C causing the vapor pressure, $P_{w,c}$ to increase from 92 Pa to 249 Pa. A change in T_C also allows the indoor relative humidity to vary up to a maximum of 30 %.

If the inlet vapor pressure remained constant and the vapor pressure, $P_{w,c}$ increased as a result of the temperature T_C rising, then the vapor pressure difference, $(P_{w,inlet} - P_{w,c})$ would decrease. The decrease in the vapor pressure difference,$(P_{w,inlet} - P_{w,c})$ resulted in a proportionate decrease in the moisture deposition rate. A reduction in the moisture deposition rate resulted in a decrease in both the moisture content profiles and surface moisture accumulation.

The moisture content profiles of zone 1 all decreased as shown in Figs. 4-24, 4-26, 4-28, 4-30, and 4-32 for each of the 5 cities. The trends were generally the same for all of the moisture content profiles except the duration at which the maximum moisture content was sustained decreased. The surface moisture accumulation for St.Johns decreased from 23.0 grams to 2.2 grams as shown in Fig. 4-29. Note that the surface moisture accumulation is uniformly distributed over the zone area. The surface moisture accumulation for Whitehorse, Winnipeg and Montreal were all approximately reduced to 1/3 of there original values as shown in Figs. 4-25, 4-27, and 4-31 respectively.

With the addition of the exterior retrofit comes a significant reduction in moisture deposition rates but at a cost of increasing the amount of water vapor exiting through the leakage sites. St.Johns for example, decreased the mean hourly moisture deposition rates from 0.0344 grams/hour to 0.0157 grams/hour but the rate of water vapor exiting the leakage site increased from 0.1331 grams/hour to 0.1639 grams/hour. This trend was similar for all 5 climatic regions. By adding the exterior retrofit, the problem of moisture deposition in the wall cavity has not been solved but only displaced from the wall cavity to the areas surrounding the leakage sites.

4.4 Variation in the Leakage Path Height

The base case simulations were set up to yield the worst case scenarios for moisture deposition throughout the year. The leakage sites were assumed to be at the junction of the wall and floor and wall and ceiling giving the maximum leakage path height possible. This section investigated and compared the results of the moisture content profile

of zone 1 and the surface moisture accumulation of Vancouver and St.Johns for a leakage path height 1/2 (0.966 m) of that for the base case (1.931 m) simulations.

Decreasing the leakage path height resulted in an increase in the velocity within the wall cavity. This increase in the velocity resulted in an increase in the mean hourly moisture deposition rate by 26 % over the base case for exfiltrating flow as seen in Table 4-3. The moisture content profiles for zone 1 for Vancouver and St.Johns shown in Figs. 4-33 and 4-34 followed the same trend as the base cases for these two cities with a slight increase in magnitude due to the increase in the moisture deposition rates. The moisture accumulation for St.Johns with a leakage path of 0.966 m shown in Fig. 4-35 reached a maximum of 23.9 grams and sustained a surface moisture presence for approximately 20 days longer than the base case simulation.

Unfortunately, similar to the dichotomy of the exterior retrofit, the reduction in the surface moisture accumulation was at the expense of a greater number of zones having the potential for bacterial growth.

4.5 Constant Exfiltration Flow

There are a number of moisture deposition models which predict the amount of moisture deposition. To date, there are no models which calculate the pressure difference across the leakage path based on the leakage and building characteristics, determine the air flow rate and then calculate the moisture deposition like the WMS model. Other models either use a predicted constant flow rate (Ojanen and Kumaran 1992) or impose pressure differential across the wall cavity, measured the flow rate (TenWolde and Carll 1992) and

then calculated the moisture deposition rate. This section compared the results from the base case for St.Johns with a constant exfiltration flow rate.

St.Johns was chosen as the base case having the largest average exfiltration flow rate of 0.0244 m^3/hour over 5852 hours. Figure 4-36 compared the moisture deposition rates for the variable and fixed flow rate of 0.0244 m^3/hour for St.Johns over a 1 year period. There was a decrease of 30 % in the mean hourly moisture deposition rate for the constant exfiltration flow rate simulation compared to the base case. There was also a difference in the sign of the moisture deposition rate as shown in Fig.4-36 for different times throughout the year. The moisture content profile of zone 1 for St.Johns for the 2 simulations was quite close during the summer, fall and spring periods and exactly the same during the winter months as shown in Fig. 4-37. As a result, the surface moisture accumulation shown in Fig. 4-38 differed only slightly between the variable and fixed flow rate models.

If the flow rate is required for a moisture deposition model, then a constant exfiltration flow rate seems like a viable alternative as long as the value of the flow rate is carefully chosen. For example, Ojanen and Kumaran (1992) assumed a constant exfiltration flow rate of 0.98 L/(m^2s) which corresponds to 7.056 m^3/hour based on a 2 m^2 exposed area. Comparing the fixed flow rate of 0.0244 m^3/hour to 7.056 m^3/hour, it obvious that the moisture deposition will be many times greater than the actual value.

4.6 Summary

Of the 5 distinct climatic regions across Canada evaluated using the WMS model, St.Johns had the greatest moisture accumulation and potential for biological activity because of its high wind speeds and moderate outdoor temperatures. The Prairie, Arctic, and Central regions represented by Winnipeg, Whitehorse and Montreal respectively all had comparable amounts of moisture accumulations and a moderately low risk of biological activity. The western coastal region of Canada represented by Vancouver had the lowest moisture accumulation but the second greatest potential for biological activity due to the mild temperatures.

Employing a 140 mm (5.5") cavity depth increased the cross sectional area, resulted in an increase in the mean volumetric flow rates and moisture deposition rates but a decrease in the air velocity. The overall effect was a decrease in the surface moisture accumulation of all of the 5 cities tested. The moisture content profiles showed no real distinguishable difference between the 89 mm (3.5") and 140 mm (5.5") cavity depth.

The addition of the exterior retrofit greatly reduced the moisture content profiles and surface moisture accumulation by raising the temperature, T_c. This increase in the temperature, T_c, caused the vapor pressure difference,$(P_{w,inlet} - P_{w,c})$ to decrease resulting in a substantial decrease in the moisture deposition rates. However, the reduction in surface moisture accumulation only transferred the moisture deposition problem from the wall cavity surface to the areas surrounding the leakage sites.

Decreasing the leakage path height by one half resulted in increase in the mean volumetric flow rates across the wall cavity. This increase in the flow rates across the wall

cavity subsequently resulted in an increase in the moisture deposition rates, moisture content profiles and surface moisture accumulation.

Utilizing a constant exfiltration flow rate proved to be a viable alternative only if the mean exfiltration rate is used in the simulation.

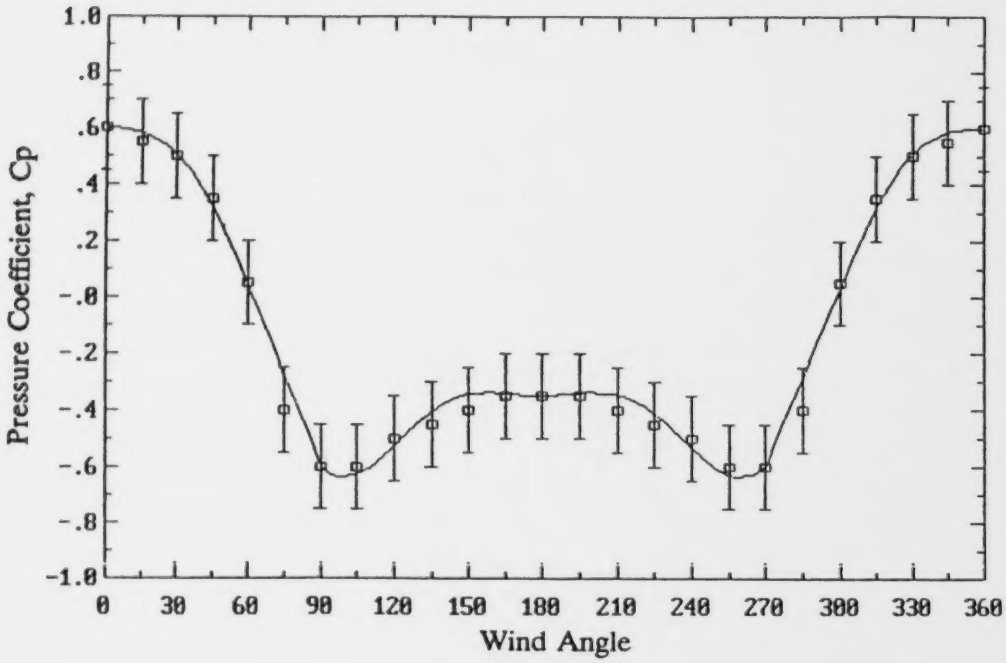

Figure 4-1 Pressure coefficients on a north wall facing (0 °) for isolated buildings over a wind angle range of 360 °.

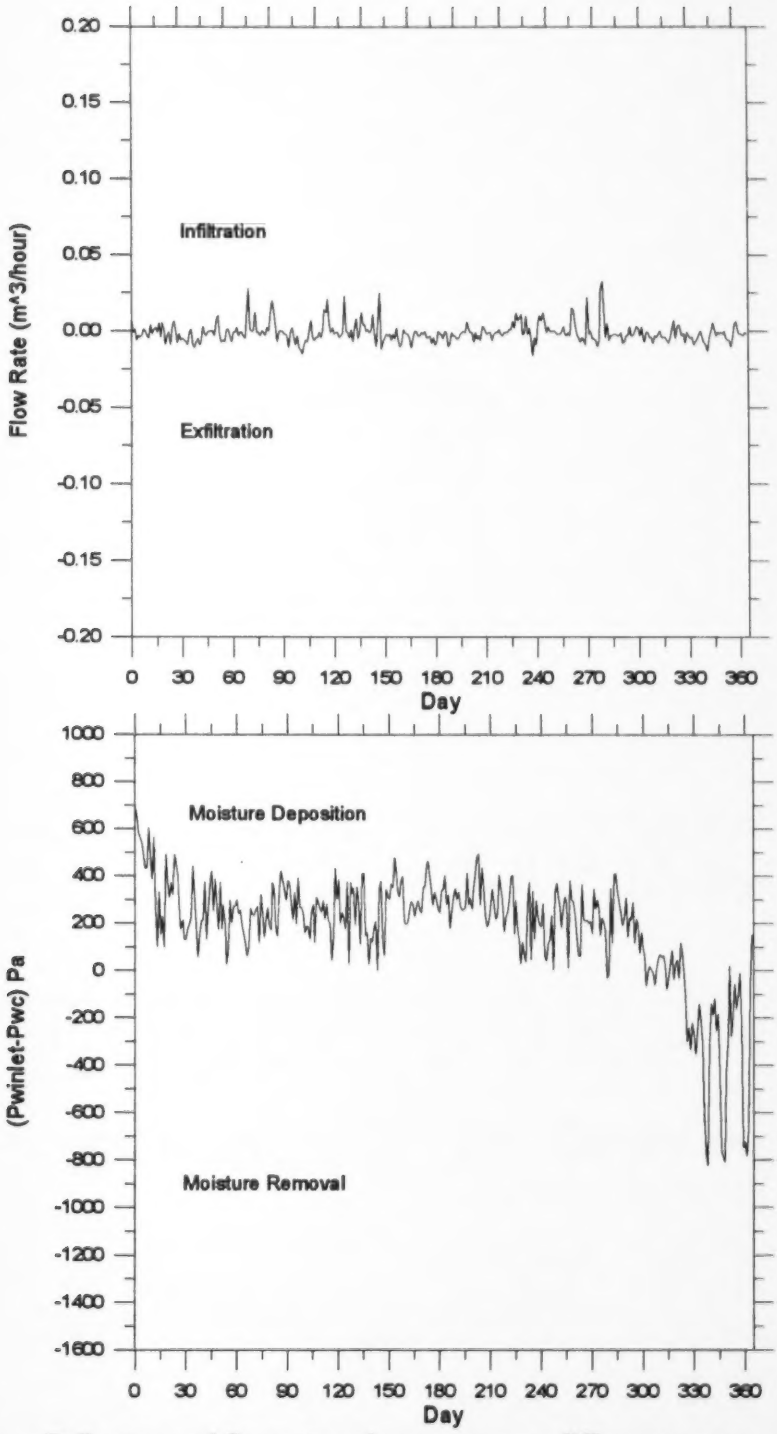

Figure 4-2 Daily averaged flow rate and vapor pressure difference over a one year period (July-June) in Whitehorse.

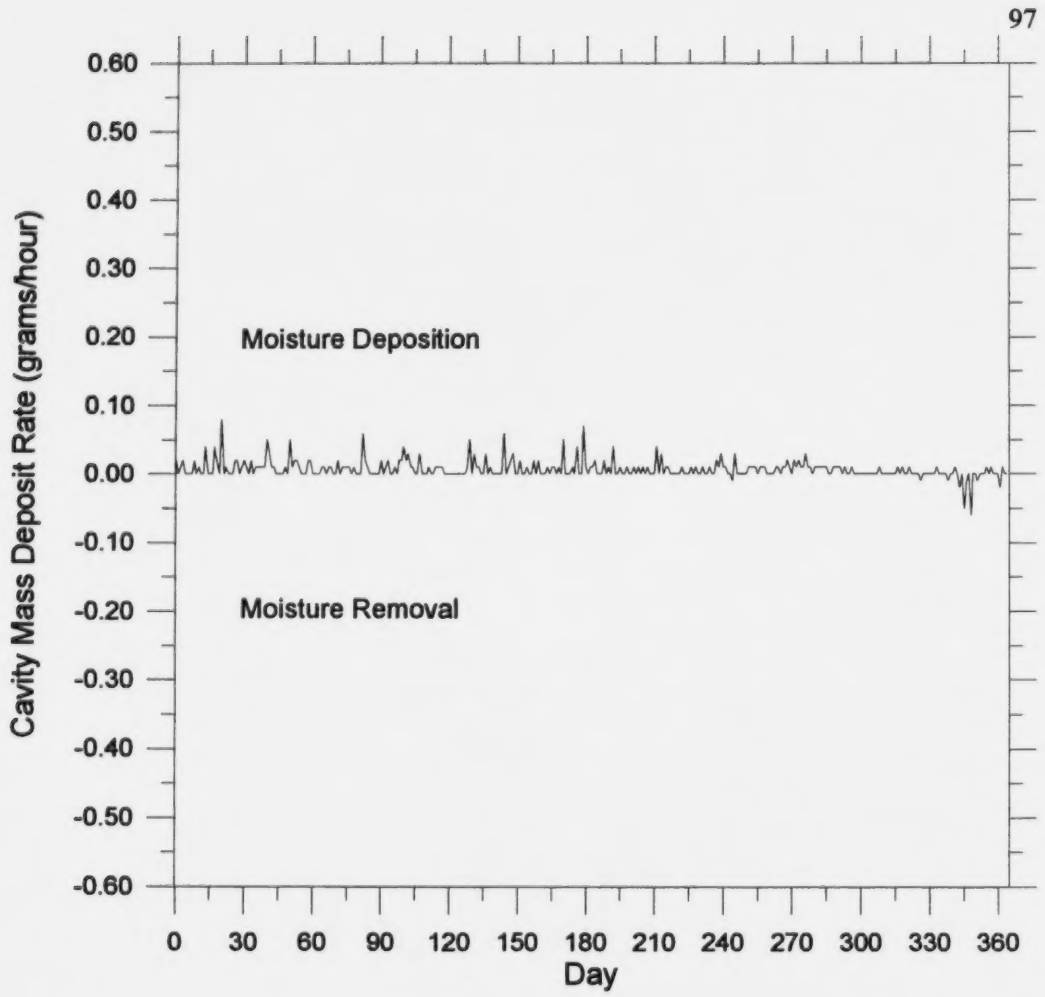

Figure 4-3 Daily averaged cavity mass deposit rate over a one year period (July-June) in Whitehorse.

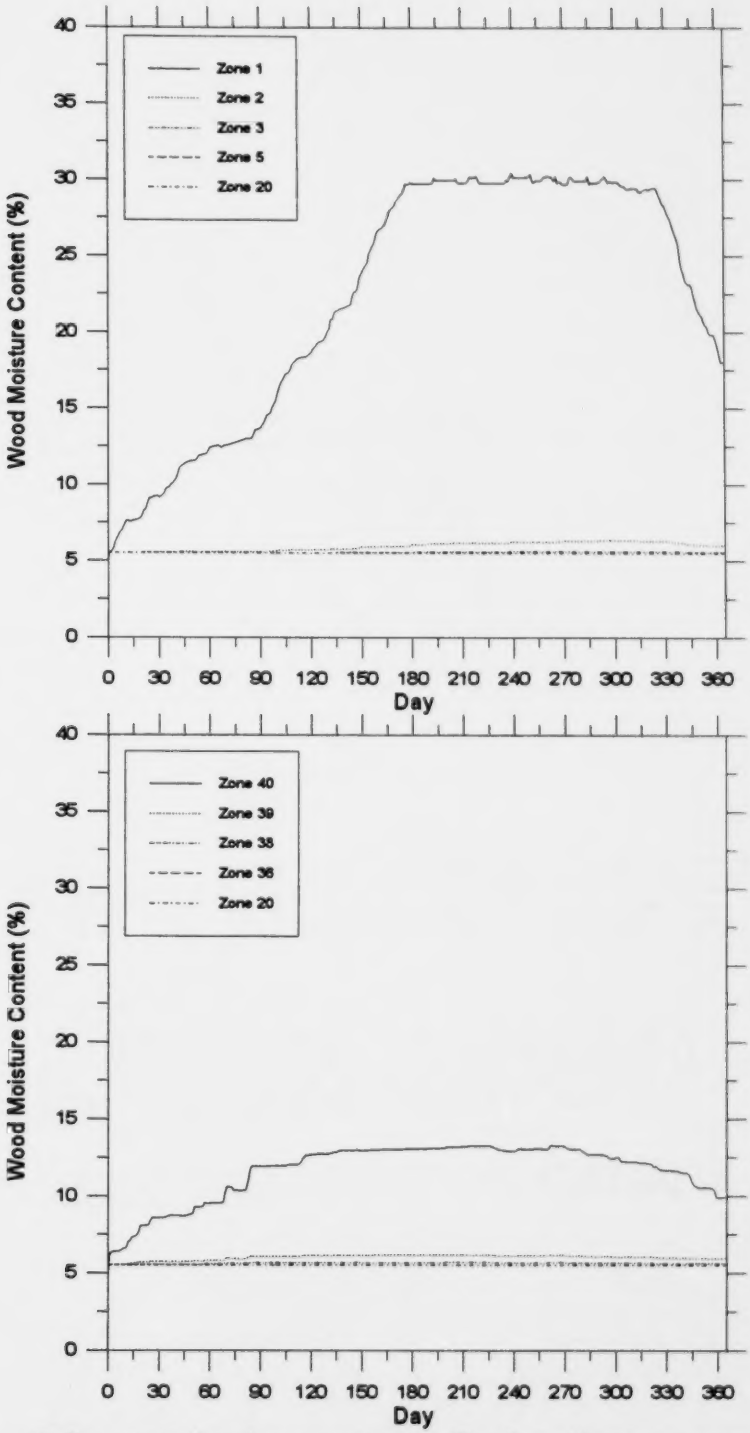

Figure 4-4 Daily averaged moisture content profiles for various zones over a 1 year period (July-June) in Whitehorse.

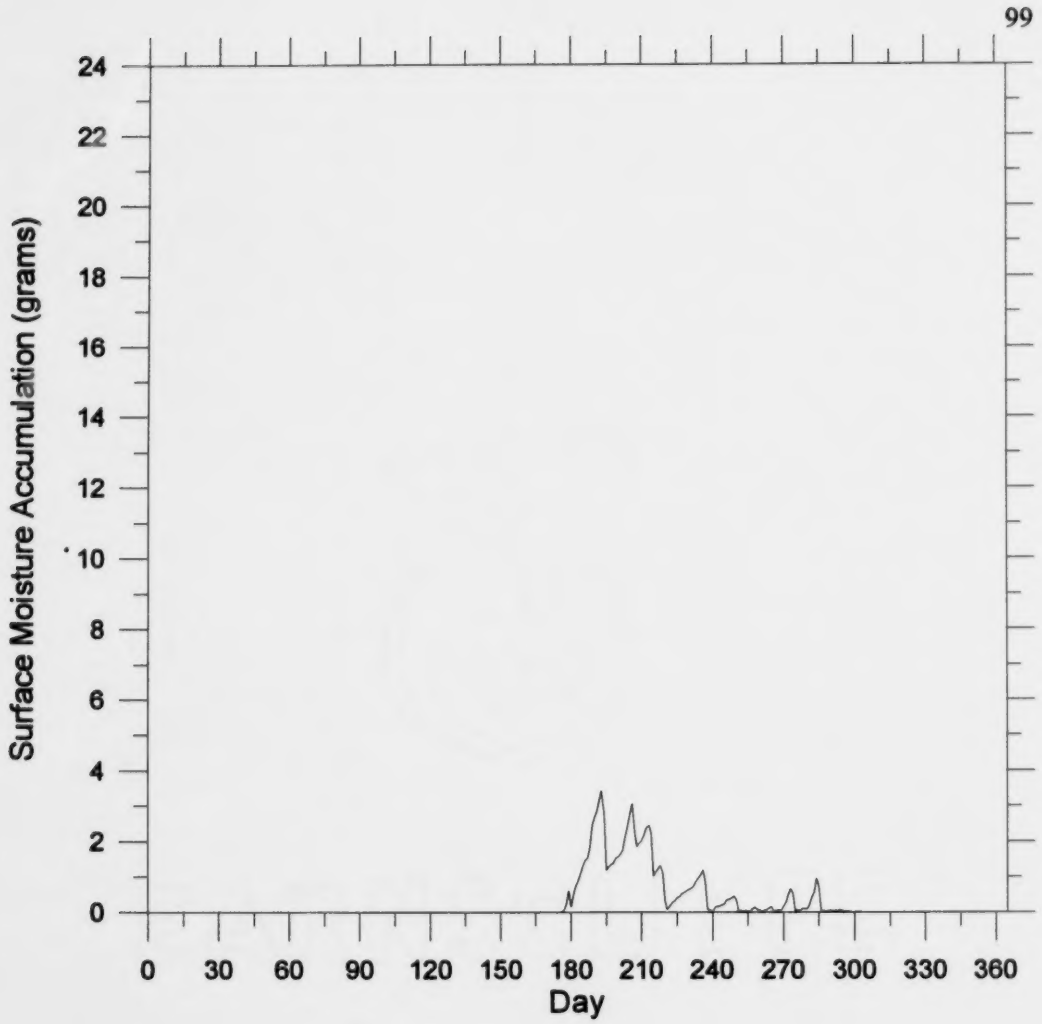

Figure 4-5 Daily averaged surface moisture accumulation for zone 1 over a 1 year period (July-June) in Whitehorse. Surface moisture accumulation is uniformly distributed over zone 1 which is 50 mm high and 368 mm wide.

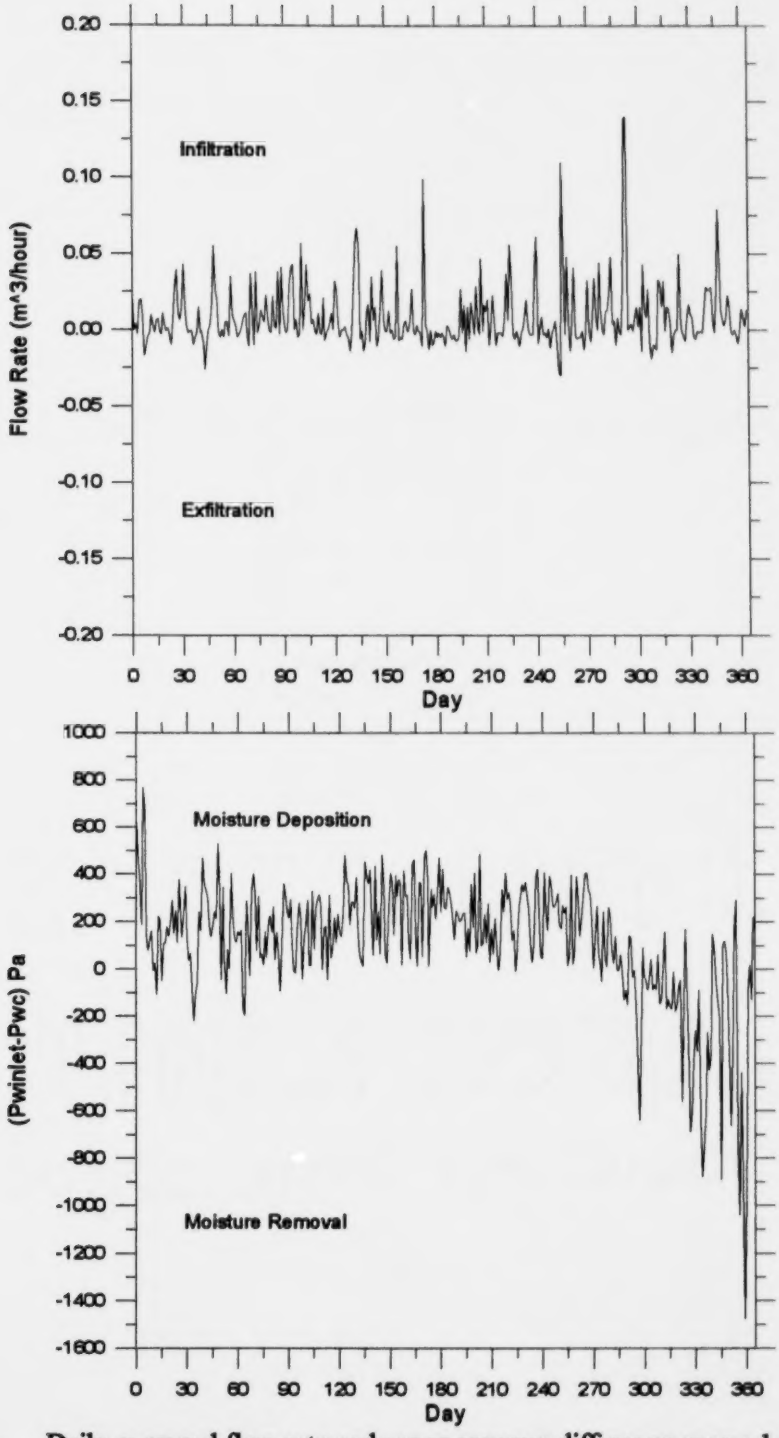

Figure 4-6 Daily averaged flow rate and vapor pressure difference over a 1 year period (July-June) in Winnipeg.

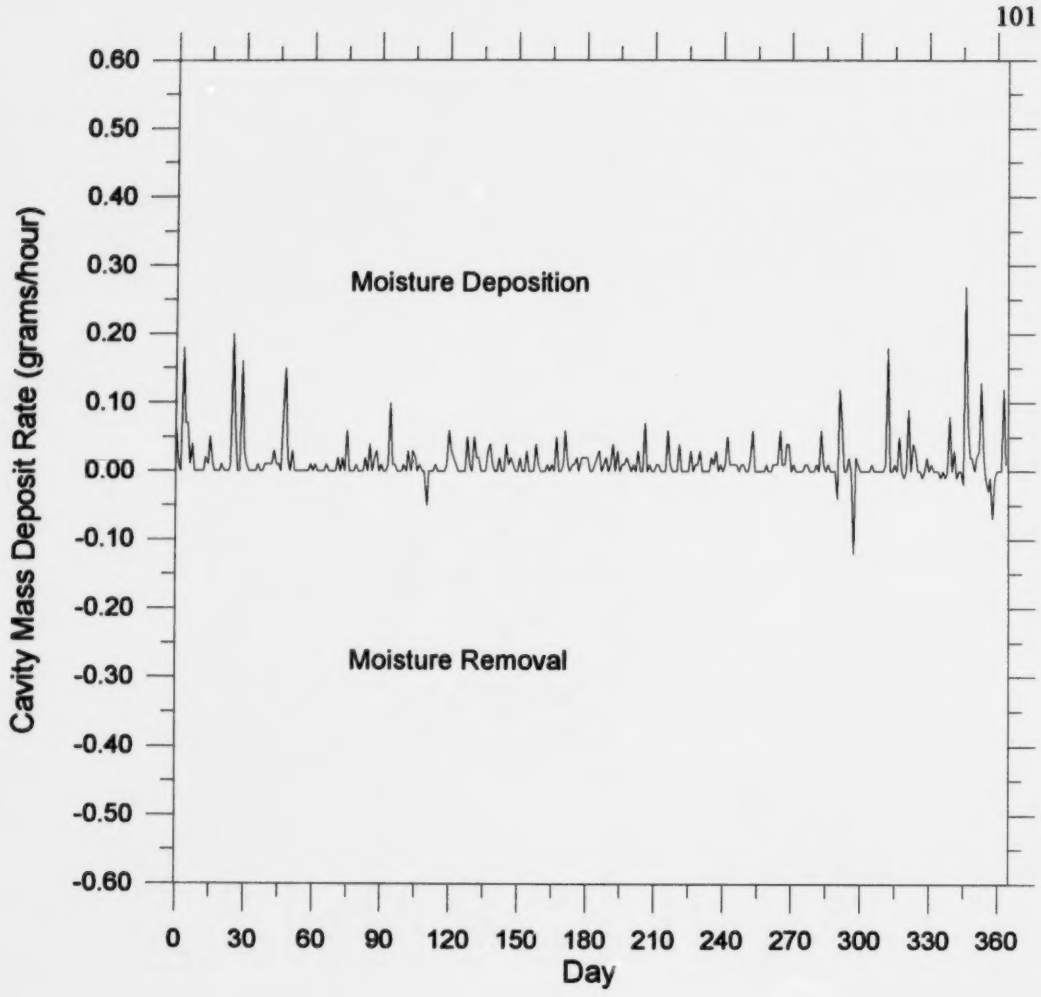

Figure 4-7 Daily averaged cavity mass deposit rate over a 1 year period (July-June) in Winnipeg.

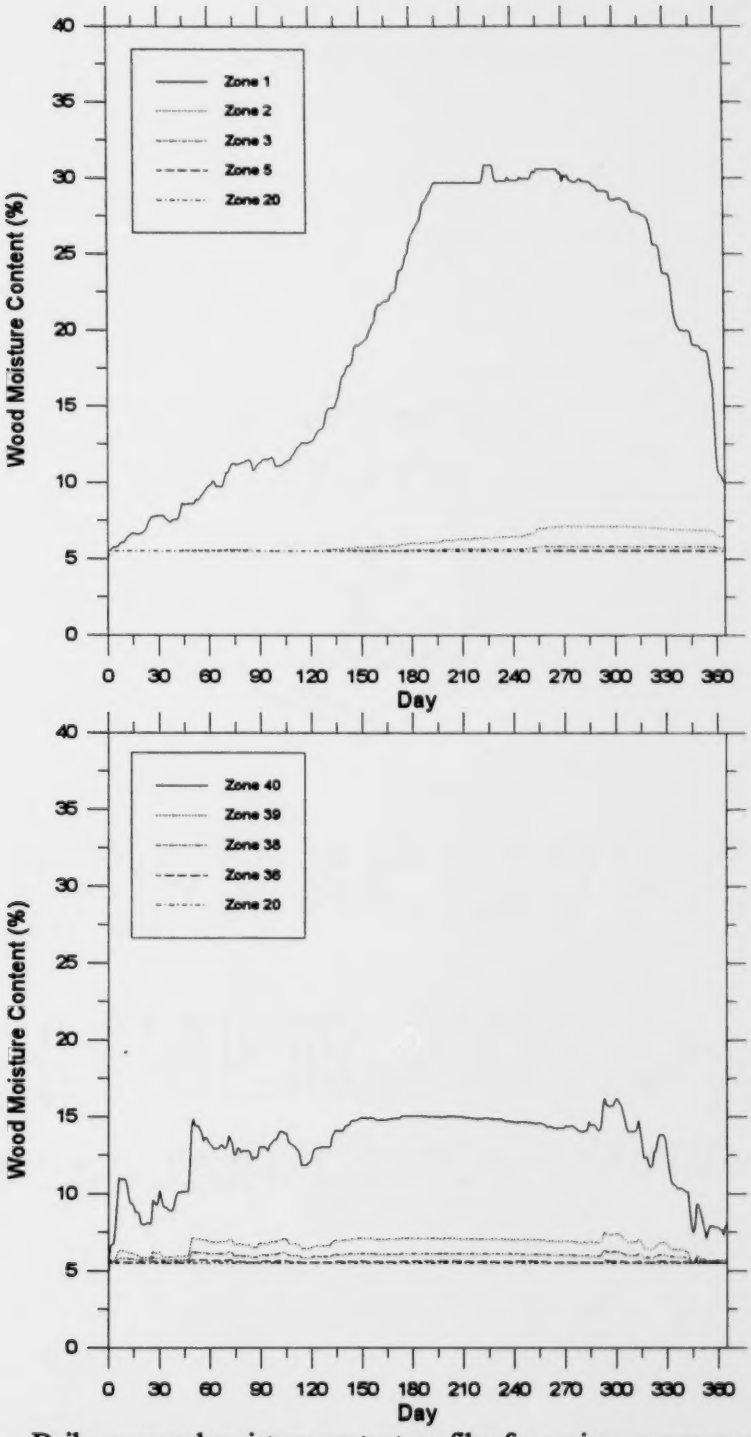

Figure 4-8 Daily averaged moisture content profiles for various zones over a 1 year period (July-June) in Winnipeg.

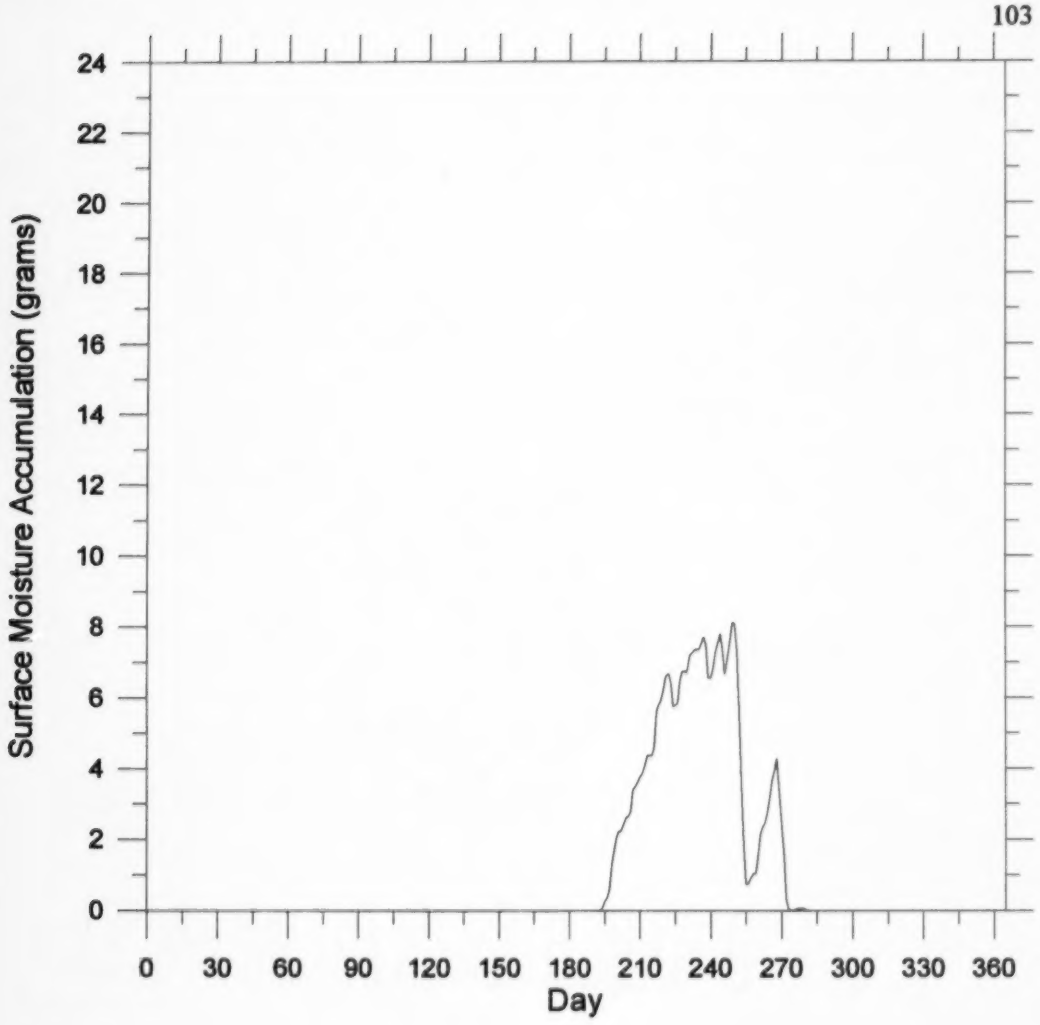

Figure 4-9 Daily averaged surface moisture accumulation for zone 1 over a 1 year period (July-June) in Winnipeg. Surface moisture accumulation is uniformly distributed over zone 1 which is 50 mm high and 368 mm wide.

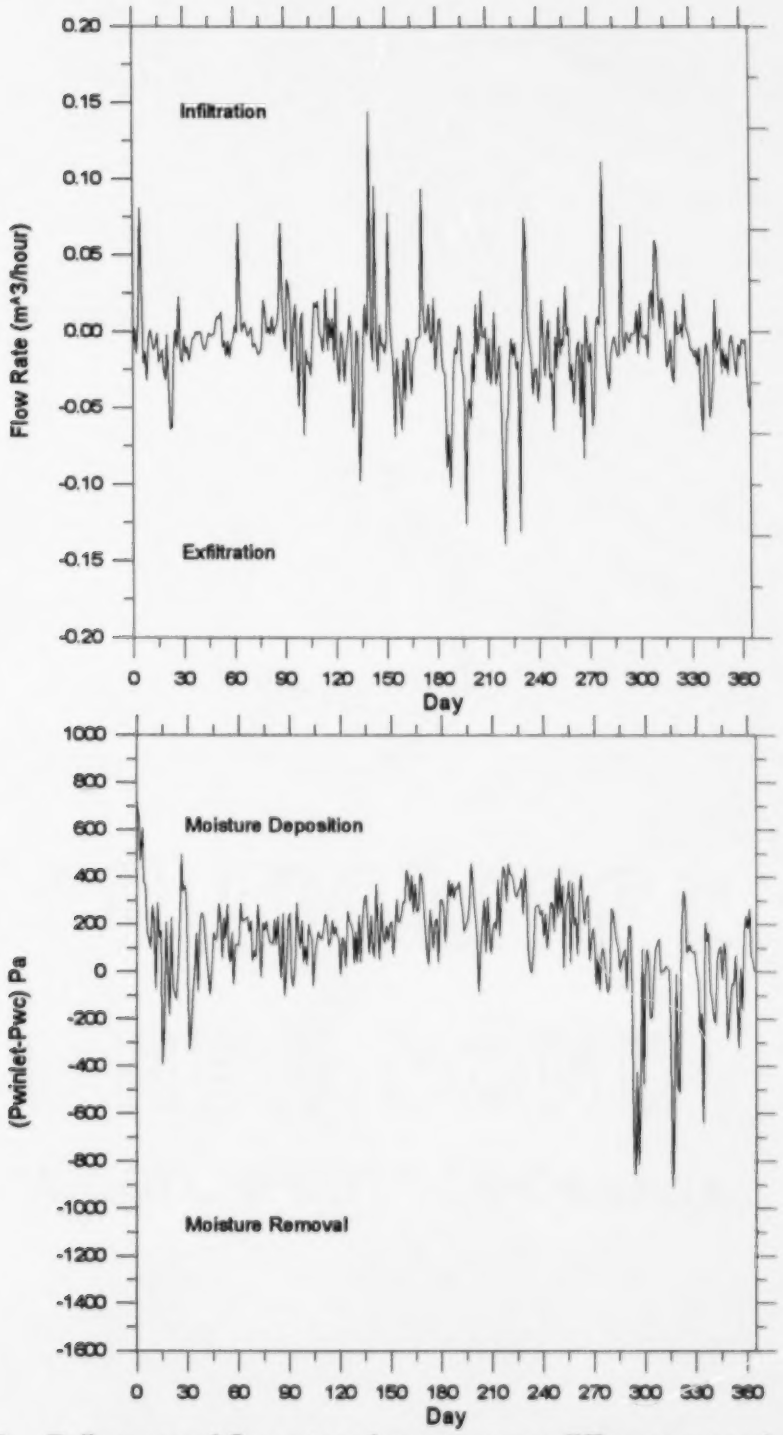

Figure 4-10 Daily averaged flow rate and vapor pressure difference over a 1 year period (July - June) in St.Johns.

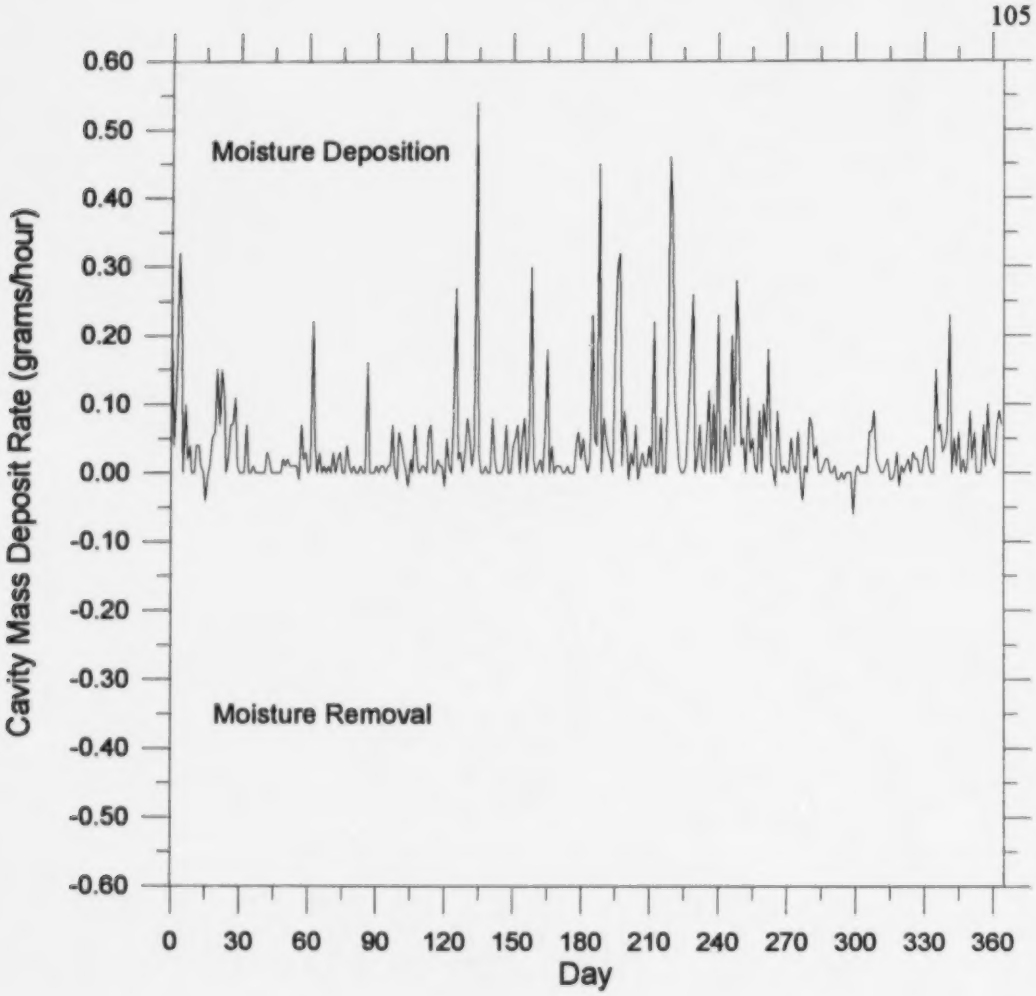

Figure 4-11 Daily averaged cavity mass deposit rate over a 1 year period (July-June) in St.Johns.

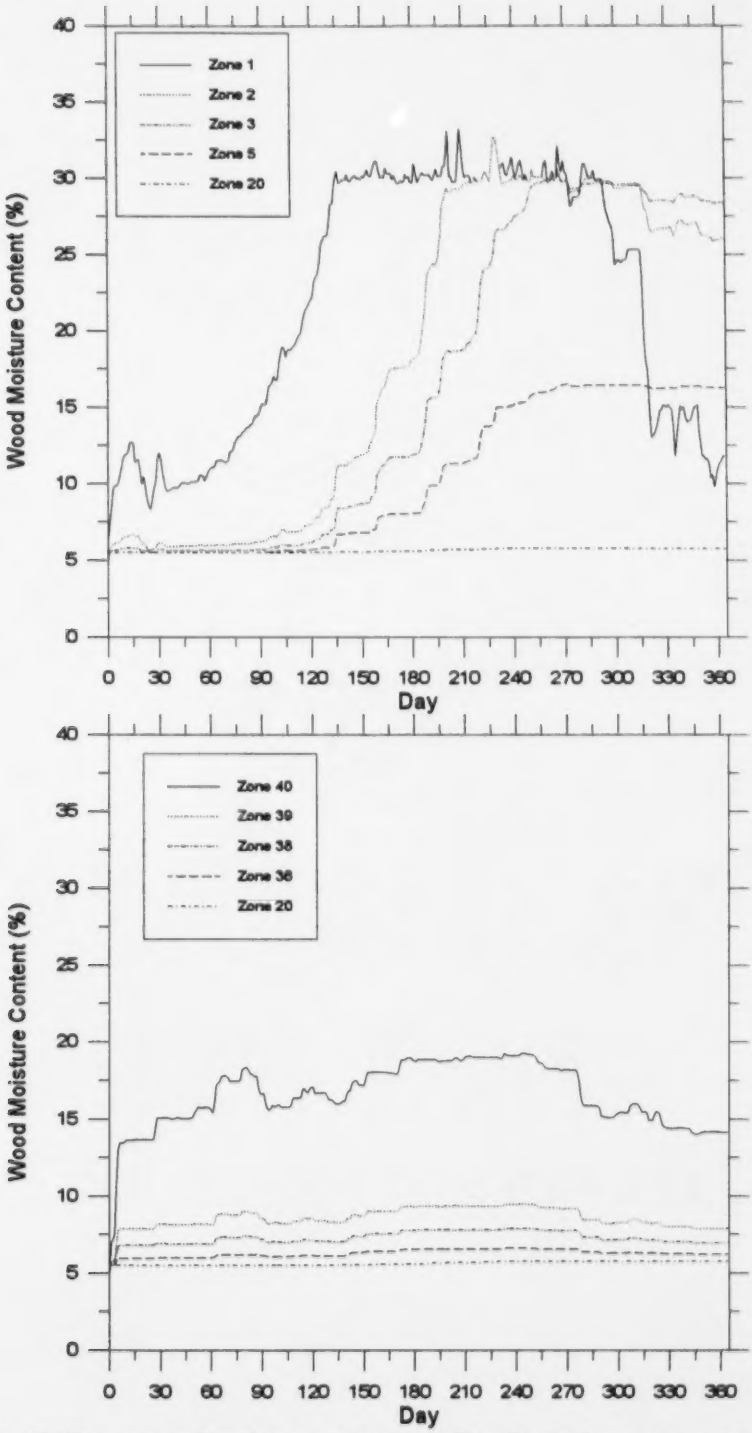

Figure 4-12 Daily averaged moisture content profiles for various zones over a 1 year period (July-June) in St.Johns.

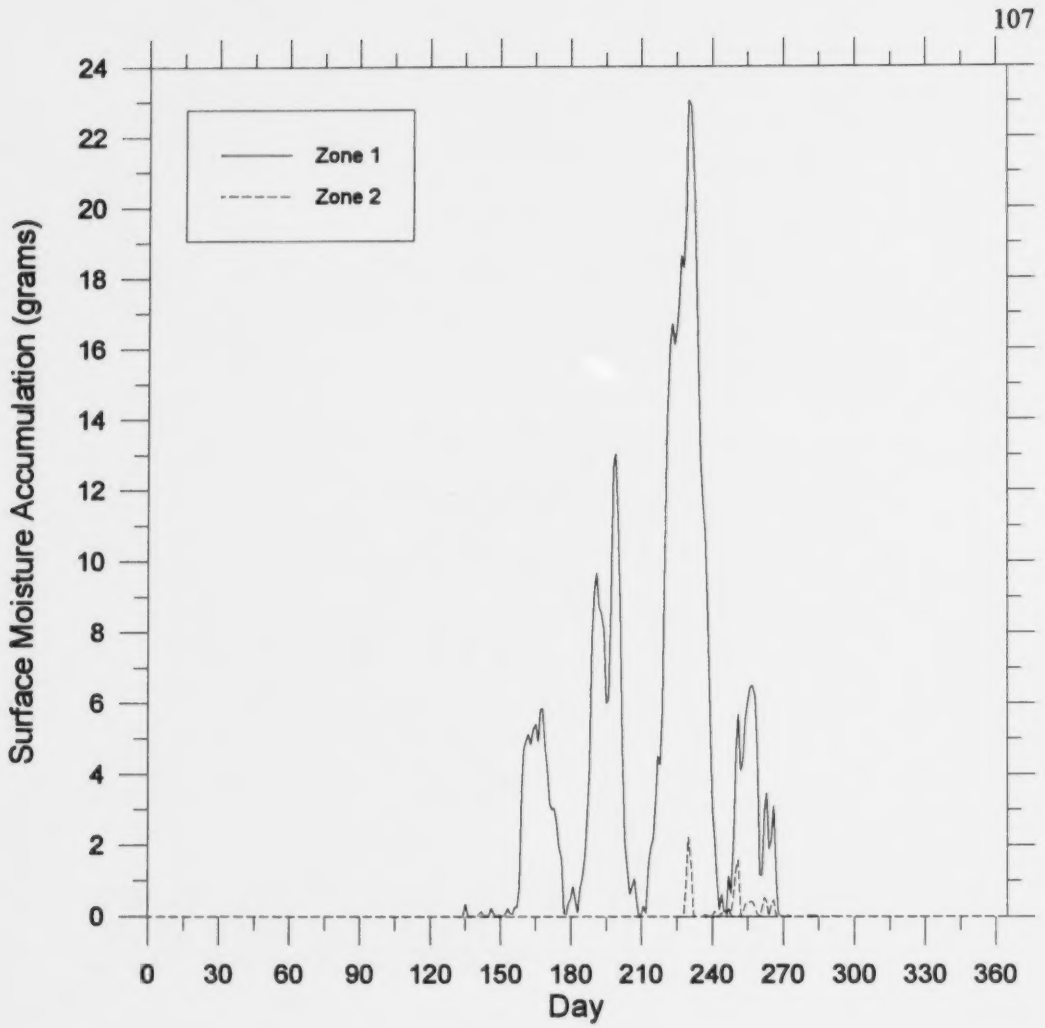

Figure 4-13 Daily averaged surface moisture accumulation for zones 1 and 2 over a 1 year period (July - June) in St.Johns. Surface moisture accumulation is uniformly distributed over zones 1 and 2 which is 100 mm high and 368 mm wide.

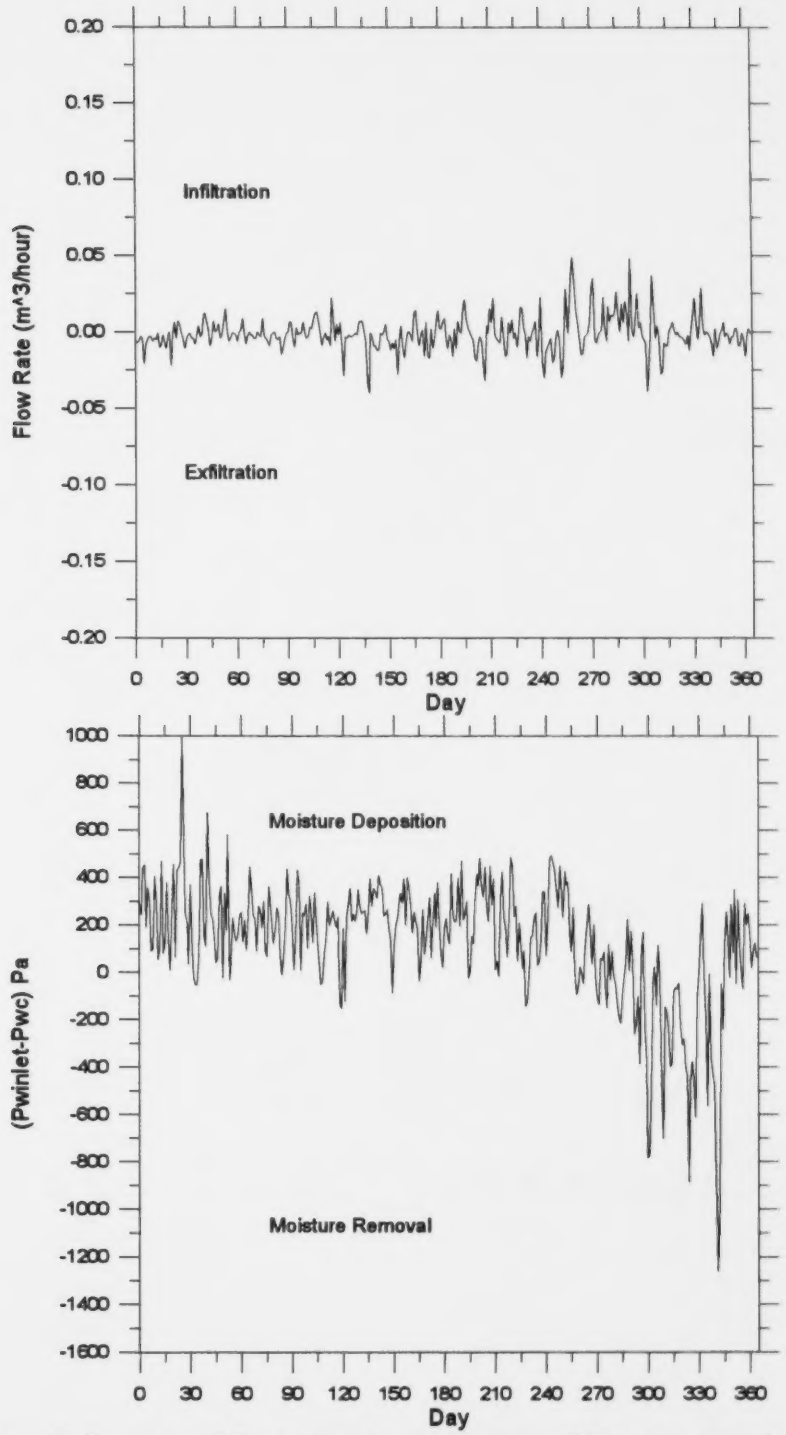

Figure 4-14 Daily averaged flow rate and vapor pressure difference over a 1 year period (July-June) in Montreal.

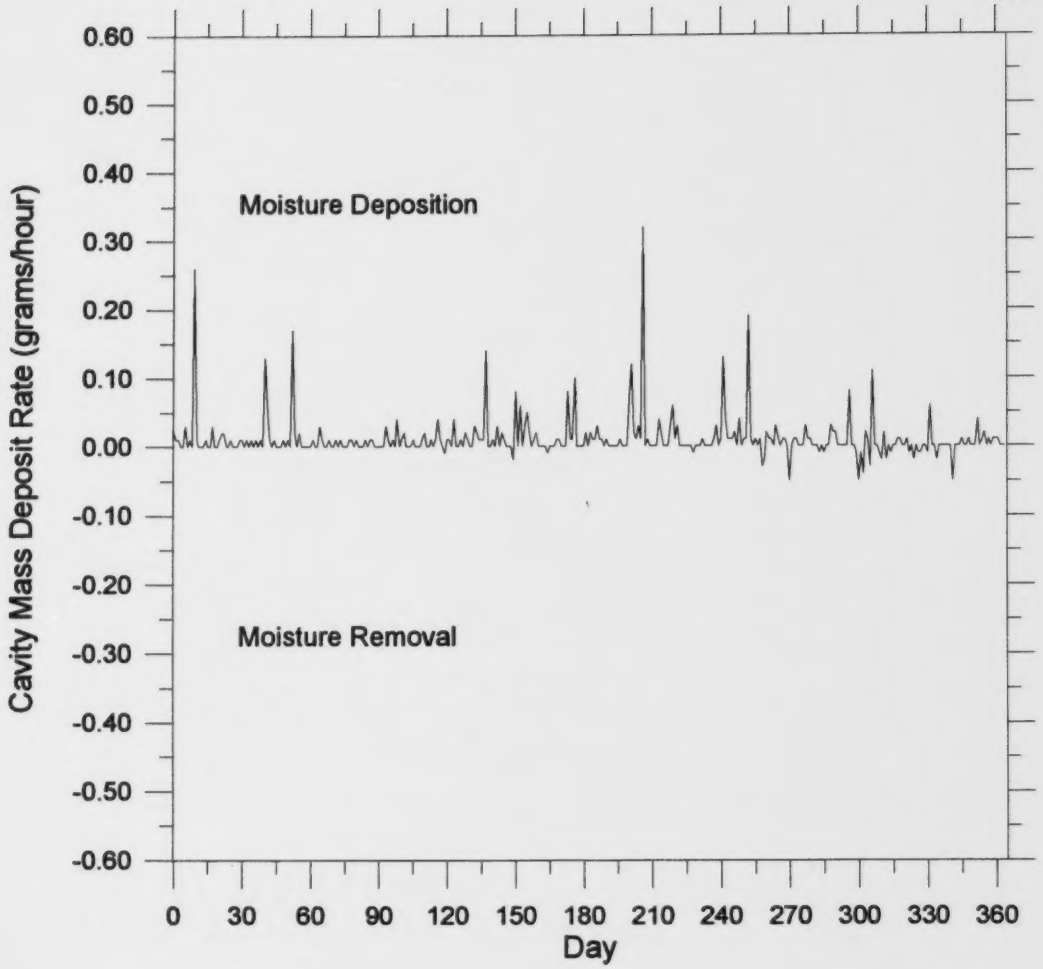

Figure 4-15 Daily averaged cavity mass deposit rate over a 1 year period (July-June) in Montreal.

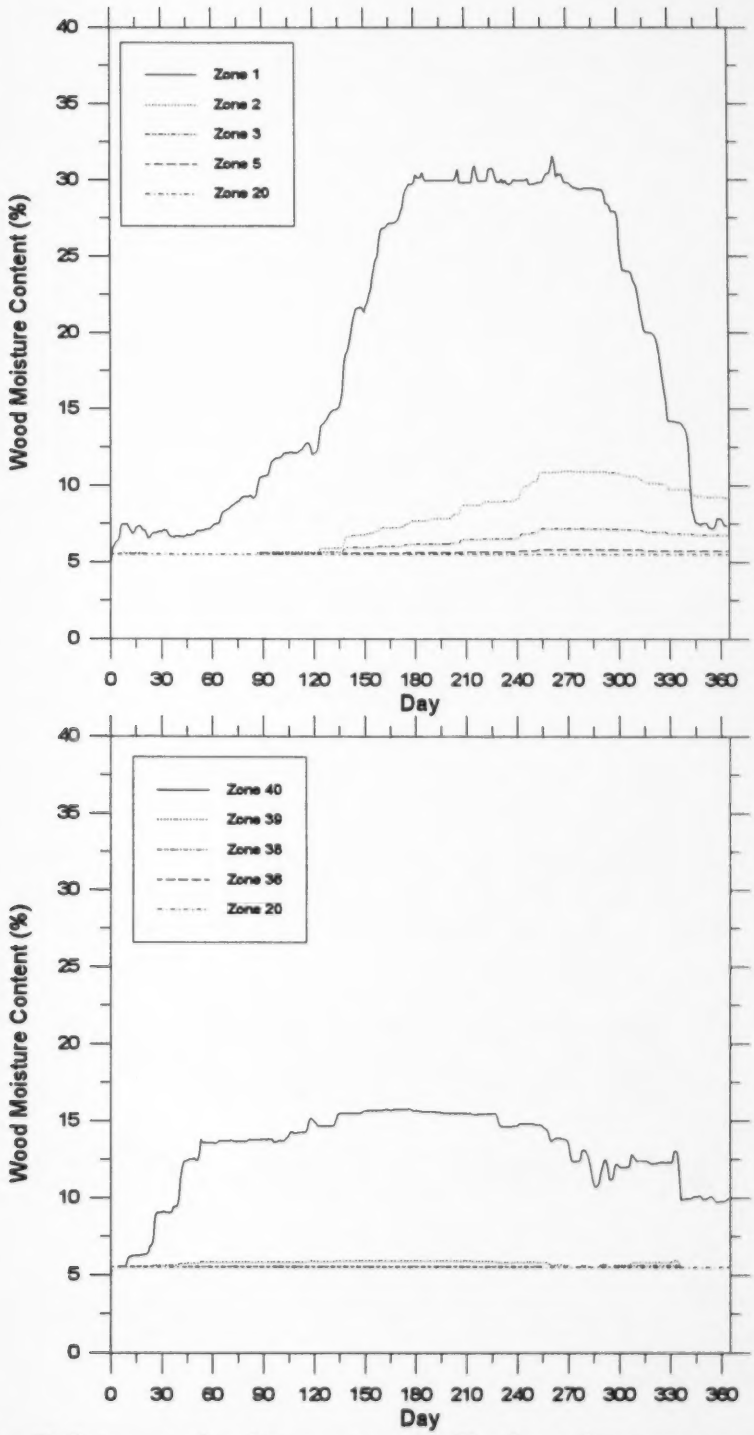

Figure 4-16 Daily averaged moisture content profiles for various zones over a 1 year period (July-June) in Montreal.

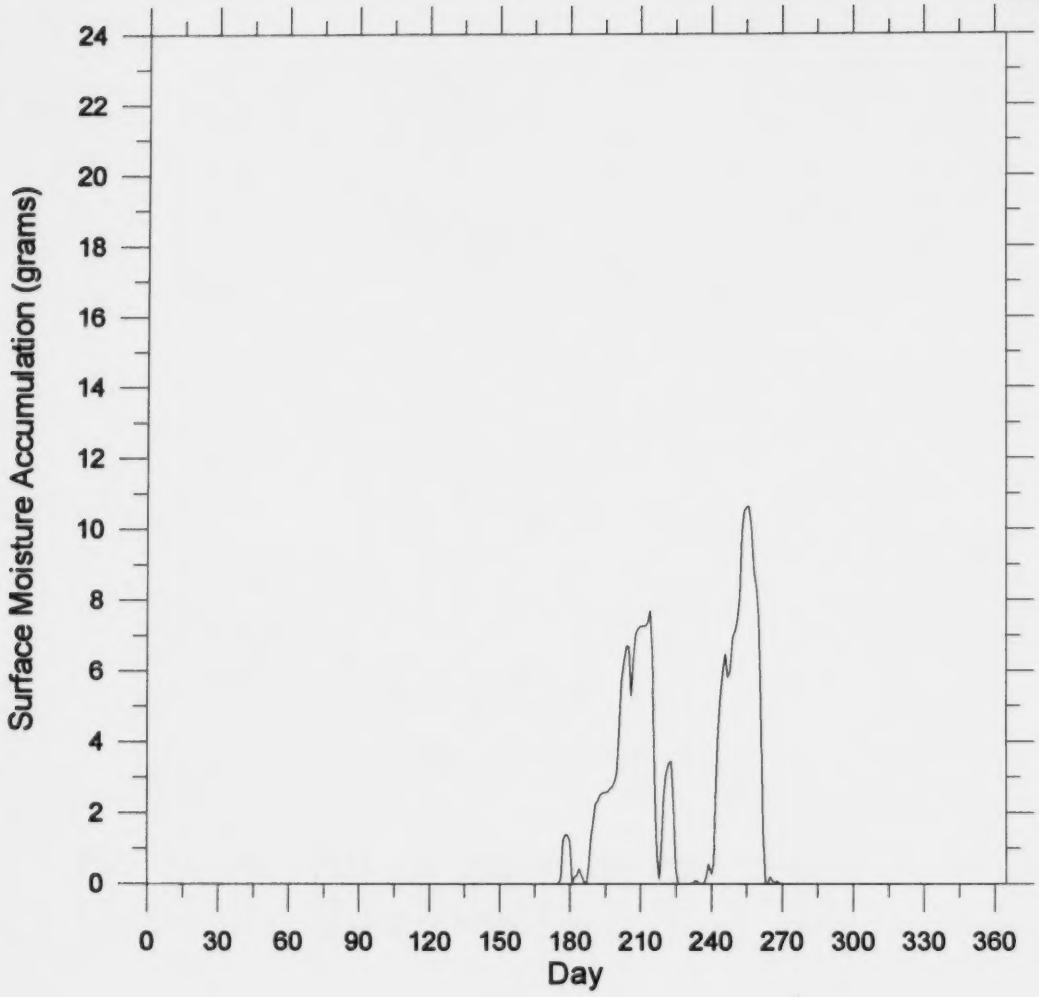

Figure 4-17 Daily averaged surface moisture accumulation for zone 1 over a 1 year period (July-June) in Montreal. Surface moisture accumulation is uniformly distributed over zone 1 which is 50 mm high and 368 mm wide.

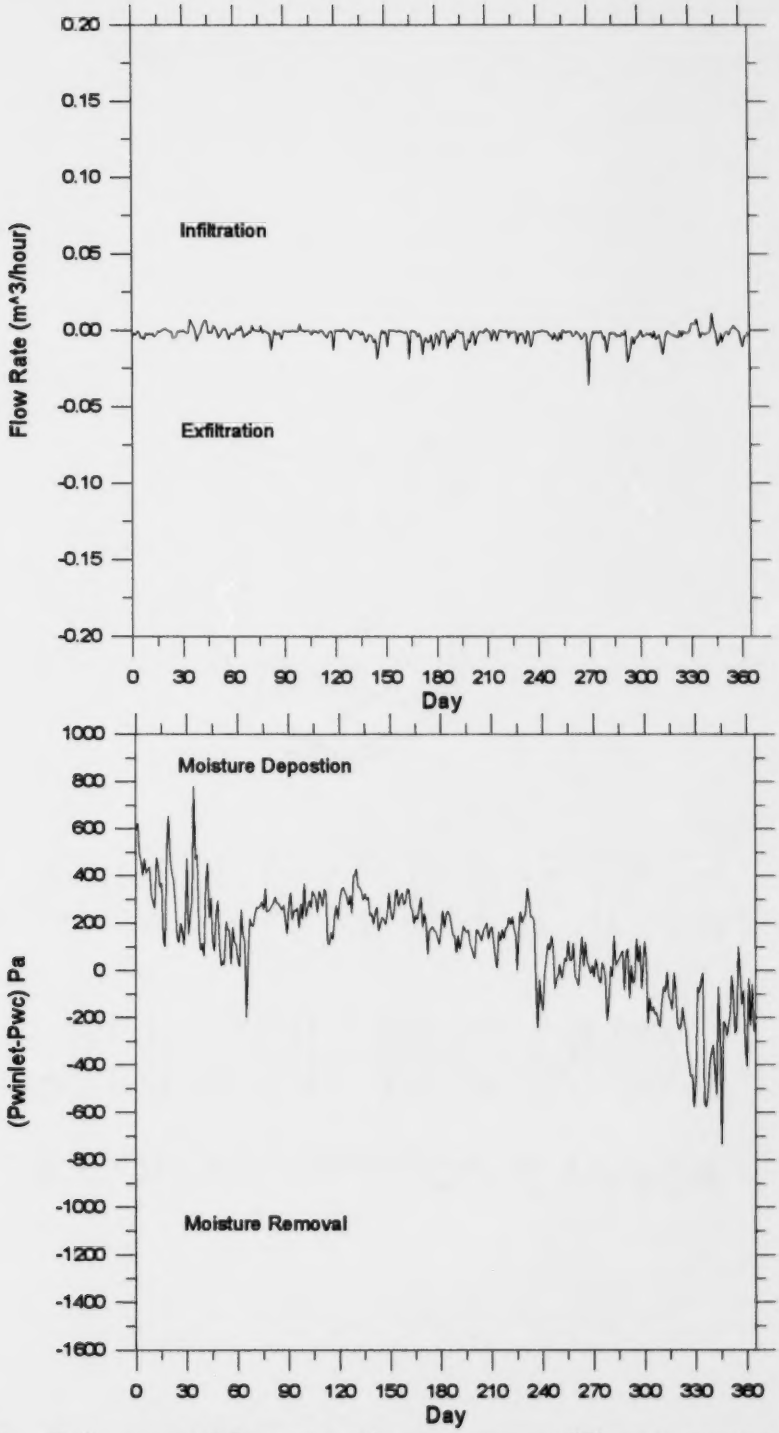

Figure 4-18 Daily averaged flow rate and vapor pressure difference over a 1 year period (July-June) in Vancouver.

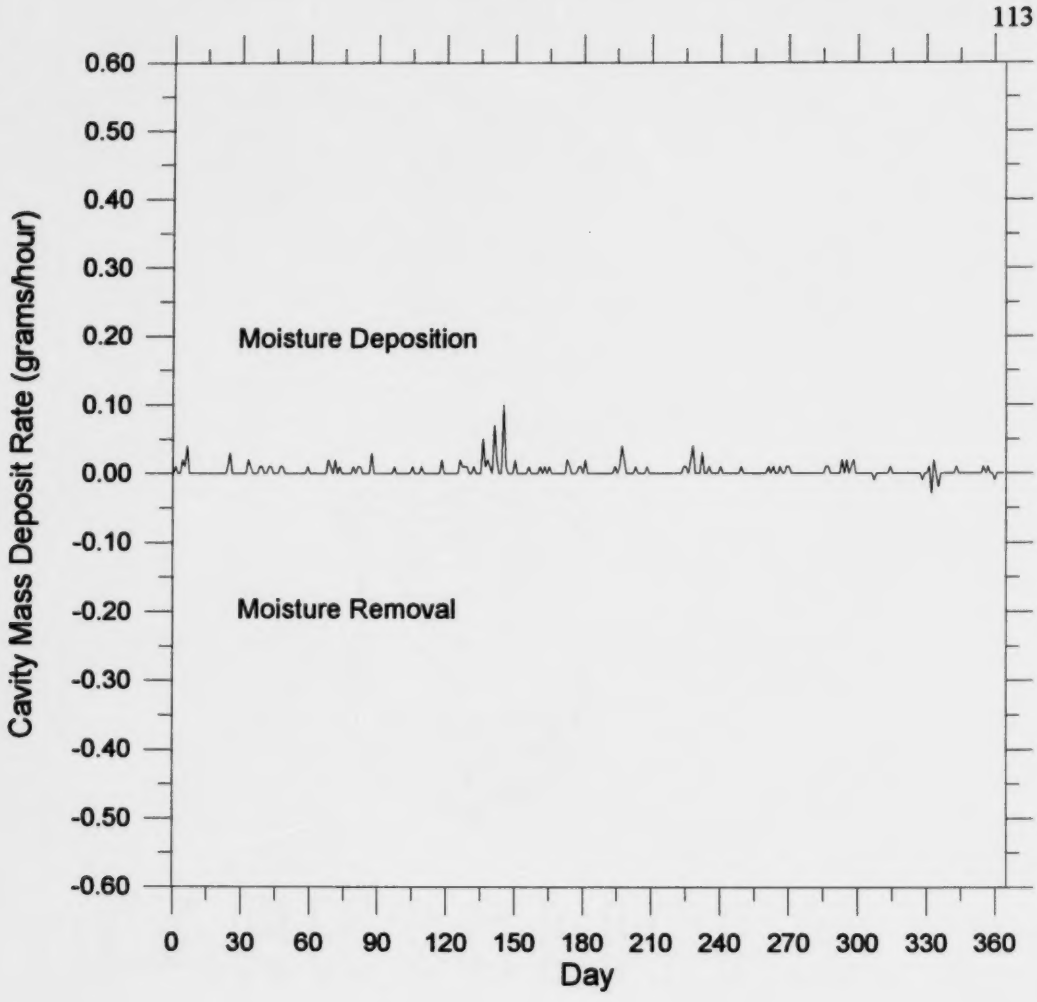

Figure 4-19 Daily averaged cavity mass deposit rate over a 1 year period (July-June) in Vancouver.

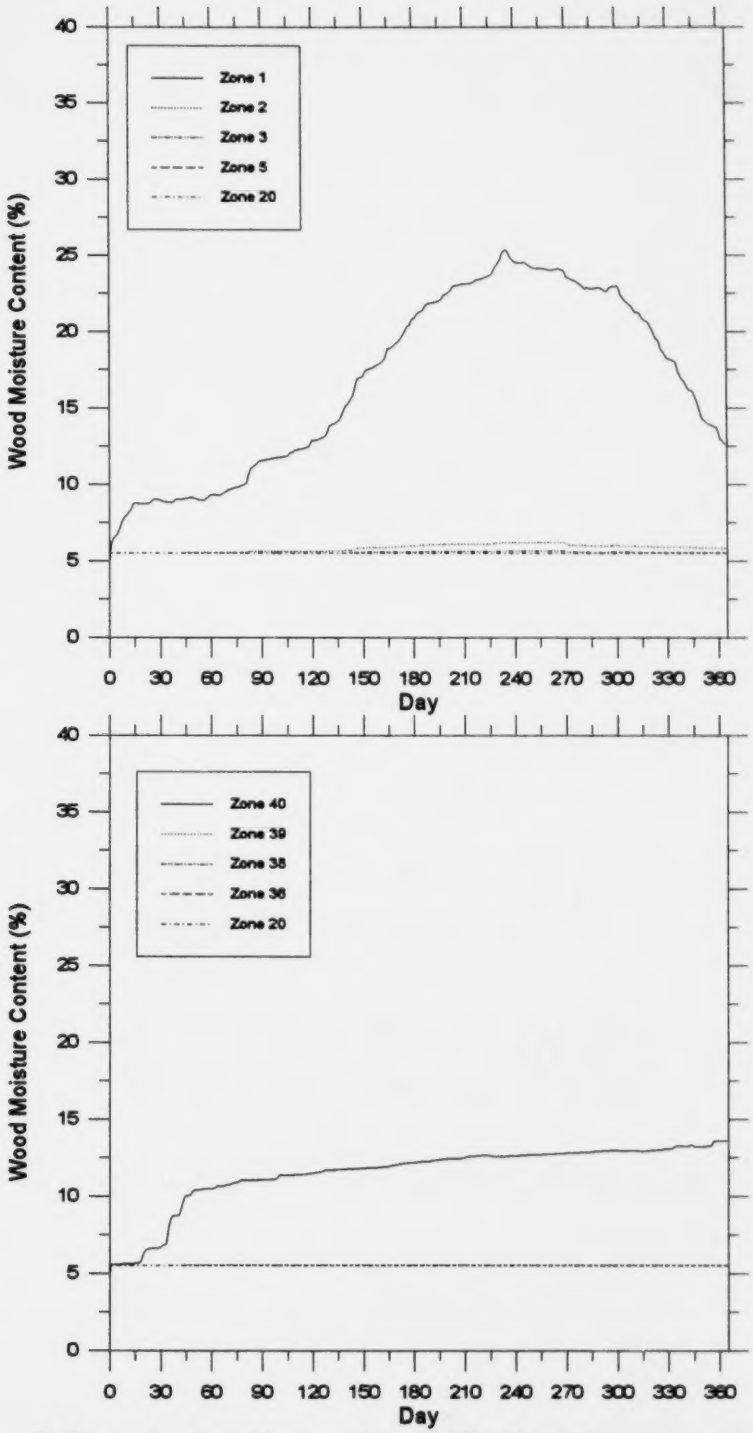

Figure 4-20 Daily averaged moisture content profiles for various zones over a 1 year period (July-June) in Vancouver.

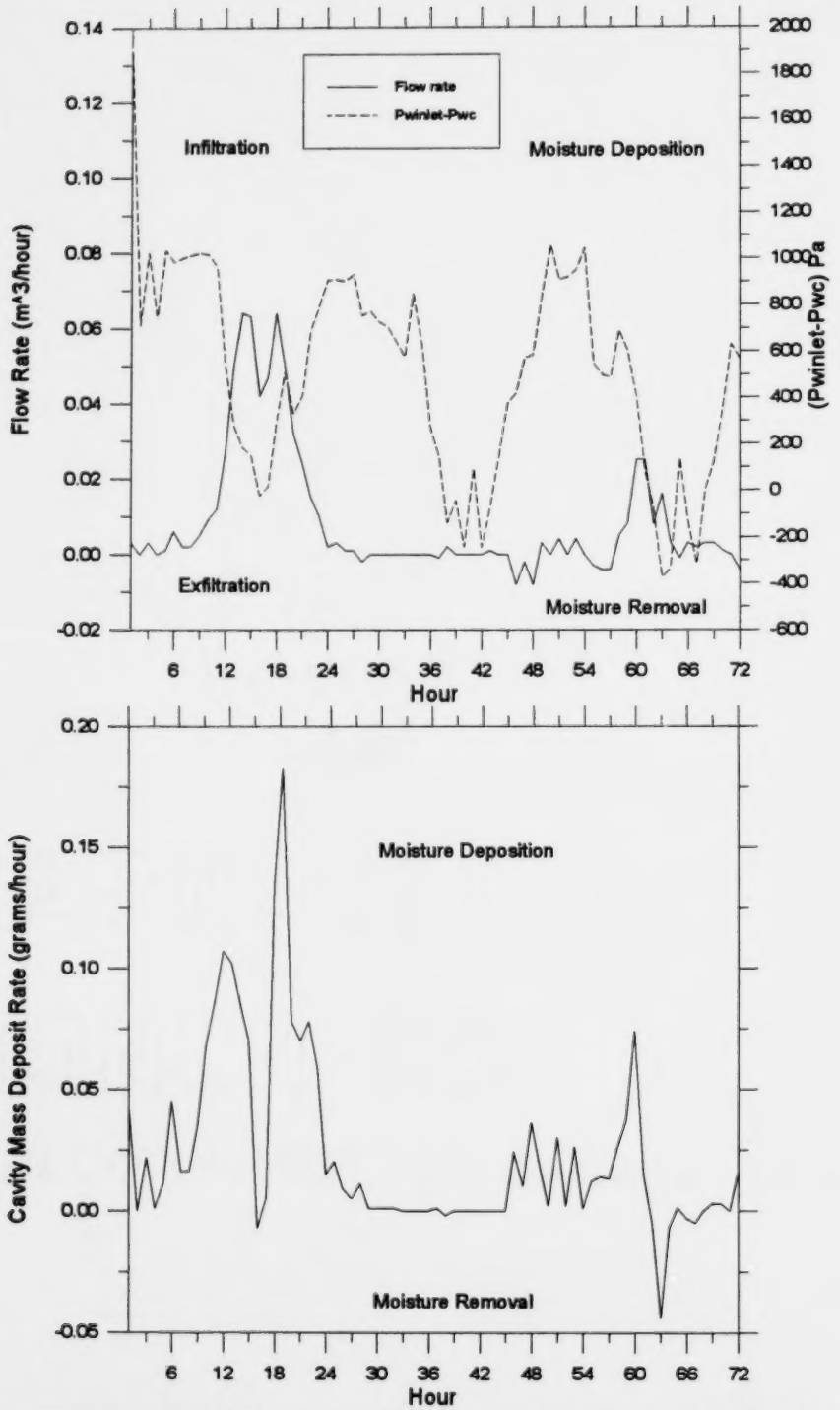

Figure 4-21 Hourly values of flow rate and vapor pressure difference (top figure) and the cavity mass deposit rate (bottom figure) for July 1 - 3 in Winnipeg.

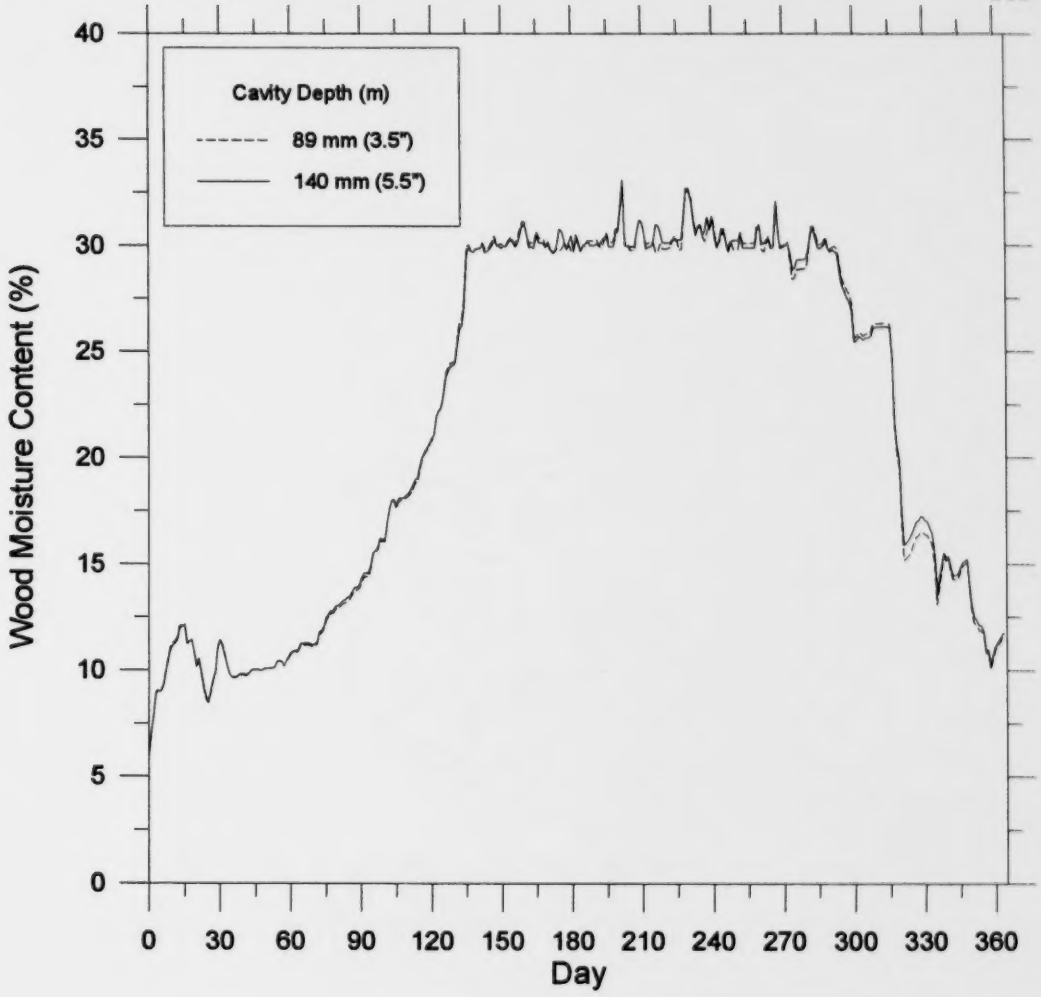

Figure 4-22 Comparison of the daily averaged moisture content of zone 1 for a cavity depth of 89 mm (3.5") and 140 mm (5.5") over a 1 year period (July-June) in St.Johns.

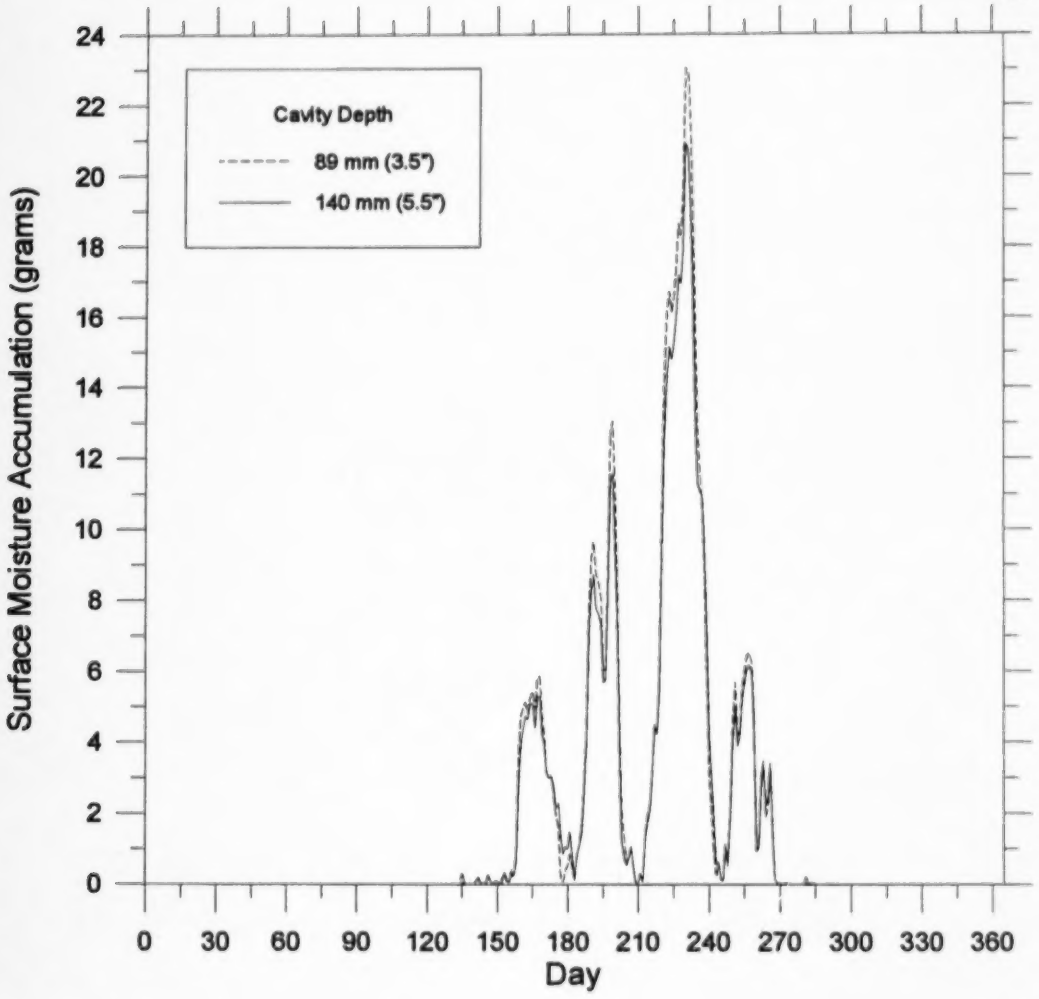

Figure 4-23 Comparison of the daily averaged surface moisture accumulation in zone 1 for a cavity depth of 89 mm (3.5") and 140 mm (5.5") over a 1 year period (July-June) in St.Johns. Surface moisture accumulation is uniformly distributed over zone 1 which is 50 mm high and 368 mm wide.

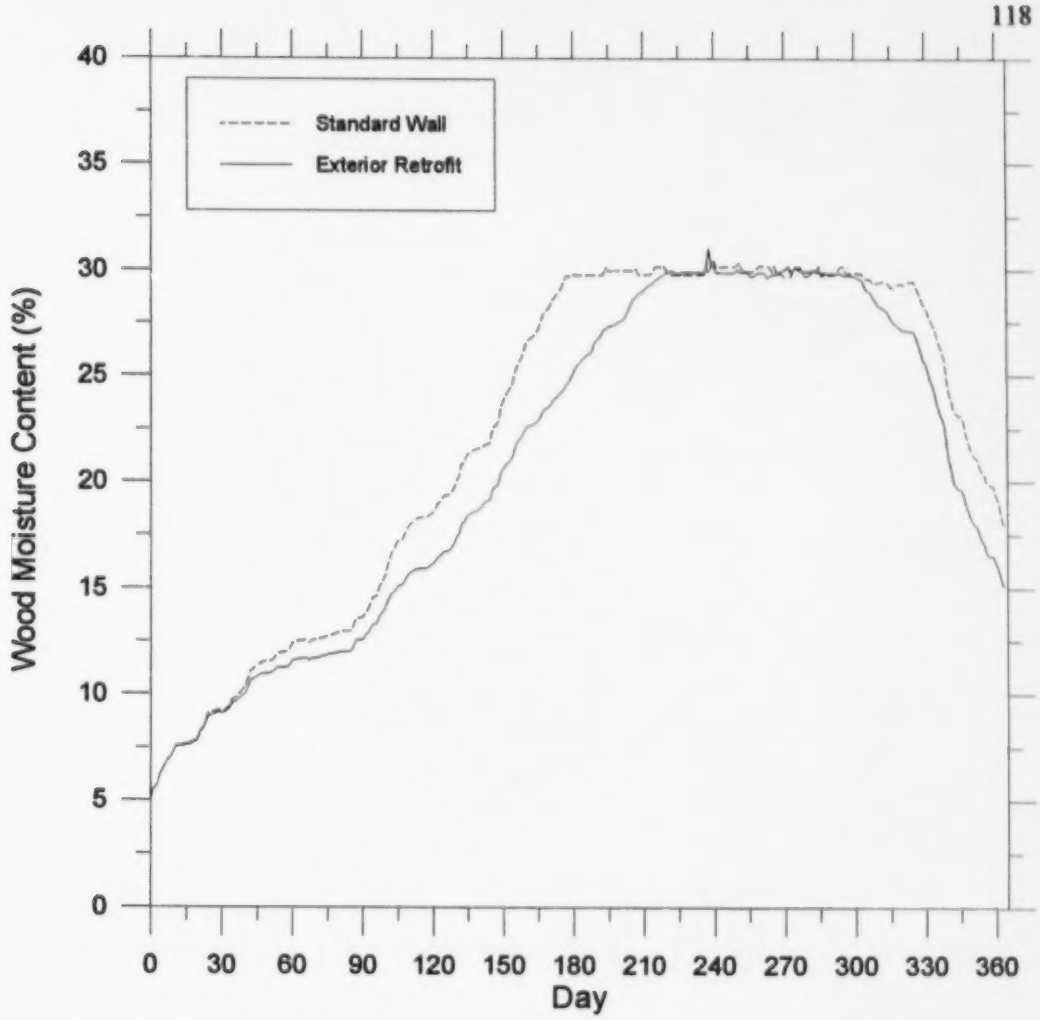

Figure 4-24 Comparison of the moisture content of zone 1 for a standard wall configuration with an exterior retrofit wall over a 1 year period (July-June) in Whitehorse.

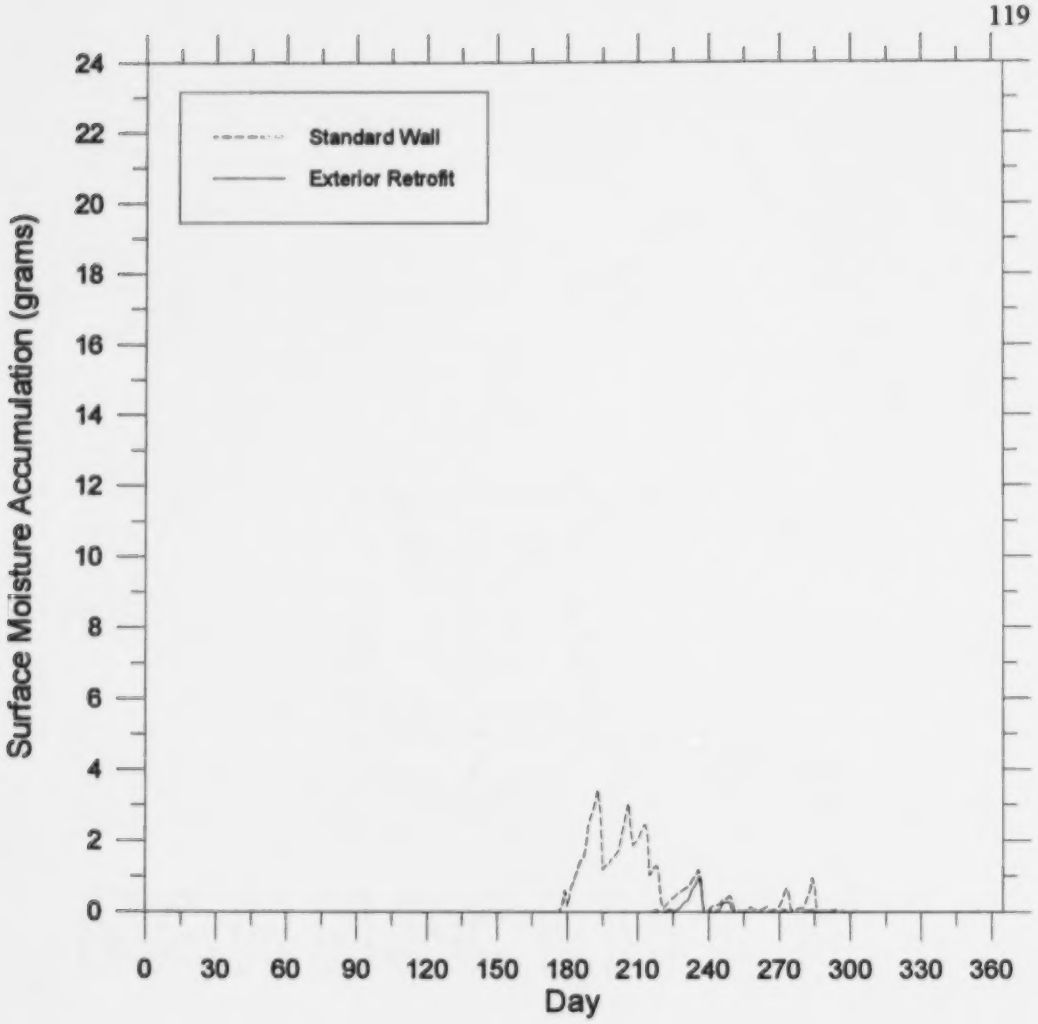

Figure 4-25 Comparison of the daily averaged surface moisture accumulation in zone 1 for a standard wall configuration with an exterior retrofit wall over a 1 year period (July-June) in Whitehorse. Surface moisture accumulation is uniformly distributed over zone 1 which is 50 mm high and 368 mm wide.

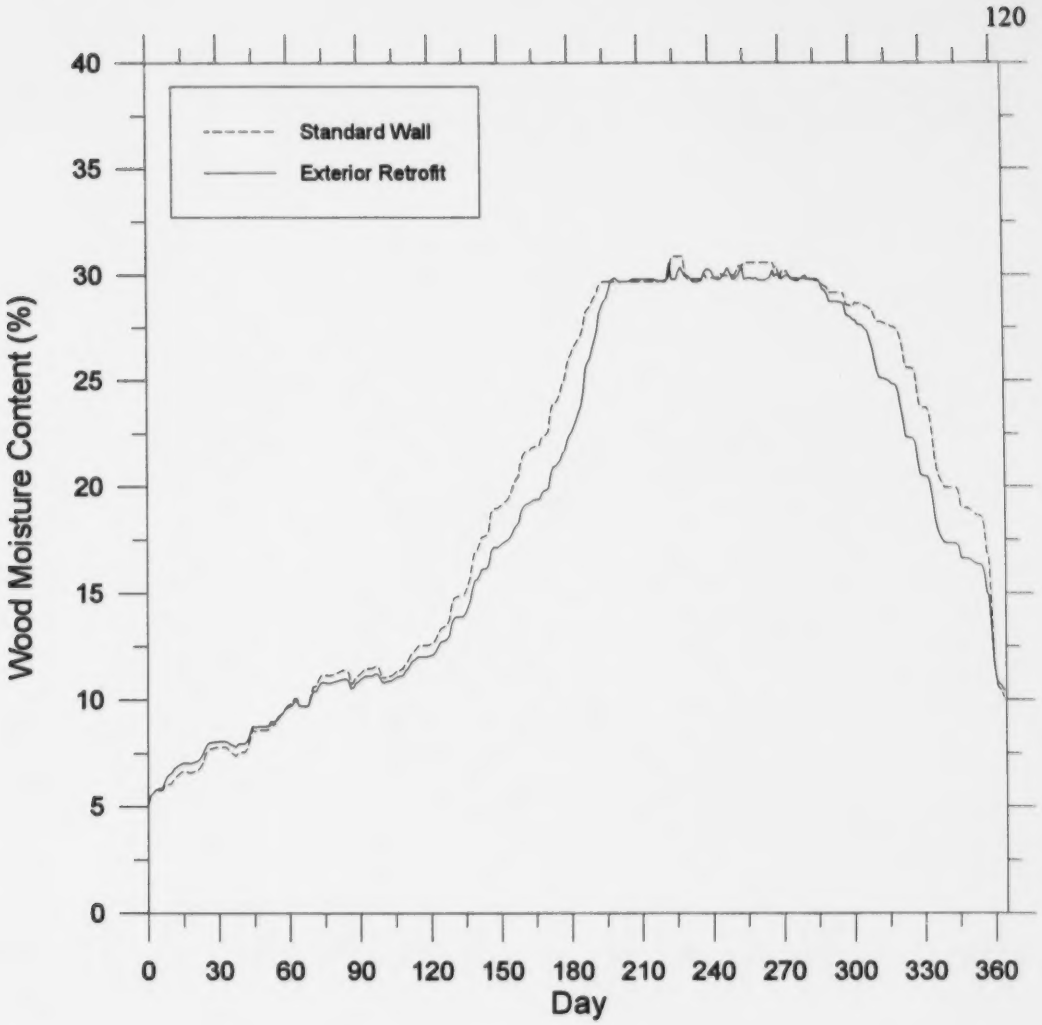

Figure 4-26 Comparison of the daily averaged moisture content of zone 1 for a standard wall configuration with an exterior retrofit wall over a 1 year period (July-June) in Winnipeg.

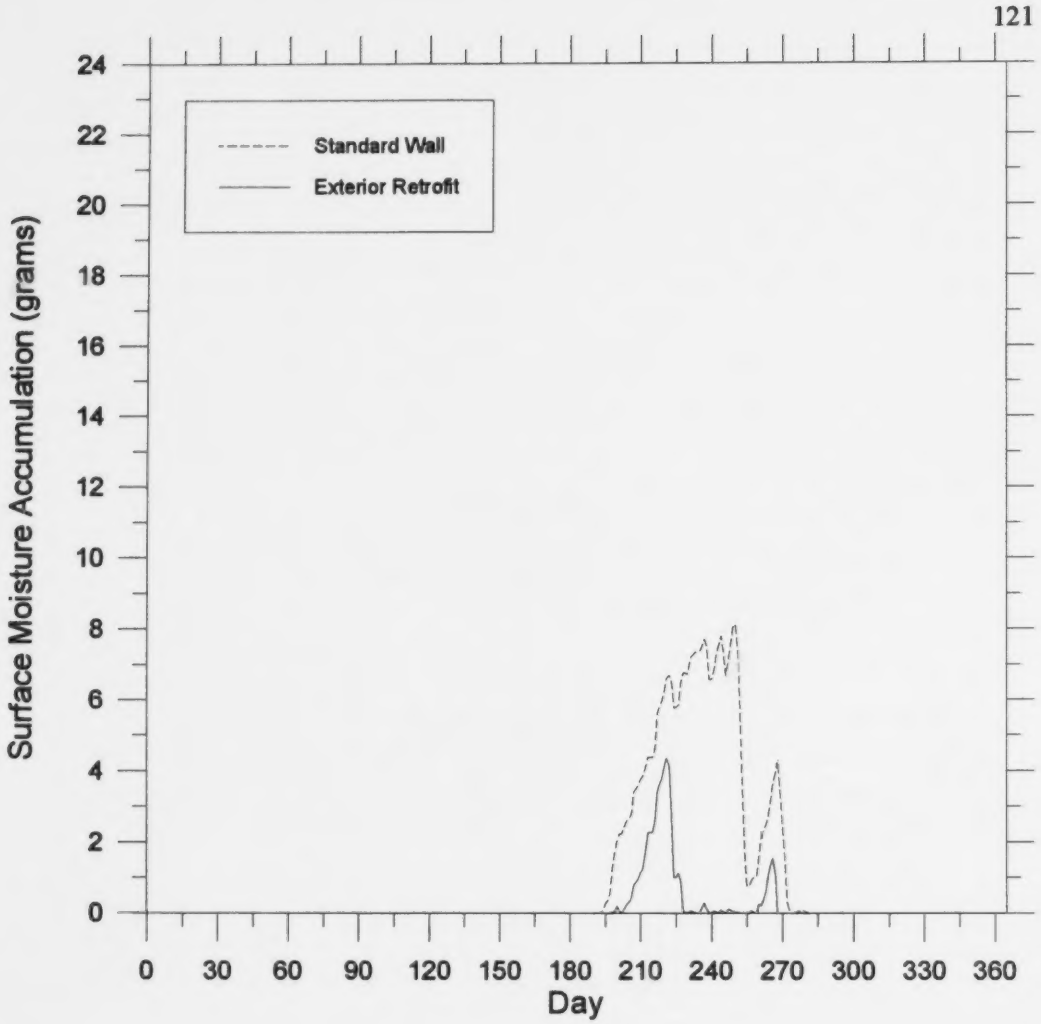

Figure 4-27 Comparison of the daily averaged surface moisture accumulation in zone 1 for a standard wall configuration with an exterior retrofit wall over a 1 year period (July-June) in Winnipeg. Surface moisture accumulation is uniformly distributed over zone 1 which is 50 mm high and 368 mm wide.

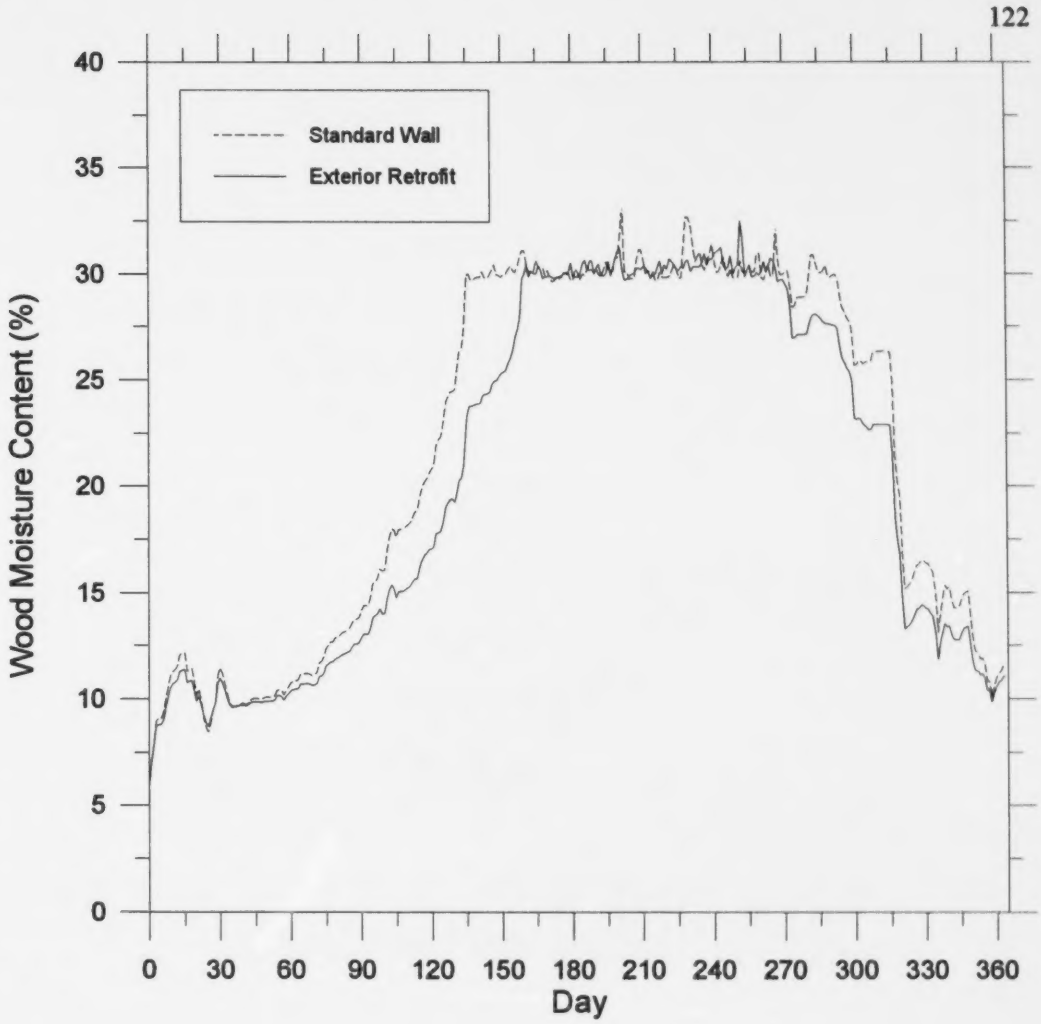

Figure 4-28 Comparison of the daily averaged moisture content in zone 1 for a standard wall configuration with an exterior wall retrofit over a 1 year period (July-June) in St.Johns.

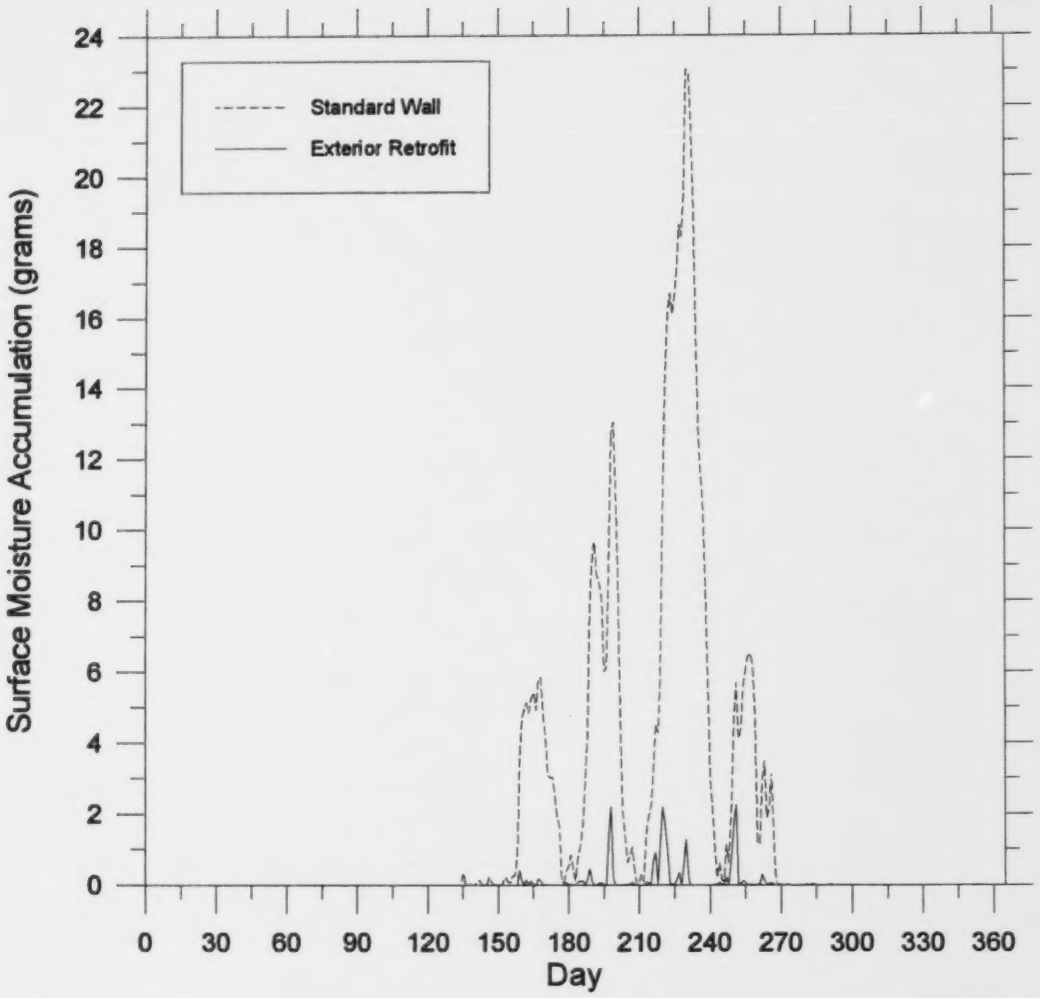

Figure 4-29 Comparison of the daily averaged surface moisture accumulation for a standard wall configuration with an exterior retrofit wall over a 1 year period (July-June) in St.Johns. Surface moisture accumulation is uniformly distributed over zone 1 which is 50 mm high and 368 mm wide.

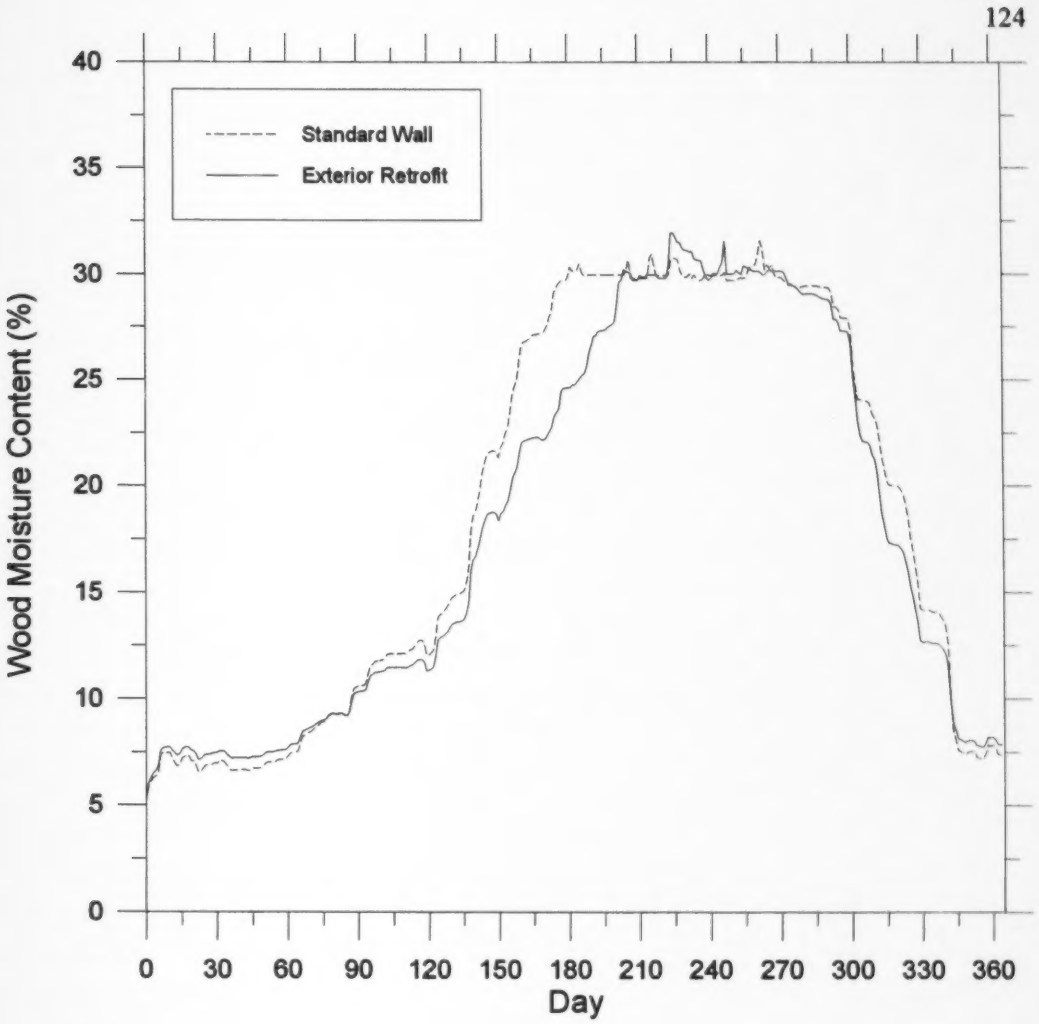

Figure 4-30 Comparison of the daily averaged moisture content in zone 1 for a standard wall configuration with an exterior retrofit wall over a 1 year period (July-June) in Montreal.

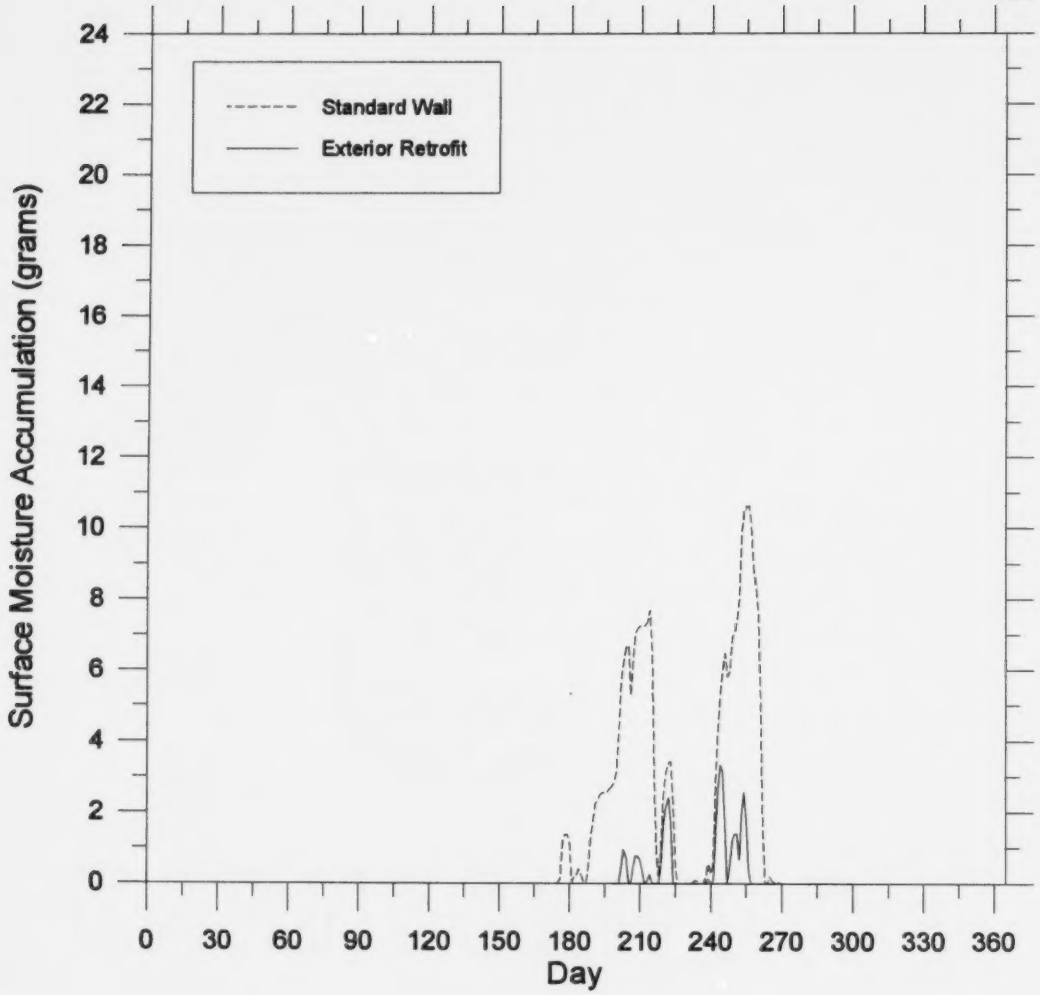

Figure 4-31 Comparison of the daily averaged surface moisture accumulation in zone 1 for a standard wall configuration with an exterior retrofit wall over a 1 year period (July-June) in Montreal. Surface moisture accumulation is uniformly distributed over zone 1 which is 50 mm high and 368 mm wide.

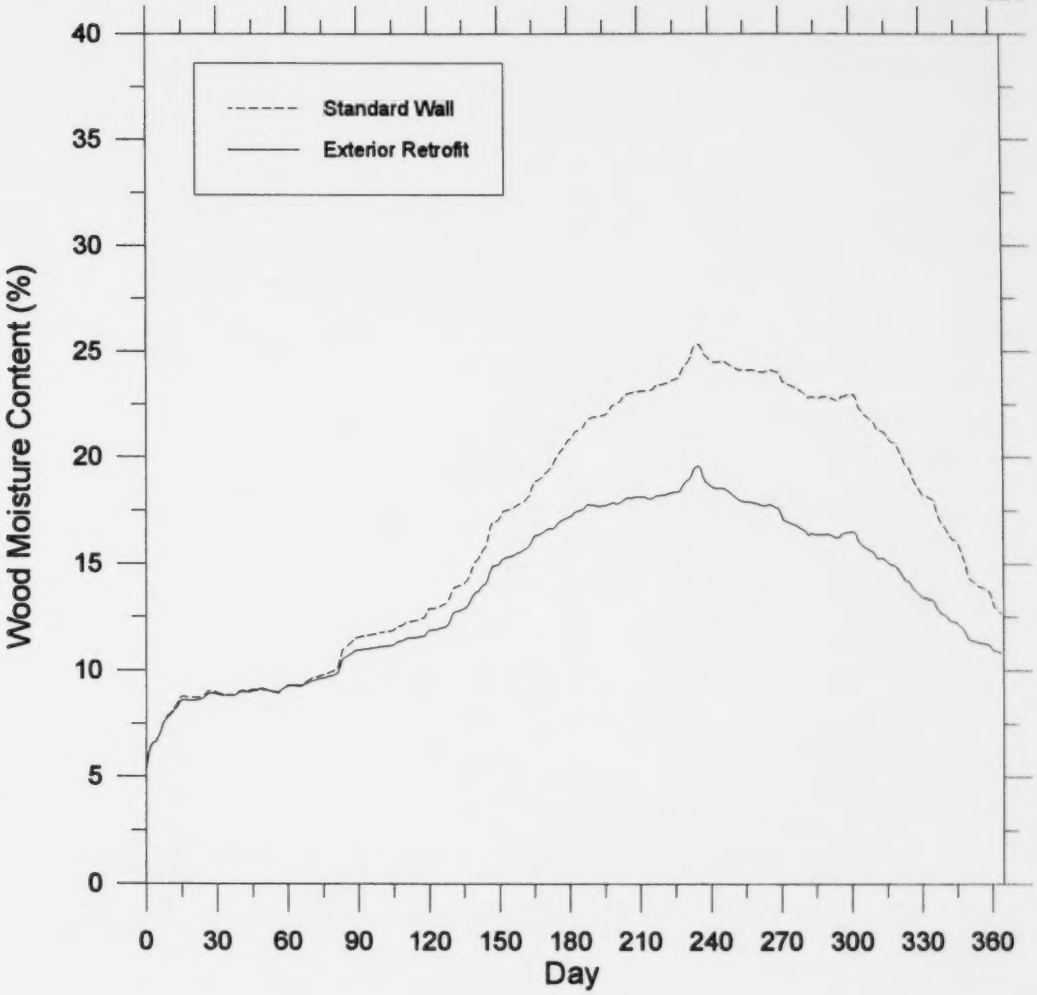

Figure 4-32 Comparison of the daily averaged moisture content in zone 1 for a standard wall configuration with an exterior retrofit wall over a 1 year period (July-June) in Vancouver.

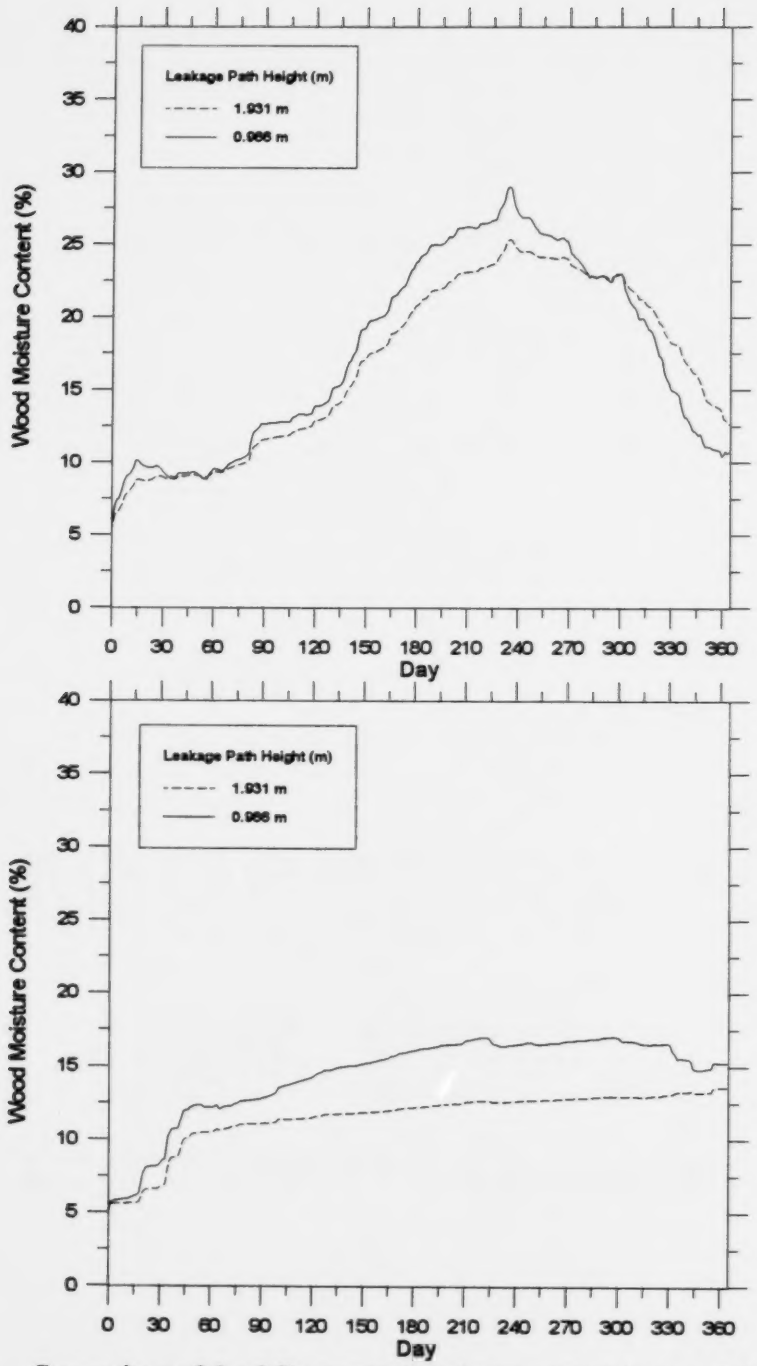

Figure 4-33 Comparison of the daily averaged moisture content in zone 1 (top figure) and zone 40 (bottom figure) for a leakage path height of 1.931m and 0.966m over a 1 year period (July-June) in Vancouver.

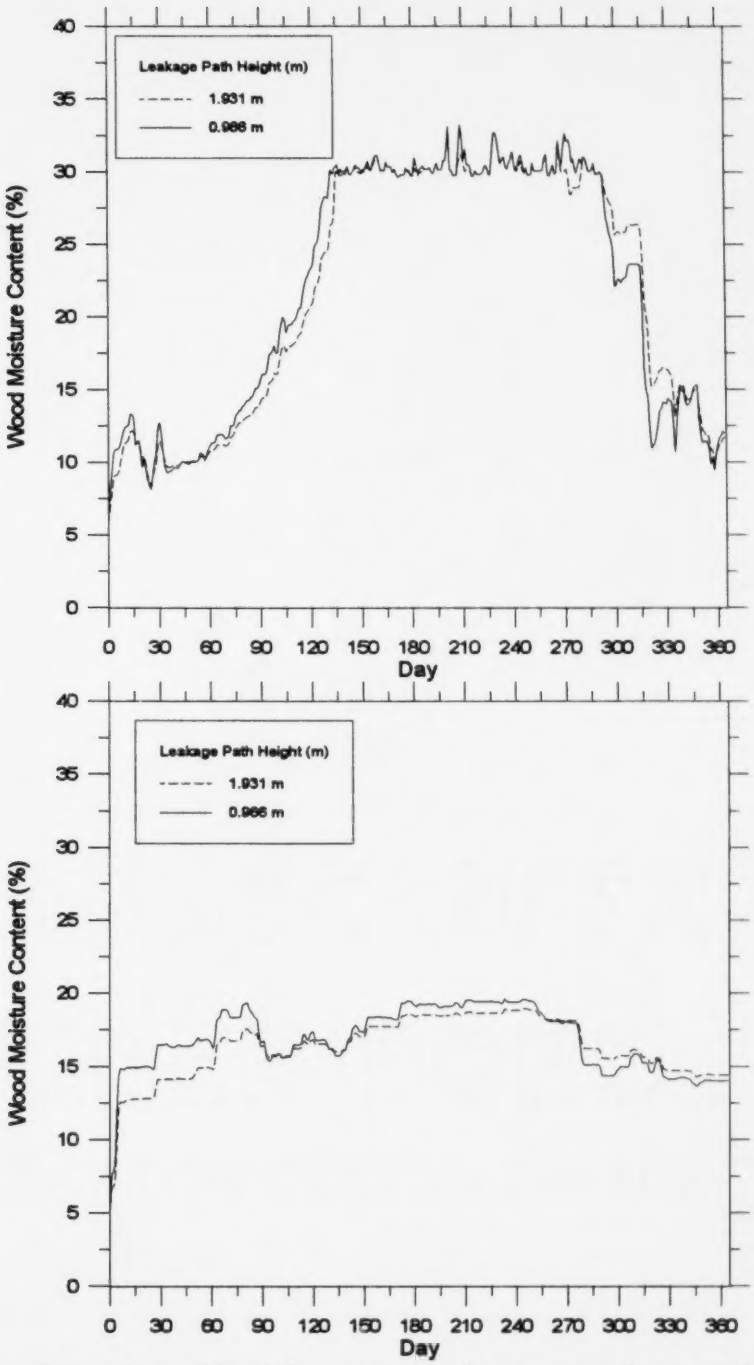

Figure 4-34 Comparison of the daily averaged moisture content in zone 1 (top figure) and zone 40 (bottom figure) for a leakage path height of 1.931 m and 0.966 m over a 1 year period (July-June) in St.Johns.

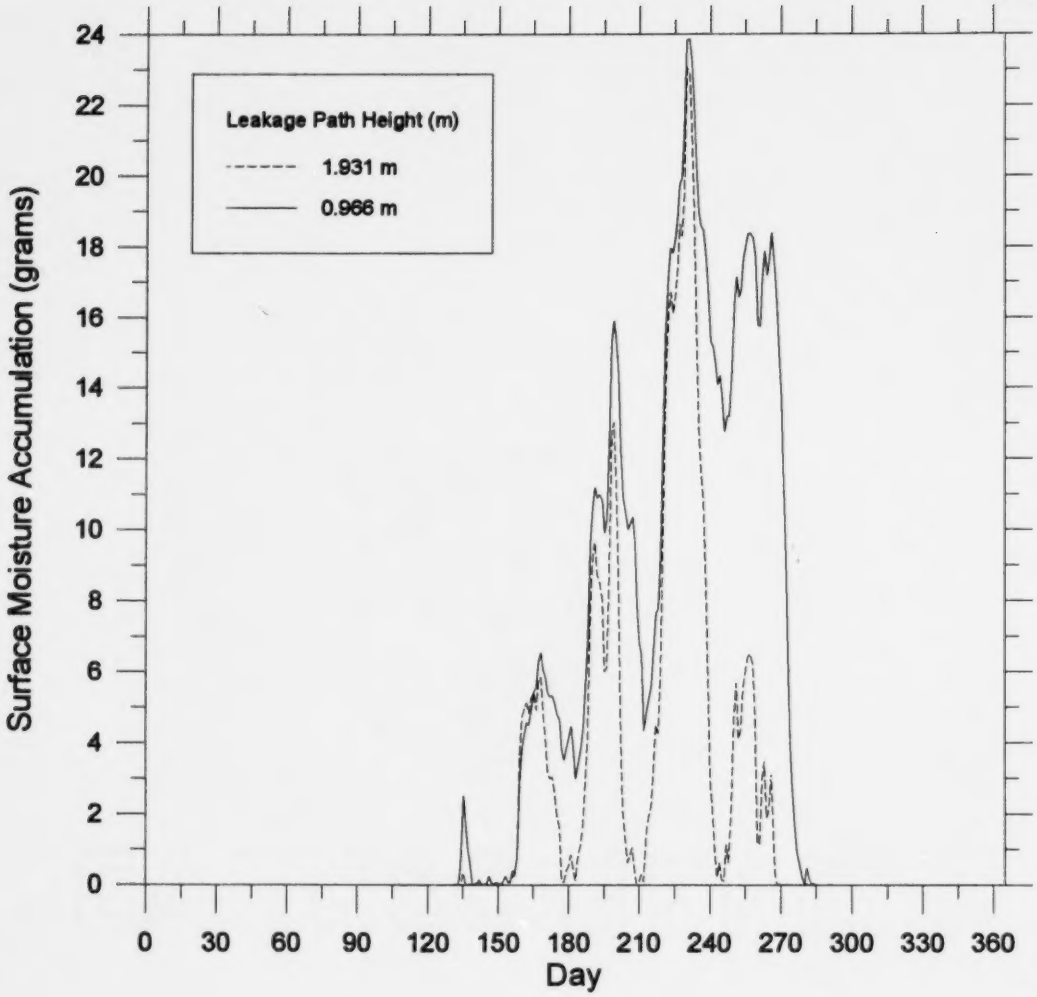

Figure 4-35 Comparison of the daily averaged surface moisture accumulation in zone 1 for a leakage path height of 1.931 m and 0.966 m over a 1 year period (July-June) in St.Johns. Surface moisture accumulation is uniformly distributed over zone 1 which is 50 mm high and 368 mm wide.

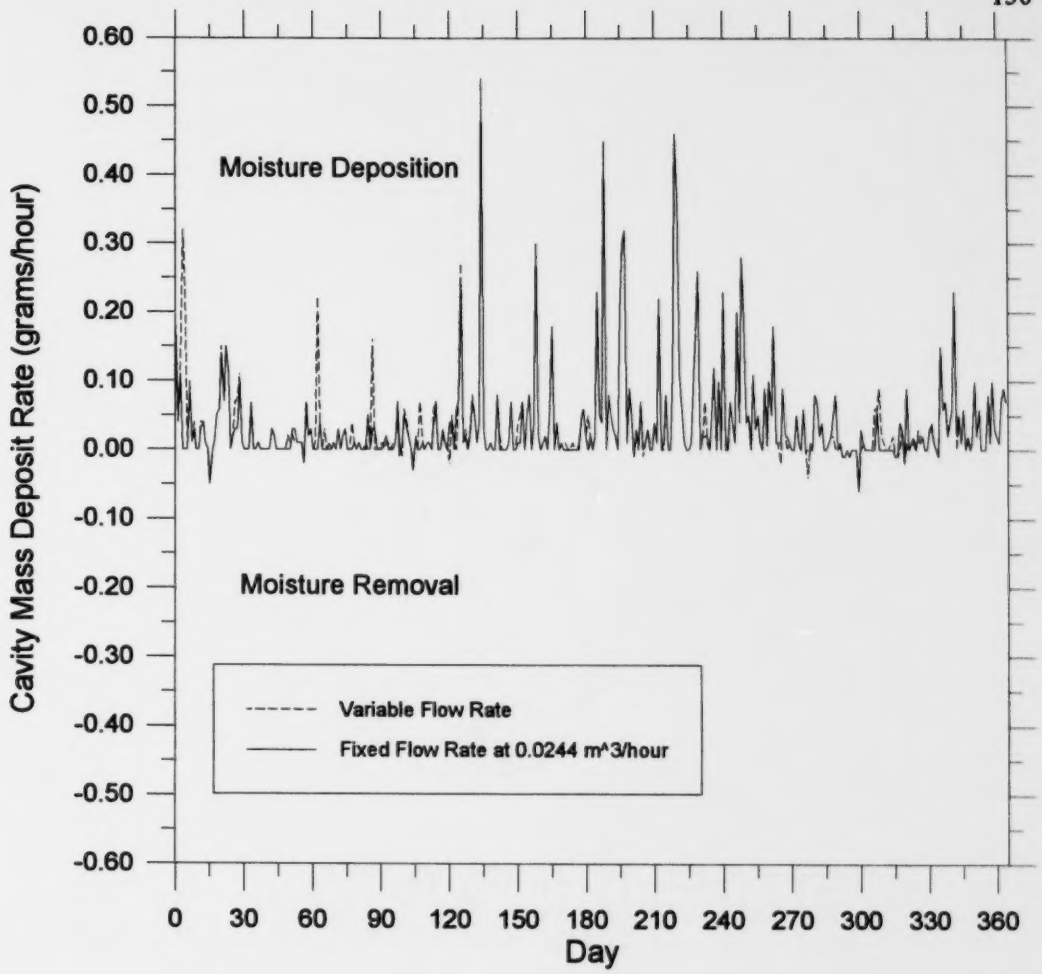

Figure 4-36 Comparison of the daily averaged cavity mass deposit rate for a variable flow rate (base case) with a fixed flow rate of 0.0244 m^3/hour over a 1 year period (July-June) in St.Johns.

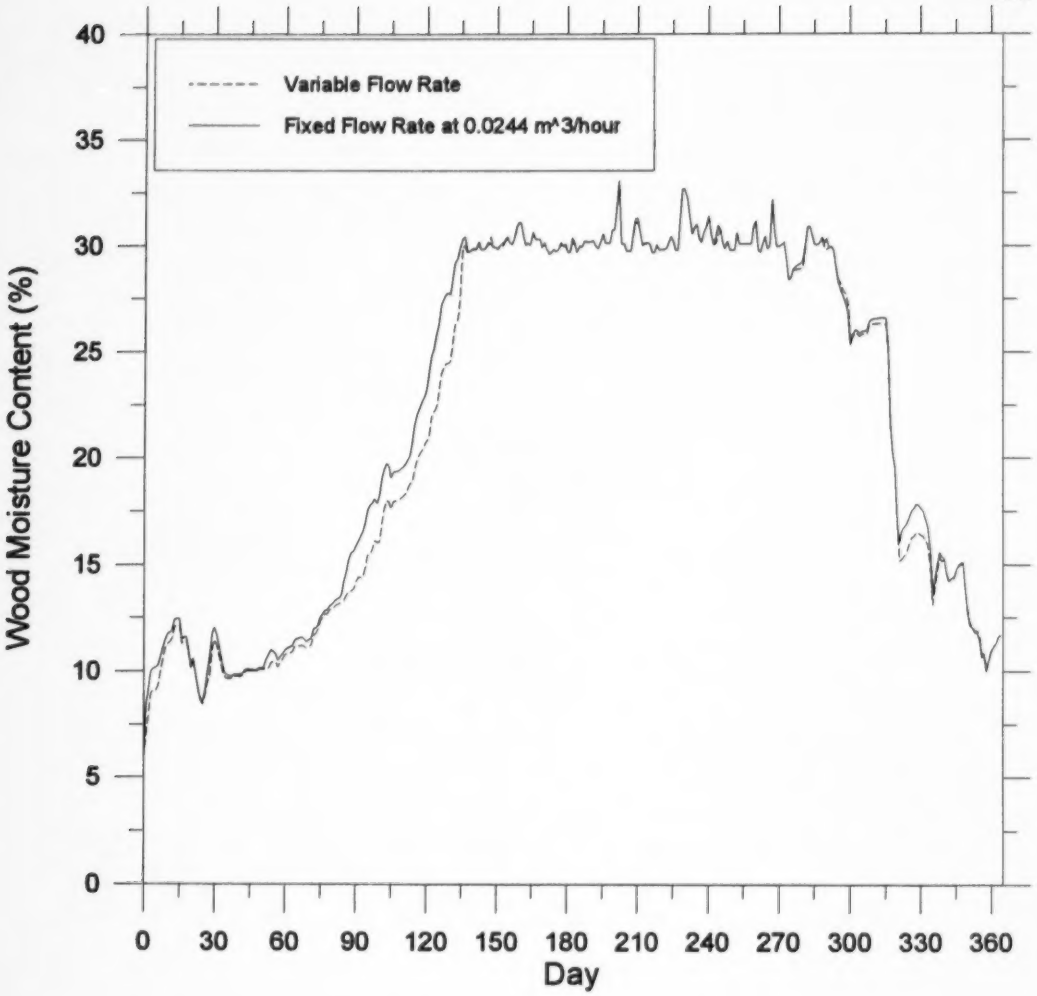

Figure 4-37 Comparison of the daily averaged moisture content in zone 1 for a variable flow rate (base case) with a fixed flow rate of 0.0244 m^3/hour over a 1 year period (July-June) in St.Johns.

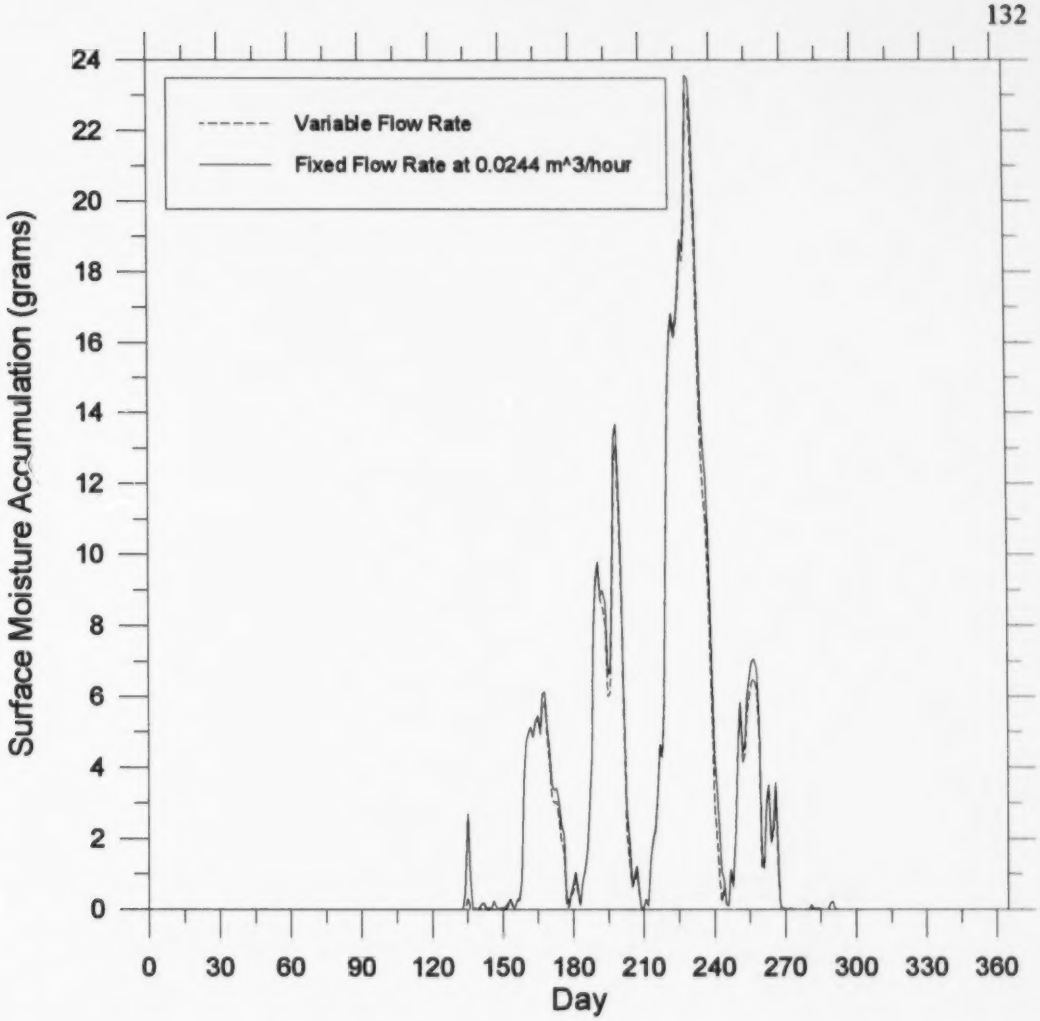

Figure 4-38 Comparison of the daily averaged surface moisture accumulation in zone 1 for a variable flow rate (base case) with a fixed flow rate of 0.0244 m^3/hour over a 1 year period (July-June) in St.Johns. Surface moisture accumulation is uniformly distributed over zone 1 which is 50 mm high and 368 mm wide.

City	Whitehorse	Winnipeg	St.Johns	Montreal	Vancouver
Hours of Infiltration	3351	4687	2908	3707	3849
$\overline{Q}$ (m^3/hour)	0.0054	0.0212	0.0215	0.0090	0.0011
Q_{max} (m^3/hour)	0.078	0.249	0.466	0.092	0.030
$\overline{\dot{M}_w}$ (grams/hour)	0.0162	0.1025	0.1034	0.0434	0.0098
$\overline{\dot{m}_w}$ (grams/hour)	0.0017	0.0007	0.0052	0.0010	0.0023
$\dot{m}_{w,min}$ (grams/hour)	-0.167	-0.639	-0.313	-0.429	-0.042
$\dot{m}_{w,max}$ (grams/hour)	0.287	0.584	0.402	0.256	0.106
$\overline{\dot{m}_{w_{exit}}}$ (grams/hour)	0.0141	0.0990	0.0944	0.0413	0.0076
Hours of Exfiltration	5409	4073	5852	5053	4911
$\overline{Q}$ (m^3/hour)	0.0050	0.0067	0.0244	0.0087	0.0056
Q_{max} (m^3/hour)	0.072	0.065	0.278	0.118	0.073
$\overline{\dot{M}_w}$ (grams/hour)	0.0336	0.0433	0.1694	0.0596	0.0419
$\overline{\dot{m}_w}$ (grams/hour)	0.0057	0.0065	0.0344	0.0082	0.0014
$\dot{m}_{w,min}$ (grams/hour)	-0.216	-0.601	-0.641	-0.924	-0.174
$\dot{m}_{w,max}$ (grams/hour)	0.166	0.168	0.861	0.359	0.140
$\overline{\dot{m}_{w_{exit}}}$ (grams/hour)	0.0282	0.0367	0.1331	0.0510	0.0402

Q is the volumetric flow rate (m^3/hour)
$\dot{M}_w$ is the mass of water vapor entering the leakage site (grams/hour)
$\dot{m}_w$ is the cavity mass deposit rate (grams/hour)
$\dot{m}_{w,exit}$ is the rate of water vapor exiting the leakage site (grams/hour)

Table 4-1 Summary of the hourly average and maximum flow rates, mass of water vapor, cavity mass deposit rates, and mass of water vapor exiting the cavity for each of the base case cities over a 1 year period.

* *positive values of flow rate are infiltration while negative values are exfiltration*

* *positive values of mass flow are moisture deposition while negative values are moisture removal*

City	Whitehorse	Winnipeg	St.Johns	Montreal	Vancouver
Zone 1	491	511	275	398	828
2	0	0	920	0	0
3	0	0	902	0	0
4	0	0	902	0	0
5	0	0	0	0	0
6	0	0	0	0	0
7	0	0	0	0	0
8	0	0	0	0	0
9	0	0	0	0	0
10	0	0	0	0	0
30	0	0	0	0	0
31	0	0	0	0	0
32	0	0	0	0	0
33	0	0	0	0	0
34	0	0	0	0	0
35	0	0	0	0	0
36	0	0	0	0	0
37	0	0	0	0	0
38	0	0	0	0	0
39	0	0	0	0	0
40	0	0	0	0	0

Table 4-2 Total number of hours showing only the top 10 and bottom 10 zones when the moisture content was greater than 20% (by weight) and the temperature of the inner surface of the exterior sheathing (Tc) was greater than 10 °C. These are potential periods for bacterial growth for the standard wall configuration for the 5 base case cities.

City St.Johns	Base Case	140 mm (5.5") Cavity Depth	25.4 mm (1") Exterior Retrofit	0.996 m Leakage Path Height	Constant Exfiltration Flow Rate
Hours of Infiltration	2908	2868	2908	3612	-
$\overline{Q}$ (m^3/hour)	0.0215	0.0245	0.0215	0.0213	-
Q_{max} (m^3/hour)	0.466	0.523	0.466	0.550	-
$\overline{\dot{M}_w}$ (grams/hour)	0.1034	0.1174	0.1034	0.1016	-
$\overline{\dot{m}_w}$ (grams/hour)	0.0052	0.0069	0.0030	0.0030	-
$\dot{m}_{w,min}$ (grams/hour)	-0.313	-0.358	-0.281	-0.370	-
$\dot{m}_{w,max}$ (grams/hour)	0.402	0.448	0.305	0.414	-
$\overline{\dot{m}_{w_{exit}}}$ (grams/hour)	0.0944	0.1063	0.0967	0.0950	-
Hours of Exfiltration	5852	5892	5852	5148	8760
$\overline{Q}$ (m^3/hour)	0.0244	0.0271	0.0244	0.0312	0.0244
Q_{max} (m^3/hour)	0.278	0.311	0.278	0.324	0.0244
$\overline{\dot{M}_w}$ (grams/hour)	0.1694	0.1866	0.1816	0.2172	0.1132
$\overline{\dot{m}_w}$ (grams/hour)	0.0344	0.0389	0.0157	0.0433	0.0241
$\dot{m}_{w,min}$ (grams/hour)	-0.641	-0.742	-0.596	-0.774	-0.635
$\dot{m}_{w,max}$ (grams/hour)	0.861	0.965	0.615	0.976	0.861
$\overline{\dot{m}_{w_{exit}}}$ (grams/hour)	0.1331	0.1458	0.1639	0.1713	0.0962

where Q is the volumetric flow rate (m^3/hour)
$\dot{M}_w$ is the mass of water vapor entering the leakage site (grams/hour)
$\dot{m}_w$ is the cavity mass deposit rate (grams/hour)
$\dot{m}_{w,exit}$ is the rate of water vapor exiting the leakage site (grams/hour)

Table 4-3 Summary of the hourly average and maximum flow rates, mass of water vapor, cavity mass deposit rates, and mass of water vapor exiting the cavity for St.Johns comparing the various wall cavity assemblies over a 1 year period.

* *positive values of flow rate are infiltration while negative values are exfiltration*

* *positive values of mass flow are moisture deposition while negative values are moisture removal*

Chapter
FIVE

CONCLUSIONS AND RECOMMENDATIONS

The simple yet comprehensive Wall Moisture Simulation Model was developed to predict moisture deposition in a wall cavity. This is the first model of its kind which determines the leakage flow rate as a function of the pressure difference across the leakage path and then determines the moisture deposition taking into account the building geometry and leakage configuration and weather data. A number of models were coupled together to achieve this task including Walker's (1993) ventilation model, Nikel's (1991) moisture deposition model, and a cavity flow model. When the ventilation and cavity flow models were coupled together they were capable of predicting the pressure difference and subsequent flow rate across the wall cavity. Once the flow rate was predicted the deposition rate along the wall cavity was determined by incorporating the moisture deposition model developed by Nikel (1991) for forced flow through a porous medium.

The results including the flow rate, vapor pressure difference, $(P_{w,inlet} - P_{w,c})$, deposition rate, moisture content profile, surface moisture deposition, and potential for biological activity were analyzed for 5 different climatic regions across Canada. The WMS model was used on a number of wall assemblies and the results for the moisture content profiles and surface moisture accumulation were compared to the base case simulations. These variations included a 140 mm (5.5") cavity depth, exterior retrofit consisting of 25

mm (1") of rigid insulation, height reduction of the leakage path and constant exfiltration flow rate.

5.1 Base Case Results

A. The greatest moisture deposition and potential for biological activity occurred in St.Johns. St.Johns representing the Eastern coastal region had strong winds and moderately high indoor-outdoor temperature differences, resulting in the greatest surface moisture accumulation and potential for biological activity.

B. Vancouver, on the other hand, representing the Western coastal region had zero surface moisture accumulation but the second greatest potential for bacterial growth. Low pressure differences and subsequent low flow rates across the leakage path were the result of low wind speeds and moderately warm outdoor temperatures.

C. Winnipeg and Montreal representing respectively the Prairie, and Central regions of Canada were comparatively similar in their surface moisture accumulation and low potential for biological activity.

D. Surprisingly, Whitehorse representing the Northern region of Canada with its very cold outdoor temperatures had a lower surface moisture accumulation than both Winnipeg and Montreal.

E. The moisture accumulated within zone 1 which was just adjacent the leakage site for all of the simulations ran except St.Johns which accumulated moisture within zones 1 and 2.

5.2 Parametric Changes to the Wall Cavity

A. A slightly lower surface moisture accumulation for the 140 mm (5.5") cavity depth resulted from a decrease in the velocity of air across the wall cavity.

B. Addition of 25 mm (1") of rigid insulation to retrofit the exterior of the house decreased the amount of surface moisture accumulation but only transferred the moisture accumulation problem from the wall cavity to the areas surrounding the leakage sites.

C. Reducing the leakage path height increased the amount of moisture deposition by increasing the pressure difference and air flow rates across the wall cavity. However, with the reduction in moisture accumulation comes a greater number of zones having the potential for biological activity along the height of the leakage path height.

D. Utilizing a constant exfiltration flow rate to predict the moisture deposition was a viable alternative only if the value is sufficiently close to the actual or true value

5.3 Recommendations

1. Experimental verification should be performed to quantify the pressure drop and flow characteristics for low Reynolds number for flow through slit openings such as those found in leakage paths found in residential building.

2. Experimental verification should be set up to verify first the pressure difference and flow rates across the wall cavity and then the moisture content profiles and surface moisture accumulation values.

3. There is a need to measure the moisture content of wood as a function of temperature and relative humidity. This has been done for temperatures above 0° C but not below 0° C.

5. The WMS model has verified the requirement to build all new residential structures with a 2" x 6" studs showing that it reduces the possibility of moisture accumulation.

6. Buildings located along the coast such as Vancouver and St.Johns should take extra precautions against biological activity along the interface between the insulation and exterior sheathing. This may entail precoating the surface with some sort of anti-fungal preservative.

References

ASHRAE (1989): **1989 Fundamentals Handbook, S.I. edition.** American Society of Heating, Refrigeration, and Air Conditioning Engineers, Inc. Atlantic

Bejan, A. (1980): **Convective Heat Transfer.** Wiley-Interscience, John Wiley & Sons, New York

Burch, D.M. and W.C. Thomas (1992): " An Analysis of Moisture Accumulation in a Wood-Frame Wall Subject to Winter Climate." In: *Proceedings, ASHRAE/DOE/BTECC/ Conference on the Thermal Performance of the Exterior Envelopes of Buildings V,* December 7-10, 1992, Clearwater Beach, Florida. pp 467-479.

Cleary, P.G. (1985): "Moisture Control by Attic Ventilation and an in situ Study." *ASHRAE Transaction*, Vol. 91, part 1

Ford, J.K. (1982): "Heat Flow and Moisture Dynamics in a Residential Attic." PU\CEES Report 147, Princeton University

Hoffman, J.D. (1992): **Numerical Methods for Engineers and Scientists.** McGraw-Hill, New York

Jones, W.R. (1987) Letter to J.D. Wilson, File Number: 814.34, September 9, 1987

Keil, D.E., D.J. Wilson, and M.H. Sherman (1985): " Air Leakage Flow Correlations for Varying House Constructions Types." In: *ASHRAE Transactions* 91, part 2. pp 560-575.

Kent, A.D.; Handegord, G.O. and Robson, D.R. (1966): " A Study of Humidity Variations in Canadian Homes." *ASHRAE Transactions,* Vol. 72, Part II, pp. 1.1-1.8.

Kreith, F and Raymond Eisenstadt (1957): "Pressure Drop and Flow Characteristics of Short Capillary Tubes at Low Reynolds." In: *Transaction of the American Society of Mechanical Engineers,* Volume 79, part 1, New York.

Nikel, K.G. (1991): M.Sc Thesis, University of Alberta

Ojanen, T and M. K. Kumaran (1992): "Air Exfiltration and Moisture Accumulation in Residential Wall Cavities." In: *Proceedings, ASHRAE/DOE/BTECC/ Conference on the Thermal Performance of the Exterior Envelopes of Buildings V,* December 7-10, 1992, Clearwater Beach, Florida. pp 491-500.

Ozisik, M. Necati (1985): **Heat Transfer, A Basic Approach.** McGraw-Hill, New York

Parmelee, G and W. Aubelle (1952): " Radiant Energy Emission of Atmosphere and Ground." *ASHVE Transaction,* Vol. 58, p 85.

Shapiro, A.H., R.Siegel, and S.J. Kline (1954): "Friction Factor in the Laminar Entry Region of a Smooth Tube." In: *Proceedings of the 2nd U.S. National Congress of Applied Mechanics,* June 14-18, 1954, Ann Harbor, Michigan.

TenWolde, A and C.Carll (1992): " Effect of Cavity Ventilation on Moisture in Walls and Roofs." In: *Proceedings, ASHRAE/DOE/BTECC/ Conference on the Thermal Performance of the Exterior Envelopes of Buildings V,* December 7-10, 1992, Clearwater Beach, Florida. pp 555-562.

TenWolde, A. and J.C. Suleski (1984): " Steady State One-Dimensional Water Vapor Movement by Diffusion and Convection in a Multi-layered Wall." *ASHRAE Transactions **91,*** Pt. 1, p.611

Tsongas, G. (1992): "A Field Study of Indoor Moisture Problems and Damage in New Northwest Homes." In: *Proceedings, ASHRAE/DOE/BTECC/ Conference on the Thermal Performance of the Exterior Envelopes of Buildings V,* December 7-10, 1992, Clearwater Beach, Florida. pp 563-571.

USDA Forest Products Laboratory (1974): **Wood Handbook: Wood as an Engineering Material.**, U.S. Department of Agriculture Forest Service Handbook No.72, Rev. Chpt 3 & 17.

Walker, I.S. (1993): PhD Thesis, University of Alberta

White, Frank M. (1986): **Fluid Mechanics.** 2 nd ed., McGraw-Hill, New York

Wilson, D.J. and I.S. Walker (1991): "Passive Ventilation To Maintain Air Quality." *Department of Mechanical Engineering, University of Alberta,* Report Number 81, March 1991. part 2.

Wilson, D.J. (1994): Personal Conversation

Appendix A

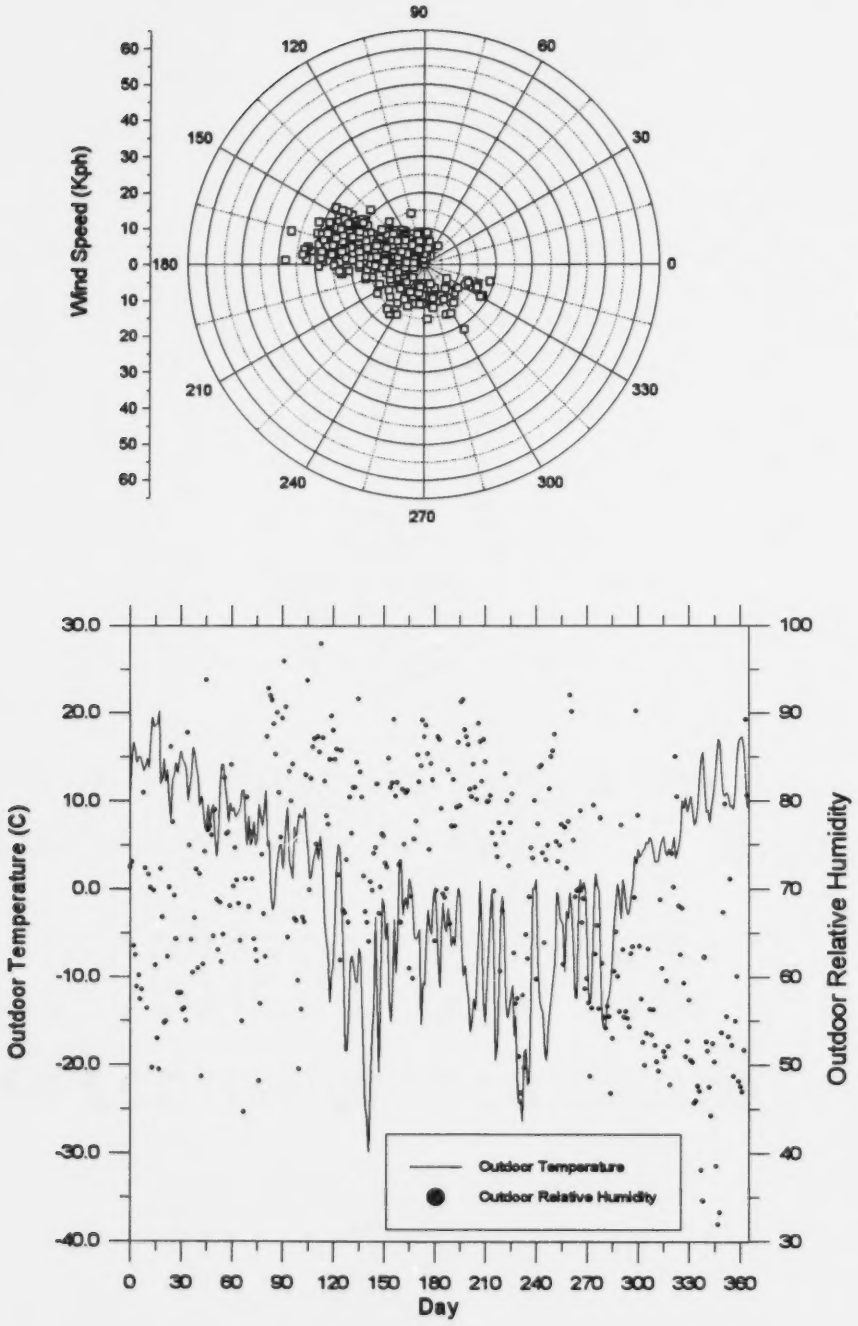

Figure A-1 Daily averaged wind speed, outdoor temperature, and relative humidity over a 1 year period (July-June) in Whitehorse.

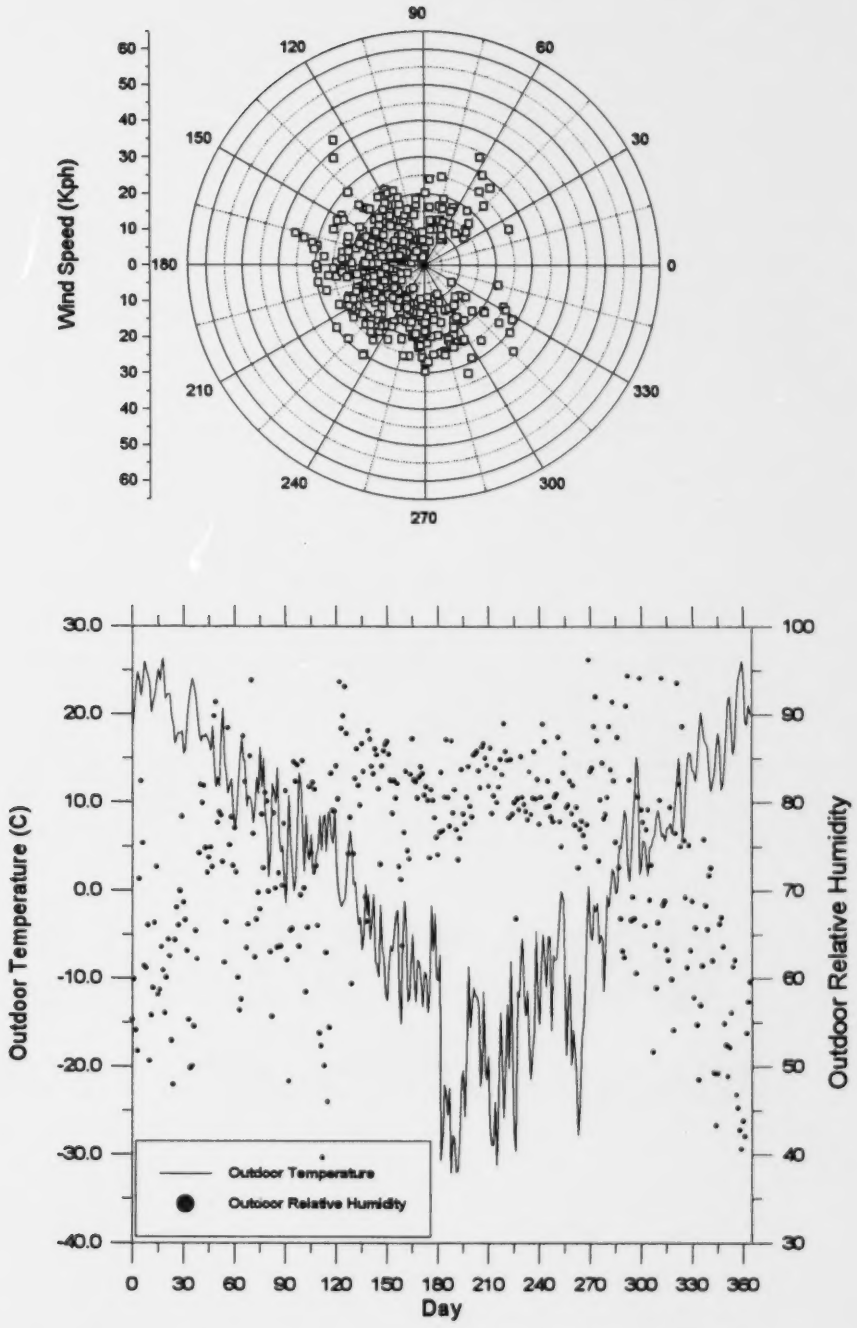

Figure A-2 Daily averaged wind speed, outdoor temperature and relative humidity over a 1 year period (July-June) in Winnipeg.

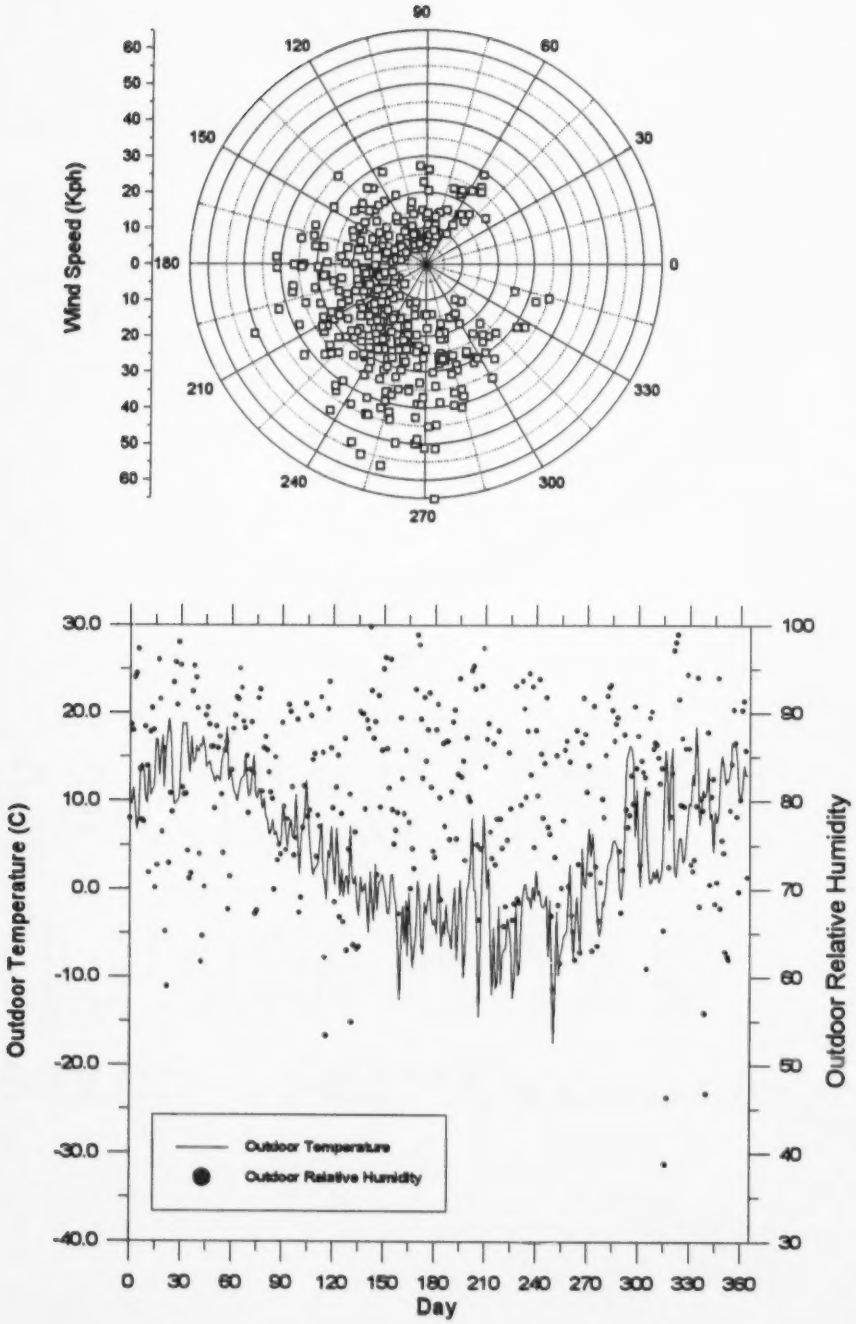

Figure A-3 Daily averaged wind speed, outdoor temperature and relative humidity over a 1 year period (July-June) in St.Johns.

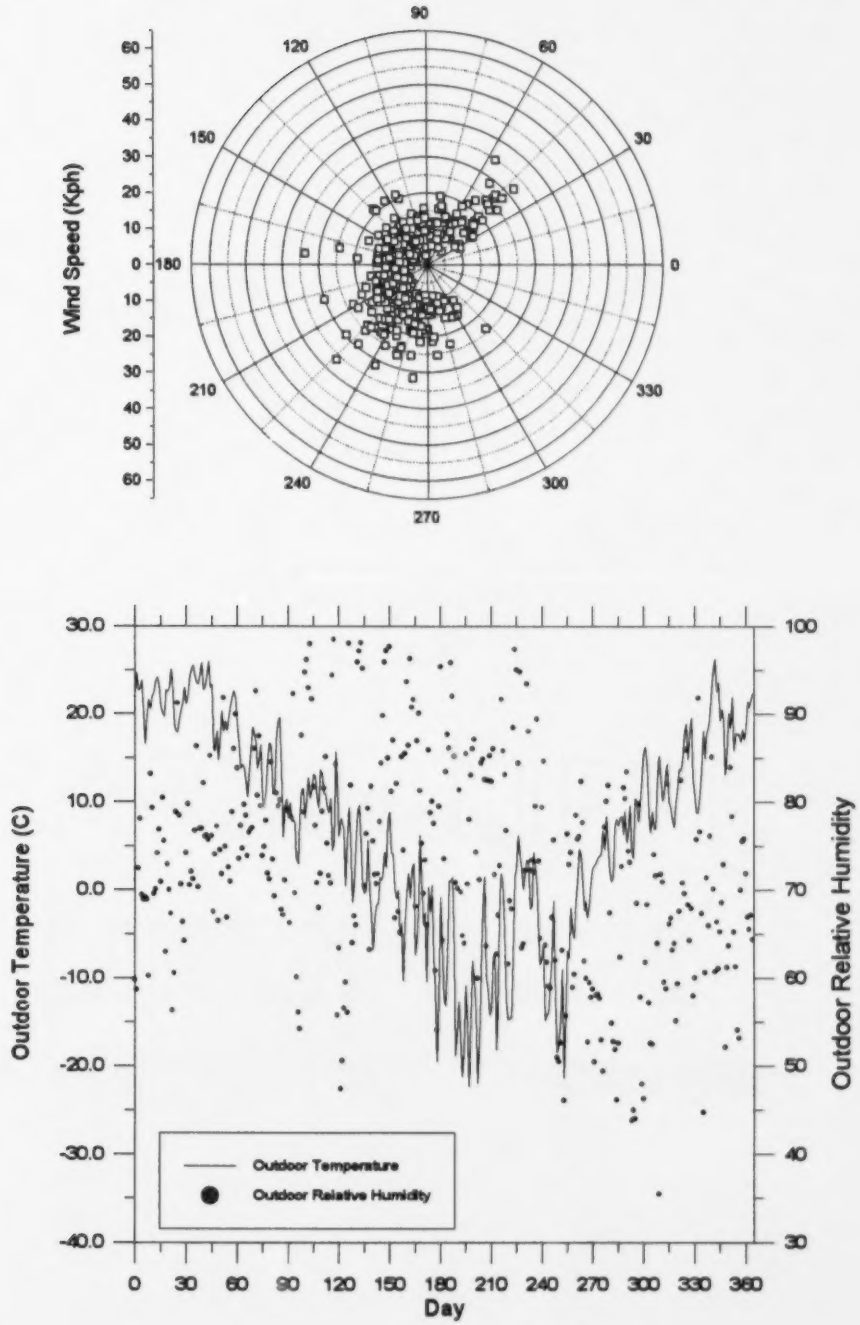

Figure A-4 Daily averaged wind speed, outdoor temperature and relative humidity over a 1 year period (July-June) in Montreal.

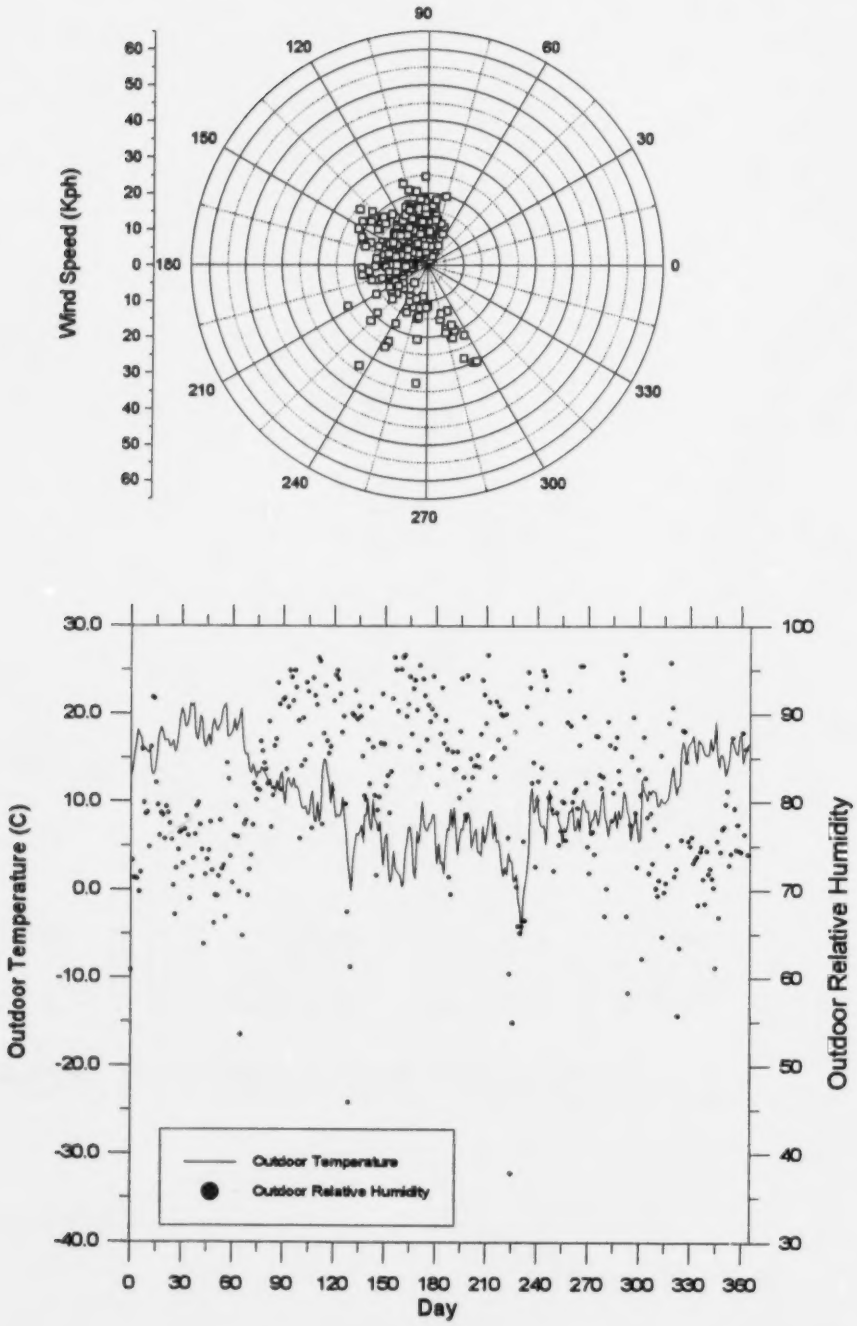

Figure A-5 Daily average wind speed, outdoor temperature and relative humidity over a 1 year period (July-June) in Vancouver.

Appendix B

Physical Constants used in WMS Model

Symbol	Description	Value
g	Acceleration due to gravity	9.81 m/s^2
D	Mass diffusivity of the insulation	2.56 x 10^{-5} m^2/s
π	Pie	3.141593
R_o	Universal gas constant	8314.41 J/kmol K
M_w	Molecular weight of water	18.01528 Kg/kmol
μ_{ref}	Reference dynamic viscosity of air	1.98 x 10^{-5} N s/m^2
ρ_{ref}	Reference density of air	1.10 Kg/m^3
K	Permeability of insulation	3.1 x 10^{-9} m^2
R_{ab}	Thermal resistance of drywall	0.079 m^2 K/W
R_{bc}	Thermal resistance of insulation	2.11 m^2 K/W
R_{cd}	Thermal resistance of exterior sheathing	0.083 m^2 K/W
h_a	Convective heat transfer coefficient (inside)	8.29 W/m^2 K
h_d	Convective heat transfer coefficient (outside)	28.40 W/m^2 K
σ	Stefan-Boltzman constant	5.669 x 10^{-8} W/m^2 K^4
ε	Long wave emissivity for exterior sheathing	0.9
α	Solar absorptivity for exterior sheathing	0.8
C_d	Discharge coefficient	0.6